PYROLYSIS OF SOME WESTERN CANADIAN COALS IN A SPOUTED BED REACTOR

by

ADNAN MOHAMMED AL-JARALLAH

B.Sc., The University of Baghdad, 1972
M.Sc., The University of Aston in Birmingham, 1975

A THESIS SUBMITTED IN PARTIAL FULFILLMENT OF

THE REQUIREMENTS FOR THE DEGREE OF

DOCTOR OF PHILOSOPHY

in

THE FACULTY OF GRADUATE STUDIES

(Department of Chemical Engineering)

We accept this thesis as conforming

to the required standard

THE UNIVERSITY OF BRITISH COLUMBIA

April 1983

In presenting this thesis in partial fulfilment of the requirements for an advanced degree at the University of British Columbia, I agree that the Library shall make it freely available for reference and study. I further agree that permission for extensive copying of this thesis for scholarly purposes may be granted by the head of my department or by his or her representatives. It is understood that copying or publication of this thesis for financial gain shall not be allowed without my written permission.

Department of chemical Eng.

The University of British Columbia
1956 Main Mall
Vancouver, Canada
V6T 1Y3

Date June, 7th, 1983

ABSTRACT

Coal pyrolysis has been studied in a 12.8 cm diameter continuous spouted bed reactor with the aim of determining conditions for maximum liquid yields from Western Canadian coals. Coals studied included two British Columbia bituminous coals and one Alberta sub-bituminous coal. The basic characteristics of the spouted bed pyrolyzer were determined by carrying out experiments over a range of spouting gas velocities and composition, coal feed rates and particle size, reactor temperatures, and bed heights. The process was assessed by measuring the yields and compositions of the tar, char, and gas. Nitrogen and nitrogen/carbon dioxide mixtures and coal of size - 3.36 + 1.19 mm were fed at atmospheric pressure to an electrically heated reactor containing sand. The tar yield was determined by sampling the outlet gas through a series of cooled impingers. The spouted bed pyrolyzer behaves in a manner similar to a fluidized bed unit, and shows a maximum tar yield with temperature at a fixed feed rate. At a given pyrolyzer temperature, the tar yield was inversely proportional to the coal feed rate over the range 0.4 to 7.6 kg/h. This effect is attributed to the detrimental effect on tar yield of the increasing amounts of char present in the reactor as coal feed rate increases. Coal type strongly influenced the liquid yields as expected. Sukunka bituminous coal from the Peace River coal field gave a maximum tar yield at 600°C of 31% wt/wt MAF coal. The corresponding gas yield was 3.6%, and the char yield was 64%. The maximum tar yield from Balmer bituminous coal from Crowsnest coal field

was 19.4% wt/wt MAF coal at 580°C while that from a high-ash Balmer bituminous coal was 12.1% at 620°C. Forestburg sub-bituminous coal from the Edmonton formation gave a maximum tar yield of 21% at 530°C and significantly higher gas yields of 20% versus 6% for the bituminous coals due to higher CO_2 production. With Sukunka coal, a steady increase in tar yield from 20.4 to 26.7% wt/wt MAF coal at 580°C was found as the average coal particle size was reduced from 2.28 to 0.65 mm. No significant effects on tar yield were found for variations in spouted bed depth, or vapour residence time over the range 0.68 - 1.15 s. No serious problems were encountered with agglomeration. Composition of gas, tar and char are presented for conditions of maximum tar yield for the various coals tested. The H/C atomic ratio of the tars was as high as twice that of the parent coal. Oxygen, sulphur and nitrogen together represent up to 10 wt% of the bituminous coal tars, which suggests considerable upgrading will be necessary to produce liquids of quality comparable to petroleum oils. The total volatiles yield data were well represented by a first order kinetic model. An activation energy of 4.71 kcal/mole was obtained for the sub-bituminous coal while that for the bituminous coals was 14.1 kcal/mole.

TABLE OF CONTENTS

LIST OF TABLES

LIST OF FIGURES

ACKNOWLEDGEMENTS

I would like to thank my advisor, Dr. A.P. Watkinson, for his guidance and encouragement.

I am grateful to Mr. Gordon Cheng for his help especially in crushing and screening most of the coal used in this study.

Thanks are also due to my colleagues, Dr. K.C. Teo and Dr. Giorgio Rovero for useful discussions, and particularly to Dr. Jim Lim for useful discussions about the kinetic model.

I am grateful to Dr. Marc Bustin and Mr. Gary Conville of the Geology Department for performing some gas and maceral composition analyses for the coals used.

Thanks are also due to the British Columbia Science Council for the Research Grant which provided the funds for the equipment and partial support and to the University of Petroleum and Minerals in Saudi Arabia which provided my scholarship.

I. INTRODUCTION

Solid fuels have inherent disadvantages for use in stationary and particularly in non-stationary applications, when compared to more convenient gaseous and liquid fuels. The atomic hydrogen to carbon ratio of coals of potential commercial interest for conversion lies typically between 0.6 to 1. This range is substantially less than the ratio for liquid and gaseous fuels which lie in the range 2 (gasoline) to 4 (methane). Therefore, the primary requirement of any coal conversion scheme is either to increase the hydrogen content or to reject carbon, thereby upgrading the hydrocarbon fraction. The latter effect can be accomplished directly by coal pyrolysis (also known as carbonization, thermal decomposition, or devolatilization) which involves heating coal in an inert atmosphere and which yields three classes of products, namely, gases, liquids, and solids (char). The nature and relative amounts of these products, though primarily dependent on the type of coal, is greatly influenced by temperature, heating rate, residence time, pressure, and gaseous environment. Reactor type, particle size, and hydrodynamic conditions are other factors which also affect the yield and quality of these products.

Pyrolysis of coal also occurs in coal gasification, direct liquefaction processes, and direct combustion. Therefore, understanding it is not only important for pyrolysis technology itself but provides a better understanding of these other coal utilization technologies.

In contrast to direct liquefaction of coal, pyrolysis processes require relatively simple equipment of low capital cost.

Depending on the process, pyrolysis may be operated at near atmospheric pressure. However, the yield of liquid per tonne of coal is lower than that achievable in direct hydroliquefaction processes, and the yield of solid char is much higher. This arises essentially because pyrolysis skims off volatile products from the coal while hydroliquefaction involves hydrogenation of various species in the coal. Thus for industrial application of pyrolysis an economical use must be found for the char which may represent at least 50 wt% of the original coal. Combustion in a utility plant or gasification to yield fuel gases are normally proposed.

Low temperature carbonization of coal with byproduct recovery of liquids and gases has been practised for many years. During the 1950's, efforts were directed toward production of char for fuel, and little attention was paid to maximization of liquid yield. Recently attention has shifted to rapid or flash pyrolysis in fluidized, entrained, or spouted bed reactors with the aim of maximizing liquid yields. Pyrolysis in spouted beds is rather a recent technique and there are few publications on it[1,2]. There are numerous articles and reviews on coal pyrolysis. The best single source is probably Elliot[3] (1981). Howard[4] (1981), Anthony and Howard[5] (1976), and Wen et al.[6] (1979) give critical reviews of experimental techniques, conditions, and kinetics of coal pyrolysis. Scott[7] (1982) presented a critical assessment of what is known and unknown in the field of pyrolysis with special reference to Canadian coals.

1.1 Objectives of this work

The objectives of this thesis were to test the feasibility of using a spouted bed for the pyrolysis of some Western Canadian coals and to determine the optimum yield of gases, liquid, and solid under different experimental conditions. Variables such as temperature, coal feed rate, particle size, vapor residence time, bed height, and gaseous medium were to be studied. The yield data was to be used to construct a mathematical model useful for design and scale-up purposes. This work was part of an over-all effort to develop a two-reactor spouted bed process in which the heat for pyrolysis is supplied by partial combustion of the product char.

2. BACKGROUND

2.1 The basic coal pyrolysis process

Coal pyrolysis involves heating coal in inert atmosphere to cause its decomposition; the primary coal pyrolysis process is simply a destructive distillation process.

Coal Particle $\xrightarrow{\text{Heating in inert atmosphere}}$ Primary volatiles + char (Tar, Carbon oxides, hydrocarbon gases and H_2O)

In practice, the primary volatiles undergo secondary reactions such as cracking or polymerization during diffusion through the internal pores of the char or contact with other char particles. These reactions occur because some of the volatiles evolve in the form of unstable radicals which are therefore susceptible to these secondary reactions given the right conditions of temperature and time.

Primary Volatiles $\xrightarrow{\text{Cracking or Polymerization}}$ Secondary volatiles + char (liquid + secondary tar, carbon oxides, hydrocarbon gases and hydrogen)

The secondary reactions mostly involve the tar and oils fractions which produce more gas and char fractions at the expense of tar. The secondary reactions are enhanced by high temperature, and the tar yield thus goes through a maximum with respect to temperature.

2.2 Coal composition and its relation to pyrolysis

2.2.1 Coal petrography

Coal is derived from plants over geological times. Coal petrography deals with the description of what is seen in coals by microscopic observation and relates the different constituents observed to plants and plant parts. The organic material in coal is a hetrogeneous mixture of "organic minerals" known as macerals. Maceral fractions are observable by microscopic examination of thin sections of coal with transmitted light (in which the different maceral types show up as various shades of reds, yellows, browns) or by examination of polished samples under reflected light (in which the macerals show up as black, white, or various shades of gray). There are numerous types of maceral components but for ease of discussion, they are often combined into three principal groups: Vitrinite, exinite, and inertinite. Exinite has the highest hydrogen content, volatile matter content, and heating value: inertinite has the least. Inertinite has the highest density and the greatest degree of aromaticity, whereas exinite is the lowest in both these properties. Thus vitrinite, by far the most abundant of the three maceral groups, usually exhibits chemical and physical properties between those of the other two. As might be expected from the order of volatile matter content, the total yield of volatiles is usually in the order exinite > vitrinite > inertinite. There are also compositional differences among the products. For example, exinite produces significantly more tar and more straight chain paraffins and olefins than vitrinite, whose products tend to be more

phenolic in nature. Thus petrographic analysis provides clues to the selection of good coals for pyrolysis processes. The rank and overall chemical composition of a coal are alone not sufficient, in general terms, to predict the pyrolysis behaviour of that coal.

2.2.2 Coal chemistry

The organic matter in coal is composed primarily of carbon, hydrogen, oxygen, nitrogen, and sulfur. Coals may be analyzed or characterized in a variety of ways. Proximate analysis determines the content of moisture, ash, volatile matter, and fixed carbon. Ultimate analysis measures the amount of the main chemical elements present. Along with heating value, these analyses help determine the rank of the coal as shown in Figure 1 and Table 1.

There have been substantial efforts to elucidate the molecular structure of coal, but the task is exceedingly difficult because of the variety of coal types, the heterogeneity of a single coal, and the complexity of individual coal constituents. Given[8] presented the hypothetical structure shown in Figure 2 as one possible arrangement of the atoms for bituminous coal vitrinite possessing 82% carbon. Although other structures have been proposed[9, 10], the Given model is generally accepted as a reasonable working structure and is suitable for this discussion of pyrolysis behaviour. A high degree of aromaticity is noted in this structure involving about two-thirds of the carbon and about 20% of the hydrogen. Condensed aromatic clusters, each comprised of one to three rings, are mostly linked in the Given model by aliphatic side chains such as methylene groups which are

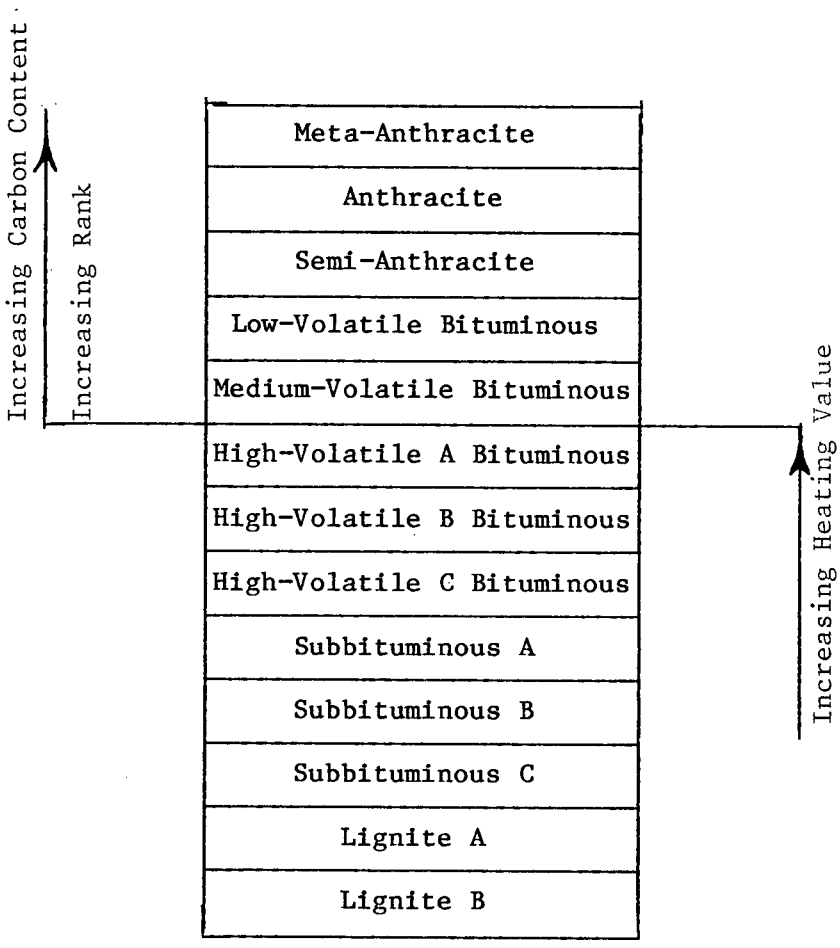

Figure 1: Classification of coals by rank (ASTM Method)

TABLE 1 Classification of Coals by Rank[A]

Class	Group	Fixed Carbon Limits, percent (Dry, Mineral-Matter-Free Basis)		Volatile Matter Limits, percent (Dry, Mineral-Matter-Free Basis)		Calorific Value Limits, Btu per pound (Moist,[B] Mineral-Matter-Free Basis)		Agglomerating Character
		Equal or Greater Than	Less Than	Greater Than	Equal or Less Than	Equal or Greater Than	Less Than	
I. Anthracitic	1. Meta-anthracite	98	...	...	2	...	...	nonagglomerating
	2. Anthracite	92	98	2	8	...	...	
	3. Semianthracite[C]	86	92	8	14	...	...	
II. Bituminous	1. Low volatile bituminous coal	78	86	14	22	...	...	commonly agglomerating[E]
	2. Medium volatile bituminous coal	69	78	22	31	...	...	
	3. High volatile *A* bituminous coal	...	69	31	...	14 000[D]	...	
	4. High volatile *B* bituminous coal	...	...	...	...	13 000[D]	14 000	
	5. High volatile *C* bituminous coal	...	...	...	...	11 500	13 000	
						10 500	11 500	agglomerating
III. Subbituminous	1. Subbituminous *A* coal	...	...	...	...	10 500	11 500	nonagglomerating
	2. Subbituminous *B* coal	...	...	...	...	9 500	10 500	
	3. Subbituminous *C* coal	...	...	...	...	8 300	9 500	
IV. Lignitic	1. Lignite *A*	...	...	...	...	6 300	8 300	
	2. Lignite *B*	...	...	...	...	...	6 300	

[A] This classification does not include a few coals, principally nonbanded varieties, which have unusual physical and chemical properties and which come within the limits of fixed carbon or calorific value of the high-volatile bituminous and subbituminous ranks. All of these coals either contain less than 48 % dry, mineral-matter-free fixed carbon or have more than 15 500 moist, mineral-matter-free British thermal units per pound.

[B] Moist refers to coal containing its natural inherent moisture but not including visible water on the surface of the coal.

[C] If agglomerating, classify in low-volatile group of the bituminous class.

[D] Coals having 69 % or more fixed carbon on the dry, mineral-matter-free basis shall be classified according to fixed carbon, regardless of calorific value.

[E] It is recognized that there may be nonagglomerating varieties in these groups of the bituminous class, and that there are notable exceptions in high volatile *C* bituminous group.

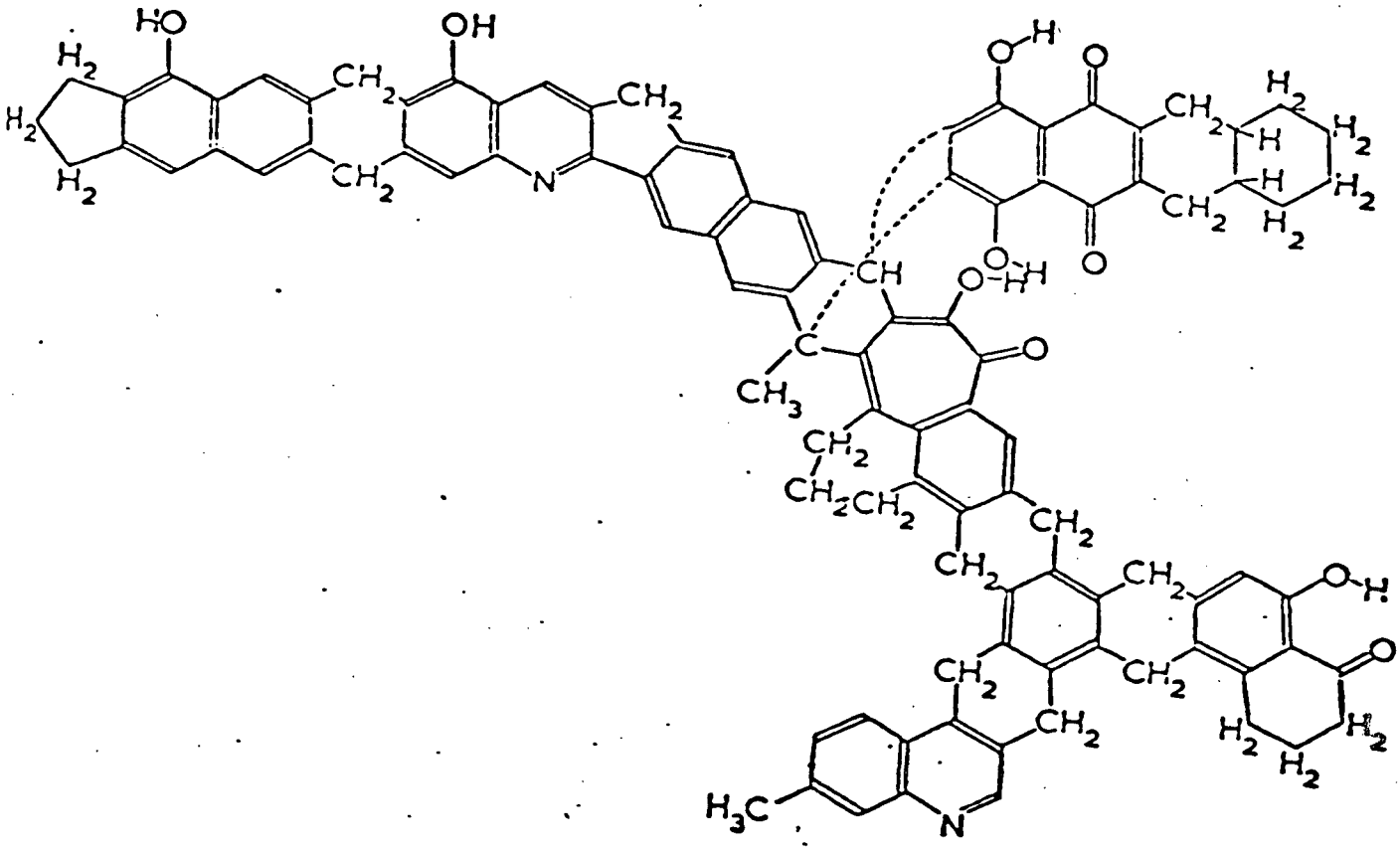

Figure 2. The Given[8] model for coal vitrinite structure.

distributed throughout the coal matrix. The nature of the linkages between clusters is a subject of considerable debate, for example see Dryden[9]. Oxygen appears predominantly in hydroxyl and carbonyl groups in all types of coal.[9] Carboxylic acid groups and ether linkages are common to lower rank coals only. The nitrogen in coal is shown in the Given model as a ring-substituted azine structure. Organic sulphur, although not shown, will also appear in heterocyclic aromatic rings as well as sulphide functional groups.

Given speculated that the course of pyrolysis anticipated from his model would consist of four steps: (i) a low-temperature (400-500°C) loss of hydroxyl groups, (ii) dehydrogenation of some of the hydroaromatic structures, (iii) scission of the molecule at the methylene bridges, and (iv) rupture of the alicyclic rings.

As there are many other models for coal chemical structure, consequently, other postulates on the course of pyrolysis such as the model of Wiser et al.[11] are available. In Table 2 Wen et al.[6] summarize the possible chemical reactions leading to various products during pyrolysis in an inert atmosphere, at conditions of moderate heating rates and temperatures, and at atmospheric pressure.

2.3 Physical factors affecting pyrolysis

2.3.1 Plastic behaviour of coals

On being heated through a certain temperature range, a plastic coal will first soften and become deformable and later resolidify to form a char. Plastic (caking) coals are also referred to as agglomerating coals under rapid heating conditions such as occur in

Table 2 - The Chemical Processes of Pyrolysis

Process	Source	Product
1. Distillation and Decomposition	Weakly bonded ring clusters	Tar and liquid
2. Decarboxylation	Carboxyl groups	CO_2
3. Decarbonylation	Carbonyl groups and ether linkages	CO (<500°C)
4. Ring rupture	Hetero-oxygens	CO (>500°C)
5. Dehydroxylation	Hydroxyl groups	H_2O
6. Dealkylation	Alkyl groups	$CH_4 + C_2H_6$
7. Ring rupture	Aromatic C-H bonds	H_2

fluidized or spouted beds. Caking type bituminous coals generally soften and become plastic when heated to about 350°C. In the plastic state, the coal particles stick to each other or to the bed material and this might lead to reactor plugging. Higher rank coals such as the anthracites and lower rank coals such as sub-bituminous coals and lignites do not become plastic when heated. One measure of the agglomerating tendency of a coal is the swelling index which is determined by a standard procedure and which is defined as the ratio of the coke to the coal volume, after heating to 1090K under nitrogen.

2.3.2 Transport processes in the reacting coal particle

The internal structure of pyrolyzing coal and that of the char product are important in the analysis of diffusional processes associated with pyrolysis reactions. The porosity of the fine structure of the char from virtually any coal increases steadily as the temperature of its formation is increased, but the accessibility of these pores to the volatiles increases with temperature up to 500-600°C, then decreases in the range 600-1000°C[12-14]. Thus, one possible explanation for the decrease in tar yield and increase in gas yield above temperatures of roughly 600°C is that the primary volatiles cannot readily escape through the pores before cracking. Accessible surface area follows a similar trend for non-agglomerating coals but is radically different for agglomerating coals, showing a sharp minimum extending over the plastic region of the coal.[15]

During the pyrolysis of plastic coals gas bubbles are formed within the fluid mass which repeatedly break through the particle

surface as pyrolysis continues.[16-17] The resulting char has a high large-scale porosity, presumably formed by entrapped gas bubbles. The growth and escape of gas-filled bubbles constitutes an important mode of volatiles transport in plastic coals. Thus when hydrodynamic and diffusional flows become greatly impeded by the essentially impenetrable pore structure developed during the period of plasticity, regions of high pressure gas form within the particle and expand against the viscous and other forces to produce growing gas bubbles that may eventually burst through the particle surface as small jets. The above noted decrease in the accessibility of the fine structure porosity of non-plastic coals also presumably leads to development of high pressure regions, but these coals cannot flow and allow the incipient bubble to expand. Hence the pressure is expected to rise until the rate of hydrodynamic flow matches the rate of volatiles generation or the particle decrepitates. Interest of some workers[18,19] in secondary reactions led to the development of bubble transport models for volatiles flow in plastic coals.

If the pyrolysis of coal particle were chemically controlled, the rate would be independent of particle size or structure, but, under a given set of conditions, heat and/or mass transfer will become limiting at some critical particle size, the identification of which requires information on the pertinent heat and mass transfer mechanisms as well as the particle residence time. For example, for the case of external heat transfer controlling, calculations by Badzioch[20] indicate that the transition from chemical to transport

processes control occurs at a particle diameter of approximately 100 μm. For systems like spouted or fluidized beds, the gas and bed to particle heat transfer coefficients can be high enough to produce significant temperature gradients within the particle, the relative magnitude and importance of this intraparticle temperature gradient is determined by the Biot number and is discussed in Section 2.5.

2.4 Effect of experimental conditions on pyrolysis

2.4.1 Effect of temperature

Temperature is the most important variable affecting the composition of pyrolysis products of a coal in a neutral atmosphere. The role of temperature includes two primary effects, one on the decomposition of the coal and the other on the secondary reactions of volatiles. The decomposition becomes apparent at 350-400°C and the products consist of a carbon rich residue (char) and a hydrogen rich volatile fraction. The decomposition continues until a temperature typically around 950°C is reached, which if maintained for an extended time results in a residue of nearly pure carbon, with a structure approaching that of graphite. In the absence of secondary reactions, the yield of a given volatile component increases monotonically with increasing temperature, hence with the extent of the decomposition reactions producing that component. In the presence of substantial secondary reactions, an increase in temperature will enhance the yield of some species and retard the yield of others, reflecting species production and consumption respectively, by the secondary reactions. The effects of temperature are clearly coupled with those of time, but

the latter plays a relatively secondary role if the rates are chemically controlled. The importance of time increases as heat or mass transfer limitations come into the picture. In general, rapid initial decomposition takes place, followed by very slow degasification of char. Pitt[21] noticed that in long holding time experiments with fluidized beds, decomposition of the coal took place at greatly varying rates. He therefore classified coal molecules into three divisions: (1) Those with a low activation energy for decomposition such that nearly complete decomposition takes place within one minute. (2) Those with intermediate activation energies such that most of the decomposition takes place between 1 to 100 minutes. (3) Those with sufficiently high activation energies to prevent any appreciable release of volatiles within 100 minutes.

Pitt also noticed that the fraction of coal molecules residing in each of the three divisions changed as the holding temperature in the bed was changed.

Table 3 shows the suggested temperature, heating rate, and residence time to be used for a desired volatile product.[6]

2.4.2 Effect of heating rate

Recent rapid heating techniques give substantially larger yields of volatiles than are obtained by the slow heating of coal in conventional packed-bed carbonization retorts. However, there apparently is some confusion and controversy whether this increase in volatile yield is due to the effect of the heating rate itself or to the avoidance of secondary reactions such as cracking or deposition. The

Table 3 - Programmed Temperature Pyrolysis

	Desired Volatile Product	Heating Rate	Temp. of Carbonization	Solid Residence Time	Volatile Residence Time
1.	Tar	Rapid	Low (~500°C)	Long	Short
2.	Liquid	Rapid	Intermediate (~750°C)	Long	Long
3.	Gas	Rapid	High (>1000°C)	Long	-[2]
4.	CH_4	Rapid	~600°C	Long	-
5.	H_2	Rapid	1000-1100°C	Long	-
6.	C_2H_2 and unsaturates	Flash	>1200°c	Long	Intermediate
7.	CO	-	Intermediate (~750°C)	Long	-

[2]The effect is either uncertain or insignificant

techniques used to achieve the rapid heating rates, such as the use of small particles and or reactor types such as fluidized beds generally tend to avoid long times at high temperature and volatile/char contact which promote secondary reactions. Howard[4] contends that the volatile yield increase probably results primarily from the associated experimental conditions employed to achieve the faster heating. To test the above argument, Anthony et al.[22] varied only the heating rate in the range 650-10,000°C/s, while holding all other variables constant in a pyrolysis experiment on both a caking and a noncaking coal. The yield of volatiles did not change significantly, thereby indicating that heating rate per se is not important with respect to volatiles yield under the conditions studied. Nevertheless, the net result of pyrolysis in reactors associated with rapid heating rates remains a higher yield of volatiles.

2.4.3 Effect of pressure

The pressure effect on pyrolysis yield is related to the enhancement or retardation of the secondary reactions of the primary volatiles. These reactions may convert some of the tars to both lighter and heavier species. At lower pressure these reactions are less favoured since there is a smaller resistance to volatiles flow out of the coal particle. Hence the tar yield increases with pressure decrease.

The majority of new pyrolysis processes are aimed at maximizing liquid yield, and hence, are operated at atmospheric pressure. There are relatively few experimental studies of the effect of pressure on pyrolysis. Anthony et al.[22] determined the weight

loss from Pittsburgh seam coal heated at different rates to 1000°C at pressures from 0.001 to 100 atm. They found that the weight loss decreased monotonically to an asymptotic value with increasing pressure, presumbably reflecting an increasing extent of cracking and carbon deposition within the particles. The weight loss also reached an asymptotic value at the lower pressure extreme. The pressure inside the particles during devolatilization probably becomes independent of the external pressure as the latter is reduced below a certain value, hence the low pressure asymptote. The approach to a limiting yield at high pressures probably reflects the depletion of species that are susceptible to the secondary reactions. Accordingly, the weight loss achieved at the high pressure extreme is the yield of nonreactive volatiles, and the additional weight loss available by reducing the pressure to vacuum represents reactive volatiles.

The main conclusion drawn from the literature about the effect of pressure on pyrolysis product distribution is that pyrolysis under high pressures produces more char, less tar, more methane, less hydrogen, and more carbon oxides.

2.4.4 Effect of particle size

The effect of particle size on the volatile yield is attributed to two main factors, namely, the extent of secondary reactions, and the rate of heat transfer to the particle. The minimum residence time to heat up the particle to the desired temperature and establish a uniform temperature throughout the particle depends on particle size, experimental conditions, reactor type, and mode of heat

transfer. At residence times greater than this minimum time for heat up, the importance of heat transfer is diminished.

In general, an increase in particle size results in a decrease in total volatile yield. As particle sizes increase, there is more resistance to the escape of volatiles, and the secondary reactions are enhanced. Tar yield decreases and yields of methane and oxides of carbon both increase.

2.4.5 Effect of coal type

The chemical and physical nature of coal has a profound effect upon its behaviour during pyrolysis. It has long been recognized that coals of different rank give markedly different products. Upon pyrolysis, lignites give fairly high yields of volatiles, but not much tar, and the chars do not agglomerate strongly. Bituminous coals can also give a high yield of volatiles, but a large fraction can be in the form of tar. Bituminous chars are also frequently swollen and/or strongly agglomerated. Anthracites give low volatile yields and do not agglomerate. The oxygen content of the coal decreases with increasing rank, as does the yield of oxygen as water plus oxides of carbon. Although the hydrogen content of the coal decreases slightly with increasing rank, the tendency to form water in the low rank coals results in the yield of hydrogen gas increasing significantly with increasing rank. The yield of methane goes through a maximum at intermediate ranks.

One of the most important differences in the weight loss behaviour of different coals is the potential for volatile yields to

exceed the proximate volatile matter content when conditions are employed that avoid extensive tar cracking and carbon deposition on particles. This potential is small to negligible for both low and high rank coals and significant for coals in the bituminous range. Badzioch and Hawksley[23] give the following empirical formula to estimate the ultimate yield of volatiles V*:

$$V^* = Q\ (1-VM_c)\ VM$$

Experimental values of Q varied from 1.3 to 1.8 depending on coal type.

2.5 Pyrolysis and heat transfer in a spouted bed

A schematic diagram of the spouted bed is shown in Figure 3. The main features which distinguish the spouted bed from the fluidized bed are the absence of the grid (distributor) and the single gas entry point to the bed which give the former a unique hydrodynamic character. A comparison between fluid-solid contacting systems given in Table 4,[24] shows the key features of spouted beds versus other reactors.

One of the main advantages of the spouted bed is its ability to handle relatively large particle size (> 1 mm) which may be too large for stable fluidized bed operations in the bubbling bed mode. It is this property that led to the development of the spouted bed in the 1950's in Canada[25] to dry wheat with air prior to storage. For details on spouted beds, the reader is referred to the book by Mathur and Epstein.[26]

One of the major problems associated with pyrolysis is the tendency for the char particles to agglomerate. Spouted beds might be

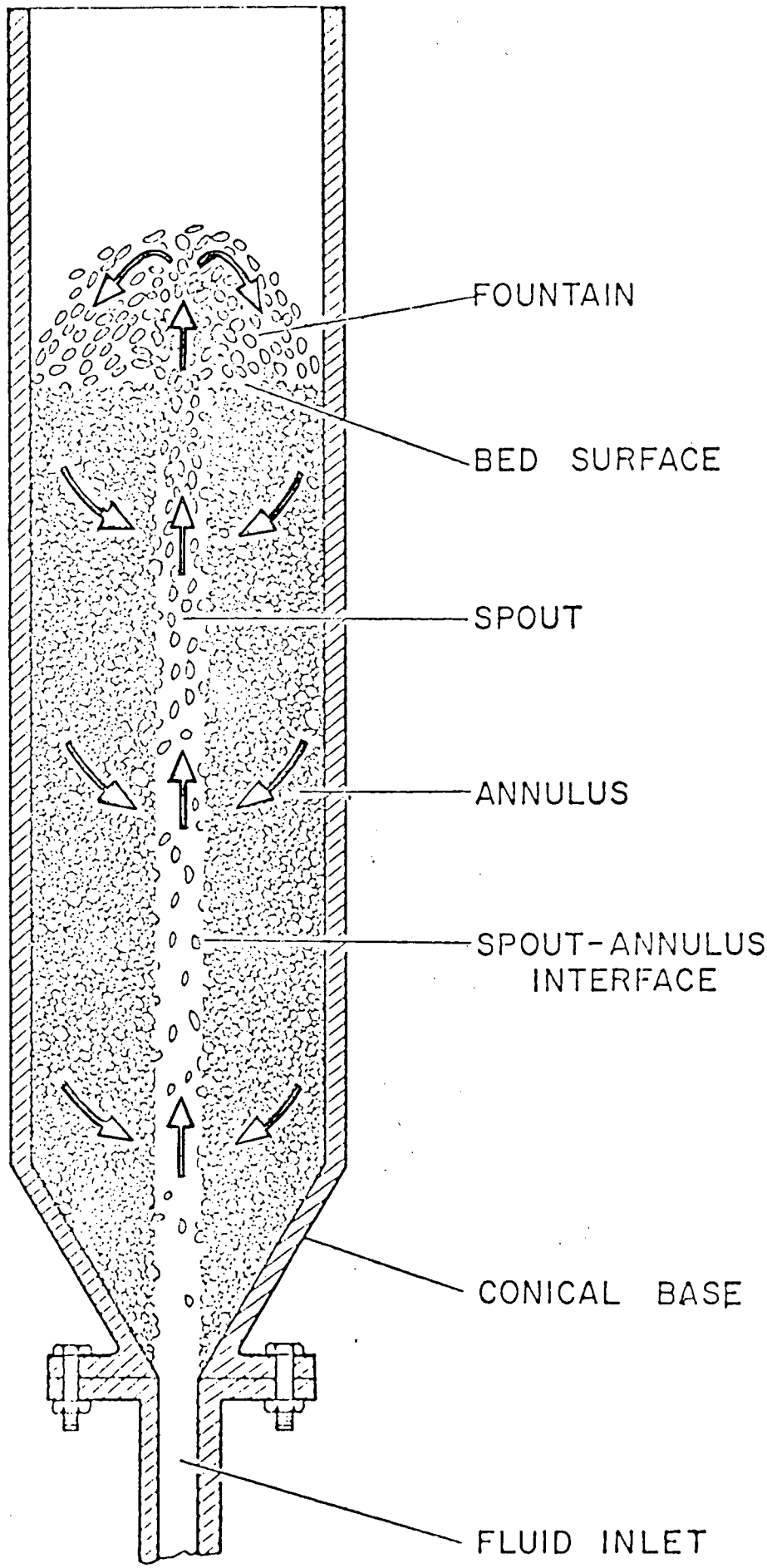

Figure 3. Schematic diagram of a spouted bed.

Table 4 - Principal Gas-Solid Contactors: Operating ranges and key advantages/disadvantages*

	Moving Bed	Fluidized Bed	Entrained Flow	Spouted Bed
Particle size	0.6-300 mm	30 μm-3 mm	< 100 μm	0.8 to 6 mm
Gas motion	up	up	up	up
Sup. Gas Vel.	<0.3 m/s	0.5-3 m/s	20-25 m/s	1-2 m/s
Gas mixing	≈ plug flow	two phases, one with considerable backmixing	≈ plug flow	two regions
Solids motion	down slowly	up and down	up	circulation up & down
Solids mixing	≈ plug flow	≈ perfect mixing (most cases)	≈plug flow	≈ perfect mixing (most cases)
Overall voidage	0.4 to 0.5	0.5 to 0.7	0.95-0.998	0.45-0.55
Attrition/Erosion	very little	some	serious	considerable attrition
Agglomeration	serious problem	may be a problem	no problem	little problem
Max. vessel dia.	4-5 m	perhaps 20 m	≈ 4 m	?
Temperature Profile	substantial gradients, gives different zones	essentially isothermal	some gradients	some gradients, esp. below spout and annulus
Key advantages	- near plug flow of gas and solids - different temperature and reaction zones	- temperature uniformity - favourable heat transfer - solids handling	- near plug flow of gas and solids	- handles large and agglomerating solids - characterization easier
Key disadvantages	- can't handle small particles - poor heat transfer - temperature control tricky - solids feed distribution	- substantial gas and solids backmixing - bypassing of gas (bubbles) - carryover of particles - scale-up difficult - attrition, erosion, agglomeration	- small residence time - attrition - need for particle capture	- limitations on d_p distribution - attrition - solids backmixing - not clear how spouted beds can be scaled up

*From reference No. (24).

more suitable than fluidized beds for pyrolysing agglomerating coals, for the following reasons: (i) The agglomeration tendency of particles decreases with increasing particle size, and larger particle sizes can be handled by spouted beds. (ii) The violent agitation in the spout region would tend to destroy any agglomerates formed in the annular region of the bed. (iii) The absence of the grid removes one possible horizontal surface on which agglomerating particles might stick.

On the other hand the volatile yield penalty associated with larger particles represents a potential disadvantage of the spouted bed system.

In a spouted bed, since the solid particles are well mixed, their average temperature in different parts of the bed would be substantially the same. Barton and Ratcliffe[27] measured the heating rate of coal particles in the annulus of a spouted bed. They found that the heat transfer coefficient increased with decreasing particle size. They also found that there was little variation in heat transfer coefficient from point to point within the bed at the same temperature. Their results were found to be about 50% higher than the heat transfer coefficient calculated from packed bed correlations.

For estimating the heat transfer coefficient in the spout, the following equation can be used:[26]

$$Nu = A + BPr^{1/3} Re^{0.55} \qquad - (1)$$

where $A = 2/[1-(1-\varepsilon)^{1/3}]$ and $B = \frac{2}{3}\varepsilon$

For the annulus region, the following packed bed correlation can be

used, although the values obtained may be somewhat low.[26]

$$Nu = 0.42 + 0.35\ Re^{0.8} \qquad - (2)$$

Calculations using equation (1) to estimate the heat transfer coefficient in the spout for typical pyrolyzing conditions showed it to be about three times higher than that in the annulus for the same particle size, but, the time which a particle spends in the spout is very small compared to that in the annulus. Therefore, the total heat transferred in the spout will be less than that in the annulus. Heat transfer from fluid to particles can either be controlled by: (i) External heat transfer: Here the resistance to heat transfer lies primarily between the coal particle and its surroundings, and the temperature within the particle may be assumed uniform. The time required to bring a feed particle at T_{po} close to the bulk solids temperature T_b is given by the following unsteady state equation:

$$\frac{T_p - T_{po}}{T_b - T_{po}} = 1 - \exp\left[\frac{-h_p A_p t}{m_p c_p}\right] \qquad - (3)$$

From this equation, the time required to heat up a 2 mm diameter coal particle from room temperature to about 99% of bed temperature (500°C) was estimated to be of the order of a few seconds. Since the practical mean residence time in the annulus is at least several minutes, the steady state concentration of bed particles having a temperature significantly below the bulk bed temperature would be small. Therefore,

the overall heat transfer rate would not normally be limited by this step of the process. (ii) Internal heat transfer: Intraparticle temperture gradients are usually ignored in fluidization because of the smaller particle size used, but with the larger size of particles commonly used in spouting, considerable internal gradients can build up within particles in certain parts of the bed. The magnitude of the intraparticle temperature differences relative to the temperature differences between the particle surface and fluid is uniquely determined by the Biot number, $Bi_H = h_p r_p / K_p$, provided that the Fourier number $Fo_H = \alpha t / r_p^2$, which is the dimensionless time variable, exceeds a minimum value of 0.2. The relative magnitude of intraparticle temperature difference decreases with decreasing Bi_H, the maximum value becoming less than 5% of the temperature difference between fluid and particle surface at $Bi_H = 0.1$.

For the present case, with coals of average particle size of 2.3 mm, and estimated thermal conductivity[28] of coal 0.069 W/mK, $h_p = 148$ W/m^{2}K[28] and the Biot number was found to be 2.46 which indicates that conditions for the development of internal temperature gradients within a particle exist. The effect of this on the pyrolysis process will depend on the particle residence time as discussed below.

Newman[29] showed that the time taken for the difference between the surface and the average particle temperature, $\overline{T}$, to attain a value which is some fraction of the difference between the initial

uniform particle temperature, T_o, and the surface temperature T_s may be found from the equation:

$$\frac{\overline{T} - T_s}{T_o - T_s} = \frac{6}{\pi^2} \sum_{n=1}^{\infty} \frac{1}{n^2} \exp\left(\frac{-\alpha t}{r_p^2}\right) n^2 \pi^2$$

Hence the time taken for the difference between the surface and the average particle temperature to be, say, only 1% of the initial difference, $T_o - T_s$, is found by solution of this equation for the Fourier modulus $\alpha t/r_p^2$ equal to 0.43. Hence for an assumed value of 1.858×10^{-4} m^2/h for the thermal diffusivity of coal, the time taken for the above event for a 2.3 mm coal particle was calculated to be 11 sec. Since the residence time in a spouted bed is normally at least several minutes, the assumption of isothermality in the treatment of kinetic data is justified.

3. LITERATURE REVIEW

3.1 Experimental

A detailed literature survey will not be attempted here. Instead, a brief review is given below with the emphasis on recent work, and on Canadian coals.

The experimental techniques are grouped into two general classes:

(i) Captive sample technique: This usally involves small samples in a crucible or on an electrically heated grid. The small scale makes it easier to operate, collect, and analyse the products. The most notable example of the crucible technique is the ASTM standard proximate analysis of coal. Crucible heating is usually at a slow rate, while the electrically heated grid provides fast heating. The latter has been used at M.I.T. over the past several years.[22, 30] Stangeby et al.[31] used the electrically heated grid technique to study the effect of heating rate on the pyrolysis of some Canadian coals. They found that heating rate has little effect on total weight loss of the coal, but a dramatic effect on the actual composition of products. High heating rates substantially increased the yield of light hydrocarbons. Furimsky et al.[32] used a modified Fischer assay retort to pyrolyse thirteen Canadian coals of different rank. They charged 70 g of coal in a retort which is weighed before and after each experiment. The retort was then heated slowly to 535°C and held at this temperature for 15 minutes; the heating was then discontinued. The difference in total weight was assumed to be equal to the yield of volatiles. They

correlated the volatiles yield with the H/C ratios and volatile matter contents of the coal. Linear correlations were observed for all bituminous coals; lignites and subbituminous coals produced low yields of liquid hydrocarbons. They explained this deviation in terms of the presence of O-containing functional groups.

(ii) Coal flow techniques: These methods are used to rapidly heat coal and usually approximate real process conditions more closely than the captive sample technique. This technique includes pyrolysis in fluidized beds and spouted beds.

A considerable amount of work has been done at the C.S.I.R.O. of Austrailia over the last five years on pyrolysis of Australian coals in fluidized beds. Tyler[33] pyrolyzed Loy Yang brown coal (< 0.2 mm) using a 3 cm diameter fluidized bed with a feed rate of 1 - 3 g/h. He obtained a maximum tar yield of 23% w/w of MAF* coal. In a subsequent study Tyler[34] pyrolysed ten bituminous coals in the reactor described above and found that the maximum tar yield is directly proportional to the coal atomic H/C ratio. He obtained a maximum tar yield of 32% at 600°C from Millmerran coal which has a H/C atomic ratio of 1.13. Edwards et al.[35] pyrolysed the same above mentioned two coals in a fluidized bed reactor with a nominal throughput of 20 kg/h and obtained a maximum tar yield of 23% at 580°C from Loy Yang brown coal and 35% at 600°C from Millmerran bituminous coal. Edwards et al.[36] compared the performances of the above mentioned two reactors and reported good agreement between them. Scott et al.[37] used a small bench scale fluidized bed reactor with a

---

*MAF = Moisture-ash free

continuous feed rate of 15 -30 g/h to pyrolyse some Canadian coals and to determine conditions for maximum liquid yield. They obtained a maximum liquid yield of 10% at 650°C and 19.6% at 750°C from Alberta subbituminous and bituminous coals respectively.

Pioneering work on coal carbonization in spouted beds was started in Australia[1,2] to test the feasibility of a continuous spouted bed reactor to handle agglomerating coals. These coals were treated successfully in the spouted bed reactor. Further studies by Ratcliffe et al.[38], Barton et al.[27], and Quinlan et al.[28] were aimed at developing a model to predict the volatile matter content of the exit char and to experimentally determine the heat transfer coefficient between coal particles and spouting gas. Tar yield was not determined quantitatively in the above studies. Ray et al.[39] studied the pyrolysis kinetics of some Indian coals in a batch spouted bed using fractional changes in the volatile matter of char as the kinetic parameter. They did not measure the yield of tar or other volatiles.

3.2 Mathematical model for coal pyrolysis

Pyrolysis of coal which occurs in nearly all coal conversion processes, is perhaps the most difficult to model mathematically. Howard[4], and Wen et al.[6] give comprehensive reviews of the various attempts to construct a mathematical model for coal pyrolysis. Attempts ranged from simple reaction models in which coal pyrolysis is considered to be a single first order reaction to models based on complex reaction schemes where pyrolysis is assumed to consist of a

large number of independent chemical reactions. Models which account for mass and heat transfer effects are also available. Table 5 summarizes some of the coal pyrolysis models.

The primary reactions in pyrolysis are generally considered to be simple organic decomposition processes, first order with respect to the decomposing component. Thus for the simplest form treating pyrolysis as a single reaction, the rate of pyrolysis is expressed as:

$$\frac{dV}{dt} = k(V^* - V) \qquad - (3.1)$$

where V is the quantity of volatiles evolved from the particle in weight percent of original coal, V* is that quantity of volatiles evolved after an infinite length of time, and k is the rate constant for the reaction. The ultimate yield V* should not be confused with the proximate volatile matter. Values of V* that are both higher[22] and lower[30] than proximate volatile matter have been reported for different sets of experimental conditions.

The rate constant in equation (3.1) is given by an Arrhenius expression:

$$k = k_o e^{-E/RT} \qquad - (3.2)$$

where k_o is the frequency factor, E is the activation energy, R is the gas constant, and T is the absolute temperature. Table 6 lists some experimental values of k_o and E and Figure 4 shows more of these values from the literature. There is little agreement on the observed rates of pyrolysis and activation energies range from 7 to 95 kcal/g-mole.

Differences in coal type, experimental equipment, and procedures contribute to this disagreement. Equation (1) in Table 5 is the same as equation (3.1) but with a different notation. It was applied by Dutta et al.[40] to the analysis of coal pyrolysis in a thermobalance. Their study showed that coal pyrolysis can be represented approximately by a single Arrhenius type equation. Ramakrishnan[41] used this equation to fit his data on the pyrolysis of some Indian coals in a fluidized bed reactor. He obtained a good fit.

Many authors have contended that a simple first order model is inadequate because it yields low k_o and E values for organic decomposition reactions which cannot be solely attributed to heat and mass transfer limitations. For the non-isothermal case, an energy balance would give the particle temperature as T = f(t). In this case the energy balance will have to be simultaneously solved with equation (3.1) to calculate the volatiles yield. Wen et al.[42] have given a treatment of this sort. However, they considered the heat of pyrolysis to be rather small, about 166.5 kcal/kg of coal and thus they ignored it in their overall heat balance. In a more recent paper Wen et al.[43] include the effects of mass transfer and secondary reactions to develop a coal pyrolysis model.

Pitt[21] proposed that pyrolysis be considered as a large number of independent chemical reactions involving the original coal molecule. Hence, for volatile component i, equation (3.1) becomes:

$$\frac{dVi}{dt} = k_i \, (V_i^* - V_i)$$

$$\text{and } k_i = k_{oi}^{-Ei/RT}$$

Depending on the bond strength, the rupture of different covalent bonds of coal molecules take place at different temperatures with different rates. Assuming that k_i's differ only in activation energy, Pitt suggested the use of a distribution function of activation energy, it is thus necessary to know one more kinetic parameter, the standard deviation σ, for the activation energy distribution function. Following the idea of Pitt, Anthony and Howard[5] proposed equation 3 in Table 5 to represent the rate of coal pyrolysis at any gas pressure in an inert atmosphere. Chang et al.[44] developed a coal pyrolysis model to predict tar, total gas as well as individual gas yields. Their model takes into account the effect of secondary cracking reactions as follows:

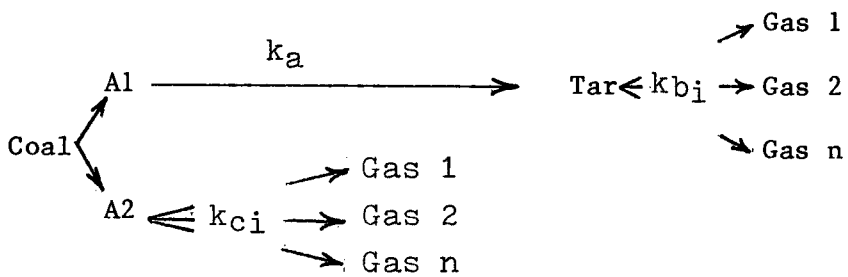

where A1 and A2 represent two major reactive portions in coal. Pyrolysis of A1 produces primary tar which subsequently cracks into smaller gaseous molecules until quenched. The tar is considered as a single species which cracks into different gases. The other portion of coal, A2, is pyrolyzed directly into gaseous molecules. They used first order kinetics. The details of the derivation of their model are given in the reference above, and the integrated final equations are presented as equation 4 in Table 5. Whereas equation 4 gives the breakdown between tar and gas, it should be noted that the models described by

equations 1-3 in Table 5 predict the total volatiles yield only. Kayihan and Reklaltis[45] derived a model for staged fluidized bed coal pyrolysis assuming first order kinetics and using the solid residence time function of a CSTR. Although their model was specifically developed for the COED* reactor concept, the general approach is applicable to any coal conversion process involving recycle of partially reacted chars. For the spouted bed reactor, Quinlan et al.[28] developed equation (5) in Table 5 to predict the volatile matter content of the char. They used a rate equation:

$$-\frac{dVM}{dt} = kVM^n$$

where VM is the volatile matter content of the char at any time t and n is the order of the reaction. They used batch data under simulated spouted bed conditions to obtain k and n. The exponent n was reported to be 17.2. For the distribution of particle residence times, they assumed an ideal backmix reactor.[46] They tested their model on six Australian coals and obtained satisfactory results. Ray et al.[39] studied the pyrolysis kinetics of some Indian coals in a batch spouted bed reactor. They could not fit their data by a single kinetic equation with respect to time. Below 400°C, the process obeyed a first order equation for the initial period followed by a zeroeth order equation at later times. At higher temperatures, the data fitted a second order equation followed by a first order one. This result illustrates the difficulties in interpreting complex pyrolysis phenomena.

---

*COED = Char - Oil - Energy - Development Project

Table 5 - Some Correlations for Coal Pyrolysis

Author	Correlation	Equation No.	Remarks
Wen et al.[42]	$\frac{dx}{dt} = k_0 e^{-E/RT} (f-x)$	(1)	Here f is the final conversion, and x is the conversion at any time t.
Badzioch & Hawksley[23]	$V = Q-VM(1-D)[1-\exp(-Ae^{-B/T_t})]$	(2)	By far the best available useful correlation applicable to bituminous coals with carbon contents of 79-92%. See original paper for correlation for the constants.
Anthony and Howard[5]	$V = V^*[1-\int_0^{\alpha} \exp(-\int_0^t k dt) f(E) dE]$	(3)	The only model that includes the pressure effect on pyrolysis in inert atmosphere, but requires that seven parameters be determined for each coal.
	where $k = k_0 e^{-E/RT}$		
	$V^* = V_{nr}^* + V_r^{**}/(1 + k_c p)$		
	$f(E) = [\sigma(2\pi)^{1/2}]^{-1} e^{-(E-E_0)^2/2\sigma^2}$		
Chang et al.[44]	$[Tar] = \frac{Aok_a}{k_b-k_a} (e^{-k_a t} - e^{-k_b t})$	(4)	This predicts tar yield, total gas yield as well as individual gas yield.
	$[Gas] = A_0\{1- \frac{k_a e^{-k_a t} - k_b e^{-k_a t}}{k_b - k_a} + G(1-e^{-k_c t})\}$		

Table 5 continued...

Author	Correlation	Equation No.	Remarks
	$[\text{Gas i}] = A_0\{\frac{k_{bi}}{k_b}(1-\frac{k_a e^{-k_b t} - k_a e^{-k_a t}}{k_b - k_a}) + \frac{Gk_{ci}}{k_c}(1-e^{-k_c t})\}$		
Quinlan et al.[28]	$\frac{\overline{VM}}{VM_0} = 1.05\ (\overline{At})^{-0.06175}$ Where $A = (n-1)\ kVM_0^{n-1}$ $\quad n \neq 1$	(5)	This predicts the volatile matter of char at any time

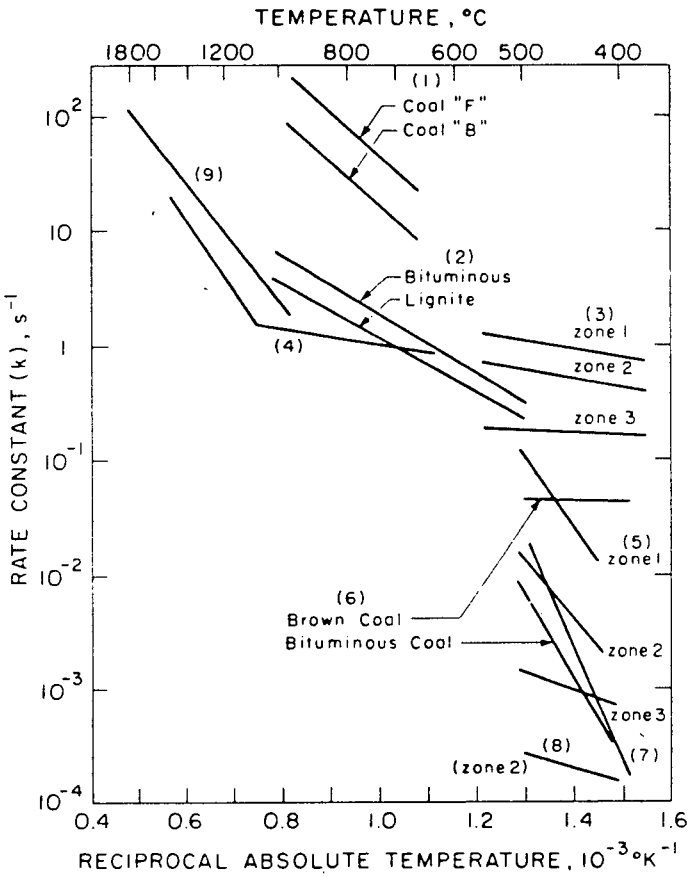

Figure 4. Comparison of simple first order pyrolysis rate constants from different investigators.*

(1) Badzioch and Hawksley[23], (2) Anthony et al.[22], (3) Shapatina et al.[47], (4) Howard and Essenhigh[48], (5) Stone et al.[49], (6) Van Krevelen et al.[50], (7) Boyer[51], (8) Wiser et al.[11], (9) Kobayashi et al.[52].

* From reference No. 4

Table 6 - Pyrolysis Rate Parameters

Investigators	Coal	VM (MAF)	E $\frac{kcal}{mole}$	k_o s^{-1}
Dutta et al.[40]			7	0.35
Badzioch & Hawksley[23]	B NBC 902	36.4	17.8	1.14×10^5
Anthony et al.[22]	Pittsburgh Seam Bituminous	46.2	11.8	706
	Montana lignite	46.2	11.3	282
Ramakrishnan[44]	Talcher Subbituminous	43.8	3.577	0.027
Quinlan et al.[38]	Liddel		95.4	0.83

3.3 Commerical and pilot scale pyrolysis processes:

An evaluation of coal pyrolysis processes is given by Holmes et al.[53] A more detailed description of these processes is given by Nowacki,[54] including the history of the process, recent developments and status. A summary of these processes is given in Table 7.

Table 7 - Pyrolysis and Hydropyrolysis Processes

Process	Coalcon		Clean Coke	Garrett	COED	C.S.I.R.O.	Lurgi-Ruhrgas	Consol
Coal	Lake de Smet		Illinois No. 6	Western Kentucky	Illinois No. 6	Wallarah, Australia	Leopold, Germany	Pitt Seam
Temp., °C	566	560	449-760	579	288-816	460	590	496
Pressure, Psi	1000	2000	80-150	14.7	6-10	300-600	14.7	10
Solids holdup time	8 min.	20 min.	50 min.	2 sec.	1-4 hr.	37 min.	2 sec.	45-120 min.
Yield, %	(a)	(b)						
Char	38.4	43.0	66.4	58.7	60.7	59.0	64.9	c
Liquid	29.0	21.3	13.9	33.0	20.1	6.6	23.4	26.0
Water	19.2	11.4	5.1	1.7	5.7	16.1	6.3	c
Gas	16.2	26.5	14.6	6.6	15.1	18.2	5.4	c
Liquid Yield as percentage of Fischer Assay	187	137	86	202	125	104	180	177
Current Status (ton/day of coal feed)	20 ton/day pilot plant operated. 2600 ton/day demo plant under design.		1/4-1/2 TPD pilot plant operational. 100 TPD demo plant under design.	4 tPD pilot plant operational.	36 ton/day pilot plant operated.	1/2 ton/day pilot plant operated.	1764 ton/day commercial plant. Operational	1.5 ton/day pilot plant operated.

a. Based upon laboratory-scale equipment. b. Based upon 20 ton/day pilot plant. c. Not available.

4. EXPERIMENTAL APPARATUS AND PROCEDURES

To carry out the objectives for the work outlined in Section 1.1, it was decided to construct a bench scale continuous feed spouted bed coal pyrolyser.

4.1 Apparatus

A schematic diagram of the experimental apparatus is shown in Figure 5. Design characteristics of the major units are listed in Table 8. A photograph of the overall apparatus is shown in Figure 6. More details on some of the units are given below:

4.1.1 Spouted bed reactor

The spouted bed pyrolyser was made of 316 stainless steel. It consisted of a main cylindrical section of 128 mm I.D. (Nominal diameter 5", schedule No. 40) by 762 mm long with a wall thickness of 6.6 mm. The main section was equipped with three Chromel - Alumel thermocouples located at 19, 38, and 57 cm above the cone outlet respectively. The main section was also surrounded by electrical heaters. A 70° cone with a wall thickness of 6.6 mm was flanged to the the bottom of the cylindrical section. This cone was equipped with a Chromel - Alumel thermocouple and a pressure gauge. A disengagement chamber of 254 mm I.D. and 6.6 mm wall thickness was welded to the top of the main section. It was also equipped with a Chromel - Alumel thermocouple and a pressure gauge. The inlet pipe to the reactor flanged to the bottom of the cone, was 15.8 mm in I.D. by 178 mm long and 2.8 mm wall thickness. This length was used as a calming section for the spouting gas. The inlet pipe protruded 3.2 mm inside the cone

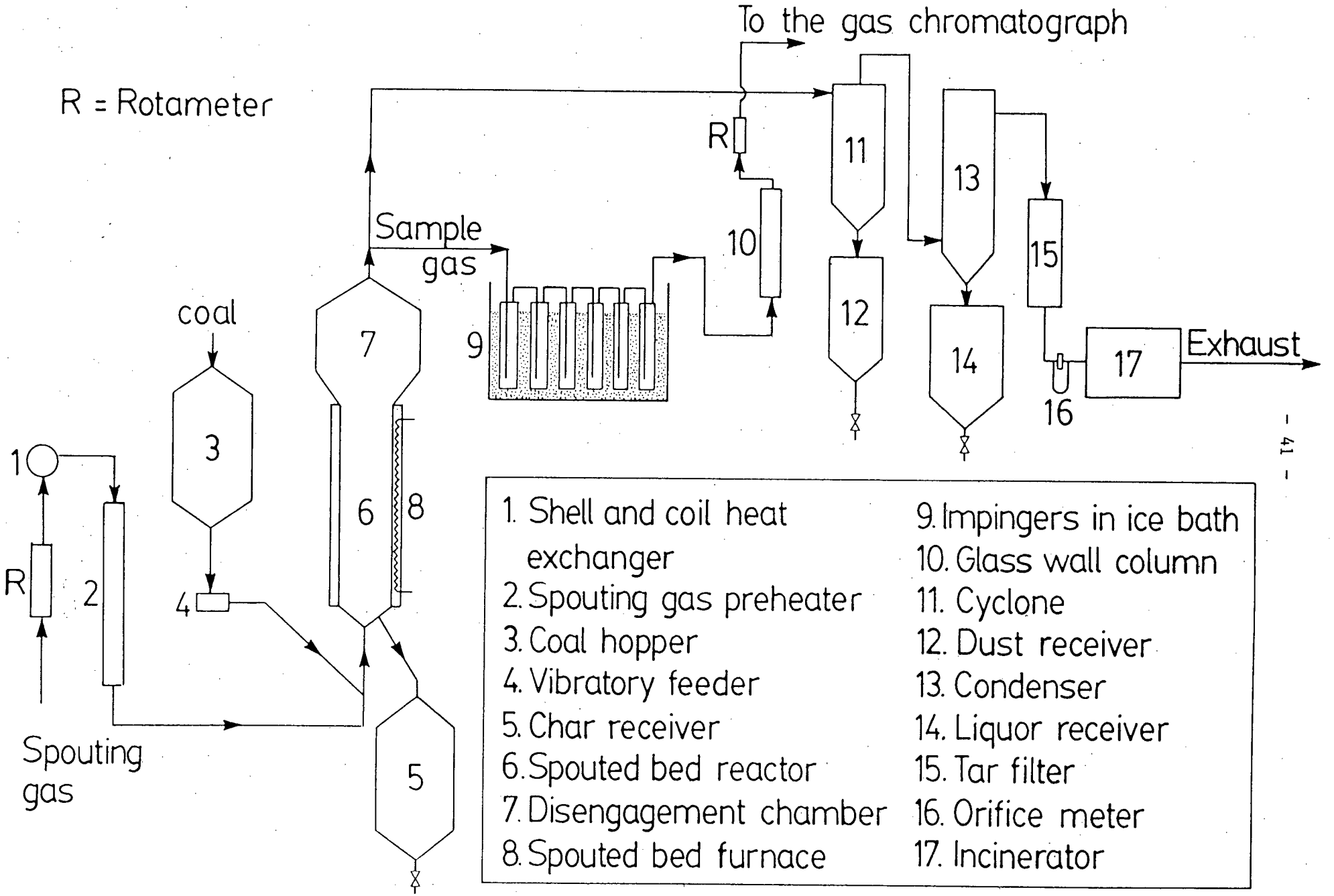

Figure 5. Schematic diagram of spouted bed pyrolysis apparatus.

Table 8 - Design Characteristics of Spouted Bed Pyrolyzer System

Reactor:	Material - 317 Stainless Steel Inside diameter - 128 mm Wall Thickness - 6.6 mm Cone Angle - 70° Disengaging section diameter - 255 mm Height (includes cone and disengagement section) - 1.22 m
Char Receiver:	Material - Mild steel Outside Diameter - 305 mm Height - 0.91 m
Coal Feed Hopper:	Material - Mild steel Outside Diameter - 305 mm Height - 0.84 m
Spouted Bed Furnace:	Electrical Rating - 9.2 kW Maximum Temperature - 1200°C Heaters: 16 1/4-Round - 152 mm high x 178 mm I.D. Heated Length - 0.61 m
Spouted Gas Preheater:	Electrical Rating - 3.94 kW Maximum Temperature - 1200°C Heaters: 4 semi-cylindrical 305 and 610 mm x 44 mm I.D. Heated Length - 0.914 m
Coal Feeder:	Syntron Tubular
Gas-Solid Cyclone:	Material - Stainless Steel Diameter - 150 mm Cylinder Height - 500 mm Cone Height 300 mm
Condenser:	Shell 316 Stainless steel Inside Diameter - 128 mm Wall Thickness - 6.6 mm Tubes 6 U-tubes .86 m long Diameter 12.7 mm Area ≈ 4130 cm^2
Tar Receiver:	Material - Glass and stainless steel Inside Diameter - 22.9 cm Height 30.5 cm
Tar Filter:	102 x 305 mm QVF glass column
Orifice Plate:	Material - Stainless steel Diameter of Orifice - 19.1 mm
Piping:	316 Stainless steel Nominal Diameter 50.8 mm

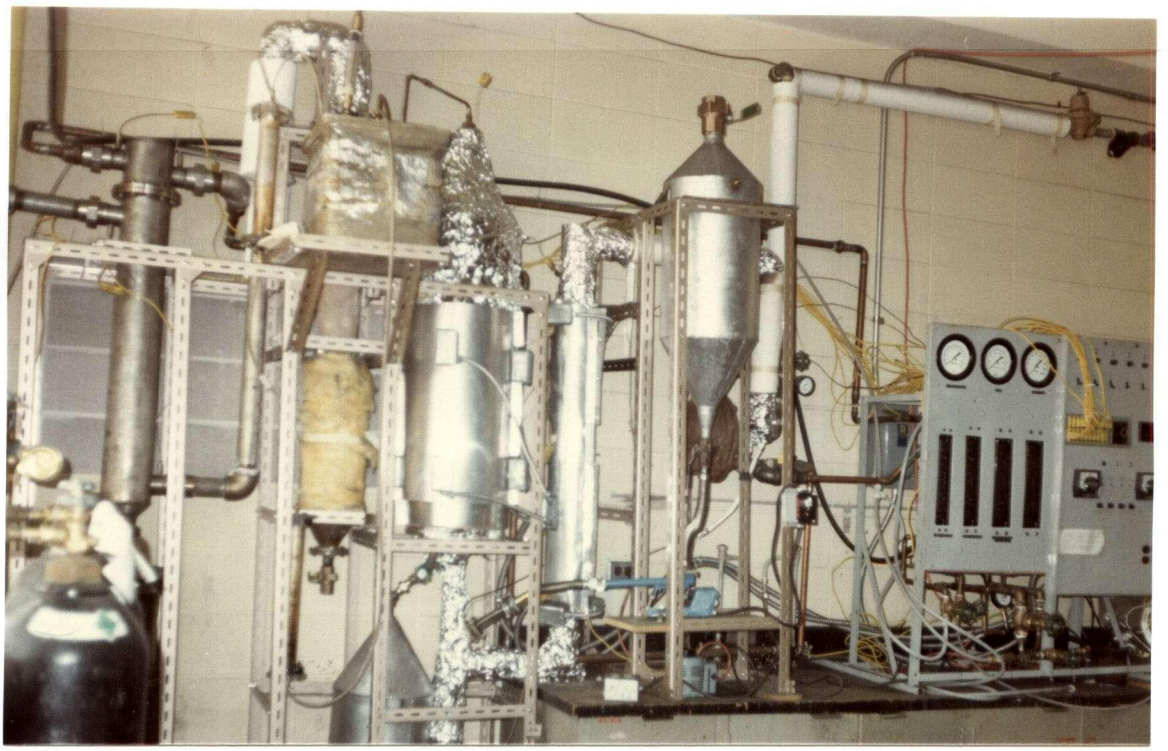

Figure 6 - Photograph of spouted bed pyrolysis apparatus.

to improve the stability of spouting as recommended in (1).

4.1.2 Coal feed hopper and feeder system

The coal feed hopper was made of mild steel, with a conical top and bottom. Its total height was 0.84 m and the diameter of the cylindrical section was 305 mm. It was fitted with a 5 cm ball valve at the top, and a 2.5 cm ball valve at the bottom. Provision for installing a pressure gauge was also available. Coal feeding was controlled by a Syntron tubular vibratory feeder. The tubular trough was 25.4 mm in diameter and 305 mm long. The vibratory feeder was equipped with a separate controller. A variac was connected to the power supply line to the controller to improve control of coal feed rate. The vibratory feeder inlet was connected to the feed hopper through a 25.4 x 381 mm stainless steel flexible tube. Its outlet was connected through another 25.4 x 305 mm stainless steel flexible tube and a 25.4 mm x 305 mm QVF glass tube fitted with flanges to the inlet pipe of the reactor. Coal fell by gravity into the inlet pipe and was blown into the reactor by the spouting gas.

4.1.3 Cyclone

The cyclone was located downstream of the reactor to separate entrained char particles and dust from the gas. Its diameter was 150 mm, cylinder height was 500 mm, and cone height was 300 mm. The cyclone was equipped with a dust receiver which was 150 mm in diameter and 500 mm high.

4.1.4 Condenser

The condenser consisted of a shell and U-tubes made of 316 stainless steel. The shell was of 128 mm I.D. by 0.86 m long with a

wall thickness of 6.6 mm. A 60° cone with a 52 mm outlet was welded to the bottom of the shell. The liquor receiver was connected to this cone by flanges. The hot gases passed through the shell while the cooling water from the building mains flowed through the U-tubes. There were six U-tubes of 12.7 mm diameter by 0.86 m long (each side). The cooling water inlet and outlet and the U-tube assembly were connected to the top of the shell by flanges. This design was adopted for ease of cleaning the condenser of tar deposits. The condenser was equipped with four thermocouples, to record inlet and outlet temperature of the gas, and inlet and outlet temperature of the cooling water.

4.1.5 Main tar filter

The tar filter was located downstream of the condenser. It was of a 102 mm diameter by 305 mm long QVF glass column connected to the pipe by flanges. A packing of glass wool was used to remove any tar droplets and/or char particles which might be carried away with the gas. This filter had two purposes; first, to clean the gas in order to prevent tar deposition on the orifice plate and downstream pipe section which might lead to blockage of the system and cause pressure rise and eventual shutdown, and secondly, to permit collection of the tar on the glass wool for qualitative analysis.

4.1.6 The impingers

Stainless steel impingers were used to condense the tar in the gas sample for quantifying the tar yield. The impinger train consisted of six impingers in series each 50.8 mm in diameter and 305 mm high as shown in Figure 7.

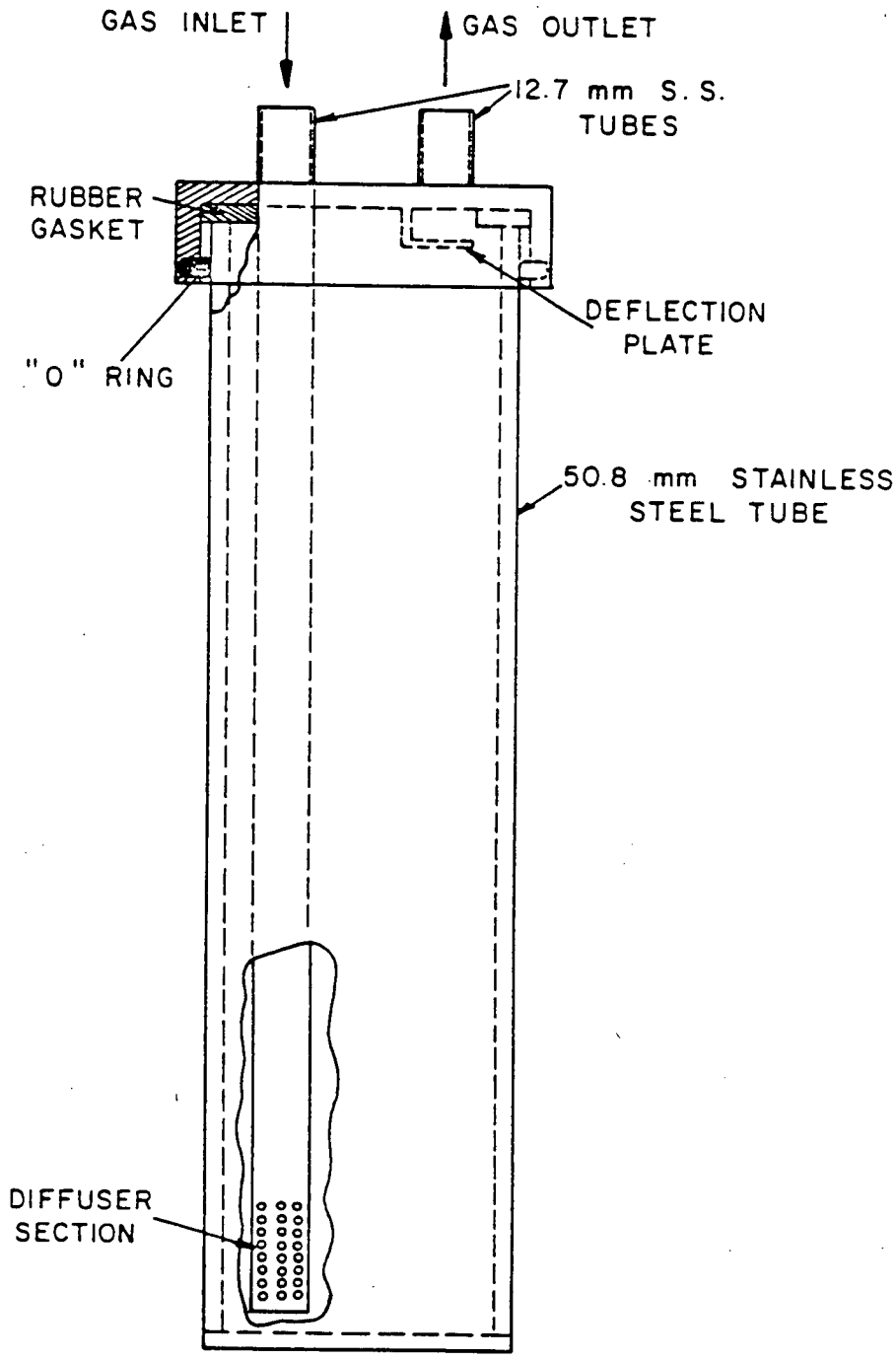

Figure 7. Impinger detail.*

* From reference No. 55

The second impinger was fitted with a thermocouple to record the gas outlet temperature. The impingers with solvents had a perforated diffuser section as in Figure 7 while in the remaining impingers the diffuser section was simply an open ended tube. The impingers train was immersed in a bath of cracked ice. The tar collection procedure is given in Section 4.2.2. A photograph of the impinger train is shown in Figure 8.

4.1.7 Spouting nitrogen supply

Since relatively large amounts of nitrogen were required for spouting, a standard size nitrogen gas cylinder was inadequate. Therefore, a liquid nitrogen cylinder 508 mm in diameter and 1.52 m high was used. It held 100 cubic meters (3531 cubic feet) of nitrogen gas stored as liquid, which is about the capacity of nineteen standard gas cylinders. It was fitted with a 3.05 m high auxiliary vaporizer to increase the nitrogen flow rate. Each cylinder usually lasted for two runs.

4.1.8 The heating system

A two stage heating system was used: The main heater on the spouted bed reactor consisted of 16 quarter-cylindrical electrical elements each of 178 mm I.D. and 152 mm height. These were mounted around the main cylindrical section of the reactor to form a shell. The heated section was 0.61 m high. The total electrical rating for these heaters was 9.2 kw. The maximum rated temperature of the inside wall of the heater was 1,200°C. An air gap of 18 mm existed between the inside wall of the heaters and the outside surface of the reactor. The

Figure 8 - Photograph of impingers train.

electrical input to the main heater was divided into two separate lines, thereby, dividing the main heater into bottom and top halves. It was possible to use both or either half; however, only the bottom half of 4.6 kw was normally used because of the limitations of the power supply and the range of bed heights explored. The temperature was controlled by an Omega controller mounted on the control panel. Thermocouple No. 6 (see Table 9) in the reactor was also used as a sensor for the controller. The reactor and downstream pipe were insulated.

The spouting gas was first preheated by condensing steam in a shell and coil heat exchanger. This heat exchanger was manufactured by Graham manufacturing company. The coil was 9.5 mm in diameter x 1.68 m long which gave an outside surface area of 0.41 m^2. The spiral heat exchanger consisted of 8 individual coils with the two ends attached to two 25.4 mm pipes. The coils were separated from each other by 3.2 mm spacers, and were encased in an one-piece metal casing. The spouting gas flowed in the coil while the steam condensed in the shell. Steam was taken from the mains at pressures up to 556.6 kPa. After the steam heat exchanger the temperature of the spouting gas was raised further by electrical heaters. These consisted of 4 semicylindrical heaters of 44 mm I.D. which were clamped around the pipe to give heated lengths of 915 mm. The total electrical rating of these heaters was 3.94 kw. The pipe section on which these heaters were mounted was packed with 12.7 mm hollow cylindrical ceramic packing pieces to increase the rate of heat transfer. An Omega controller, identical to the one used for the main heater, was used to control the temperature of the spouting gas. In

addition to the above heating devices two 25.4 mm x 1.22 m tape heaters were wrapped around the pipe section between preheater and reactor. The electrical rating for each of these two tape heaters was 624 watts. The preheater and downstream piping section were insulated.

4.1.9 Temperature measurements

The temperature throughout the apparatus was measured by Chromel-Alumel thermocouples with 316 stainless steel sheath of 1.6 mm diameter and 305 mm length. There were sixteen thermocouples in the locations shown in Table 9. These thermocouples were connected to the jack panel on the control panel by thermocouple extension wires. This jack panel was in turn connected to a multiple (18) channel switch and a digital display for temperature in degrees centigrade.

4.1.10 Coal preparation and storage

Coal was crushed and screened using a Hammer mill in this department. After screening to the desired size (-3.36 + 1.19 mm), it was stored in sealed drums. Representative samples of the coals were sent to General Testing Laboratories of Vancouver for proximate, ultimate, and free swelling index analyses.

4.2 Experimental procedures

4.2.1 General experimental procedure

Coal crushed and screened to the desired particle size was loaded into the coal hopper. The impingers for tar collection were prepared as explained in Section 4.2.2 below. The exhaust fan was turned on. Air was then turned on at a low flow rate to prevent sand particles from dropping into the spouting gas inlet pipe. Air was used

first for spouting to heat up the bed of sand to the desired temperature in order to save nitrogen. Five kg (more or less depending on bed depth) of Ottawa sand of size range - 14 + 20 U.S. standard (average particle diameter 1.12 mm) was loaded at the top of the reactor from an opening which was capped by a threaded fitting. Air flow was adjusted to the operating flow. The main reactor heater, spouting gas preheater, steam to the steam heat exchanger, tape heaters (sometimes, depending on desired temperature) and the cooling water for the condenser were all turned on. Temperature controllers for the main heater and the spouting gas preheater were set at the desired reading. The heat-up time was approximately 2-3 hours depending on the run temperature. The bed of sand was usually heated to a temperature higher than the run temperature to offset the drop in temperature which occurred after the commencement of coal feeding. After reaching the desired temperature, spouting nitrogen was turned on while the air flow was shut off. Nitrogen was blown in for about 500 mean gas residence times (10 minutes) to purge the air before coal feeding was started. The coal feeder controller was set at the desired point and the feeder turned on. The time at which coal feeding started was recorded. Achieving steady state temperatures in the bed took about 20 minutes or more (depending on type of coal and coal feed rate) after the start of coal feeding. The gas sample pump was then turned on and tar collection started (see Section 4.2.2 below). The time at which the gas sample pump was turned on was recorded. Gas sample flow rate was adjusted to the desired rate and the gas sample rotameter reading was recorded. Tar collection lasted for one hour during which a few gas samples were analysed on the gas

chromatograph, all temperatures and pressures throughout the system were recorded, and the spouting gas rotameter reading was taken. Orifice manometer readings were taken before and after coal feeding. After one hour of tar collection the coal feeder, the gas sample pump, all the heaters were turned off, and the time recorded. The system was quenched by cold nitrogen which bypassed the preheater. It was necessary to quench the bed especially when using caking coals to prevent the formation of lumps of char and sand. The quenching nitrogen flowed through the system for about 30-45 minutes to cool the apparatus to a temperature of about 100°C before the nitrogen was turned off. Cooling water for the condenser was then turned off. The impingers and tubes were dismantled and washed with solvents to recover the tar as explained in detail in Section 4.2.2 below. After the system was cold (usually the next day), the reactor, the dust receiver, the liquor receiver were all emptied and their contents weighed. The coal feed hopper was also emptied of unused coal to determine the coal feed rate. The main tar filter was opened and the glass wool removed and put in a labeled plastic bag. The filter was filled with a clean glass wool for the next run. A char sample was also stored.

4.2.2 Tar collection method

The tars are collected by isokinetic sampling of the pyrolyzer off gas upstream of the cyclone (details for calculating gas sample flow rates are given in Appendix A). After the temperature reached steady state in the reactor, the tar collection pump was turned on and a metered quantity of the gas passed through a series of

impingers (Figures 7 and 8) to condense the tar. As described above the six impingers were immersed in a box of cracked ice. The first two of these contained water (in the lower quarter) to cool down the gases and to condense some tar. The gas left the second impinger at a temperature less than 20°C. The third and fourth impingers each contained a mixture of 100 ml methylene dichloride solvent and 50 ml water. Methylene dichloride is a strong solvent for the tars. Most of the tar was collected in these two impingers. The fifth impinger contained 150 ml of methanol to dissolve the rest of the tar and also to trap any of the methylene dichloride solvent that might have evaporated with the gas. The sixth impinger contained 150 ml water in order to trap any methanol that might have evaporated with the gas. The tar collection lasted for one hour. The tar was recovered from the impingers by the following method: The impingers containing the solvents were emptied into one beaker and the impingers containing the water were emptied in a second beaker. All the empty impingers and tubes were repeatedly washed with a mixture of methylene chloride and methanol to recover the tar deposited on the walls. The washing solution was added to the first beaker. The amount of tar in the second beaker was small, and was recovered by solvent extraction in a separating funnel using the above solvents. The extract was added to the first beaker. Any char particles that might have been entrained with the gas were filtered out. The solvents (and water as an azeotrope) were removed by evaporation under vacuum in a filtering flask. The flask was immersed in a water bath which was set first at about 50°C and then raised to about 95°C. After the evaporation, the tar was weighted and the weight recorded.

4.2.3 Gas analysis

The gas analysis was performed in a Hewlett - Packard 5710A gas chromotograph with 3388A automatic integration system. The chromotograph was equipped with a 3.2 mm x 2.13 m molecular sieve A column to separate hydrogen, oxygen, nitrogen, methane, and carbon monoxide and a 3.2 mm x 3.96 m porapak Q column to separate carbon dioxide. This latter column can also resolve C_2's. The G.C. was equipped with a thermal conductivity detector. At a column temperature of 80°C, the time required for complete separation of the six above gases was about thirteen minutes. After the gases leave the impingers, they are passed through a column packed with glass wool and drierite for cleaning and drying before they were pumped to the G.C. The analysis was done on a dry basis. The gas sample was taken automatically by the G.C., and the analysis done during the tar collection period. Usually four gas samples were analysed and average values reported for each run. Provisions for withdrawing gas samples by a syringe were available just downstream of the glass wool-drierite column and the orifice.

4.2.4 Char determination and analysis

After each run, the reactor and the dust (entrained char) receiver were emptied and the contents of each one were separately weighed. By subtracting the weight of original Ottawa sand from the total weight of the above, the weight of the char produced was obtained. The weight of the material from the dust receiver was taken to represent the solid entrained, although a small quantity of solids undoubtedly passed through the cyclone.

Selected char samples from each coal were sent to an outside laboratory for analysis.

4.3 Experimental problems, observations, and developments

1. Solid feeding was the first major problem. The pressure in the coal feed hopper had to be balanced with that in the reactor in order for the feed rate to be constant. The vibratory feeder requires smooth pipes and tubes downstream of the feeder to insure free flow of solids. The presence of any obstacle such as pipethreads, pipe edges or reducers leads to accumulation of the solids and eventual blockage. The vibratory feeder works fairly well provided the above conditions are met, but it is very sensitive to vibration settings and therefore rather difficult to control. A variac was connected to the controller of the feeder improved control. The coal should be free of fines and had to be carefully screened to insure a steady feed rate.
2. A rather large temperature drop was noted between the reactor and condenser. This must be avoided to prevent tar condensation on the inside walls of the pipes. The pipes downstream of the reactor were well insulated and temperature drop was reduced (Table 9).
3. Initially, tar droplets deposited on the orifice plate and eventually blocked the flow. The filter downstream of the condenser was then installed and no serious deposition was noted on the orifice afterwards. The glass wool filter

packings had to be replaced after each run or the pressure would rise in the system and force a shutdown.

4. Sand of small particle size (~0.5 mm) was used initially to conserve spouting nitrogen. Spouting was unstable especially at high temperature which was characterized by severe fluctuations of the orifice manometer and the pressure gauges. Sand of a larger particle size (U.S. standard - 14 + 20 and average diameter of 1.12 mm) was then used and stable spouting was obtained.

5. RESULTS AND DISCUSSION

5.1 General considerations

Over 85 runs were performed on four different types of coal. All yield results are reported as weight percent on a moisture and ash free (MAF) basis. Results are not normalized to 100%.

The tar yield is calculated from the weight of tar collected from the sample gas, the mass flow rate of the sample gas, mass flow rate of the total gas output from the reactor and the coal feed rate. The total gas yield is calculated by conducting a gas material balance using nitrogen as the key component. The total gas output measured by the orifice was in good agreement with the one calculated by material balance. Sample calculations of tar and gas yields are given in Appendix A. The char yield is calculated from the weight of char remaining in the reactor and cyclone after the run and the total coal fed. The char yield should be the most reliable of the yields reported because virtually all the char remains either in the bed or in the dust receiver. A very small amount of char escapes from the cyclone, but, this amount is negligible compared to the quantity of char collected. Small errors will exist in the gas yield value, largely because hydrocarbon gases of molecular weight higher than CH_4, and gaseous sulphur and nitrogen compounds are not measured. However, even if these gases are produced in the temperature range studied, their quantities are expected to be very small. The tar yield undoubtedly is the least reliable. It is probably underestimated, because during solvent evaporation some of the lighter liquid hydrocarbons could be lost. However, using a less severe evaporation procedure could leave some

water with the tar fraction which would result in exaggerated yields of tar. Therefore, it was decided to opt for a conservative estimate of tar yield. Thus, the tar yield reported comprises liquids retained after the water and solvents are evaporated.

The effect of temperature on product yield was investigated for all types of coal studied. The effect of coal feed rate was investigated for Forestburg coal and some confirmatory runs were performed on Sukunka coal. The effects of other variables, namely, particle size, vapour residence time, bed height, and gaseous media were studied using Sukunka coal only. While studying the effect of one variable, other variables were kept constant. The coal particle size used throughout most of this study is -3.36 + 1.19 mm. The height of the static bed of sand in the reactor is 38 cm except where otherwise stated. The minimum spouting velocity, estimated using the Mathur-Gishler equation[26] was between 0.85 and 0.95 m/s depending on temperature. The spouting velocity used was up to about 20% higher than the calculated minimum spouting velocity. The vapour residence time in the reactor (from reactor bottom to impingers inlet) is estimated to be 0.98 s while that in the bed of sand is less than 0.5 s.

Tables showing the tar, char, and gas yields from all coals are given in Appendix B. In repeated tests tar yields were found to have a reproducibility of about ± 5%, char yields ± 2%, and gas yields ± 3%.

5.2 Temperature profile

Table 9 illustrates typical examples of the temperature profile throughout the apparatus during two runs. The reactor is heated

Table 9 - Temperature Profile in the Apparatus

Thermocouple Number	Location	Temperature °C Run No. 33 (Forestburg Coal)	Run No. 45 (Sukunka Coal)
1	30 cm upstream of spouting gas rotameter	18	18
3*	Reactor inlet pipe, 19 cm upstream of reactor inlet	525	527
4	Reactor cone, 2 cm from the base of the cone	530	597
5	19 cm above the base of the cone	525	594
6	38 cm above the base of the cone	540	600
7	57 cm above the base of the cone	516	583
8	Centre of disengagement chamber	427	518
10	Main condenser inlet	179	250
11	Main condenser outlet	33	63
14	9 cm upstream of orifice meter	27	43

*Shows the result of the preheater

up to the location of Thermocouple No. 6. The bed height is estimated to be slightly below the position of thermocouple No. 6. Hence thermocouples No. 4, 5, and 6 record the bed temperature. These thermocouples protrude into the annulus about 2.5 cm from the inside wall of the reactor. The temperature of the run is taken to be the average of these three which are usually uniform throughout the run and have about the same temperature with a difference within 1%. The readings shown in Table 9 are instantaneous temperatures at a time about half way through the run. The small fluctuations in temperature were recorded throughout the run, and the average bed temperature for run No. 33 is calculated to be 530°C and for run No. 45 is 600°C.

5.3 Entrainment of char

Some typical examples of the extent of char entrainment are shown in Table 10. These values are calculated by dividing the weight of material collected in the cyclone by the total amount of char obtained for that run. It is assumed that all the material collected in the cyclone is char dust i.e., there is insufficient sand attrition to produce significant entrainment of sand. From Table 10, it is evident that in general for all the coals shown, the percentage entrained increases with superficial velocity as would be expected. Scott et al.[37] and Tyler[34] who used small fluidized bed pyrolysers also reported that most of their char was retained in bed. They reported that the reason for this is the agglomeration of coal particles with the bed of sand. In this work, some agglomeration of coal with the sand was noted in the case of Sukunka and Balmer coals. Also the disengagement chamber apparently has been efficient in reducing the amount of

Table 10 - Entrainment with different coals

Run No.	Coal	Temperature °C	Superficial Velocity* of Spouting N_2, cm/s	Entrainment wt % of Char
35	Forestburg	500	87.2	5.2
34		540	91.7	12.3
40		560	96.4	14.1
59	Sukunka	540	94.9	14.2
52		550	101.2	23.2
54		615	109.2	28.8
72	Balmer A	535	99.4	13.5
69		600	107.3	16.5
78		650	117.6	22

*Calculated at temperature

entrainment. However, it should be noted here that char entrainment is not necessarily undesirable in this kind of work provided that the particles residence time in the reactor is sufficient for complete devolatilization (pyrolysis). For the case of coal gasification or combustion recycling of the cyclone catch is probably important.

The entrained particles are of very fine size and far smaller than the fresh coal feed. For example, the mean diameter of a sample from the cyclone catch from Run No. 59 is 0.061 mm. The size distribution of this sample is given in Table 11. From this table, it seems that reducing the spouting velocity to the minimum spouting velocity is not likely to reduce the amount of entrainment due to the very fine size of these particles. A photograph of the cyclone catch is shown in Figure 9d.

5.4 Forestburg coal

Forestburg coal is a sub-bituminous coal from the Edmonton formation in Alberta, and it was supplied by Luscar Ltd. Its proximate, ultimate and maceral composition is given in Table 12. The proximate and ultimate analyses were done by an outside laboratory, and the maceral analysis was done in the Department of Geological Sciences. Forestburg coal is a non-agglomerating coal with a swelling index of unity. For this reason, this coal was used first to test and debug the apparatus.

5.4.1 Effect of coal feed rate and char accumulation

Experiments were run over a range of coal feed rates from 0.39 to 7.64 kg/h. The tar yield dropped off while the gas and char

Table 11 - Size distribution of a sample from the cyclone catch of run No. 59 (Sukunka).

Tyler Mesh Range	Average diameter, mm (d_i)	Weight, g	Weight Fraction (X_i)
- 32 + 35	0.46	0.6	0.016
- 35 + 48	0.36	1.3	0.035
- 48 + 60	0.274	1.1	0.029
- 60 + 115	0.188	9.2	0.247
-115 + 200	0.1	7.8	0.209
-200 + 250	0.069	3.9	0.105
-250 + 0	0.032	13.4	0.36

$$\text{Mean Diameter} = \frac{1}{\Sigma \frac{x_i}{d_i}} = 0.061 \text{ mm}$$

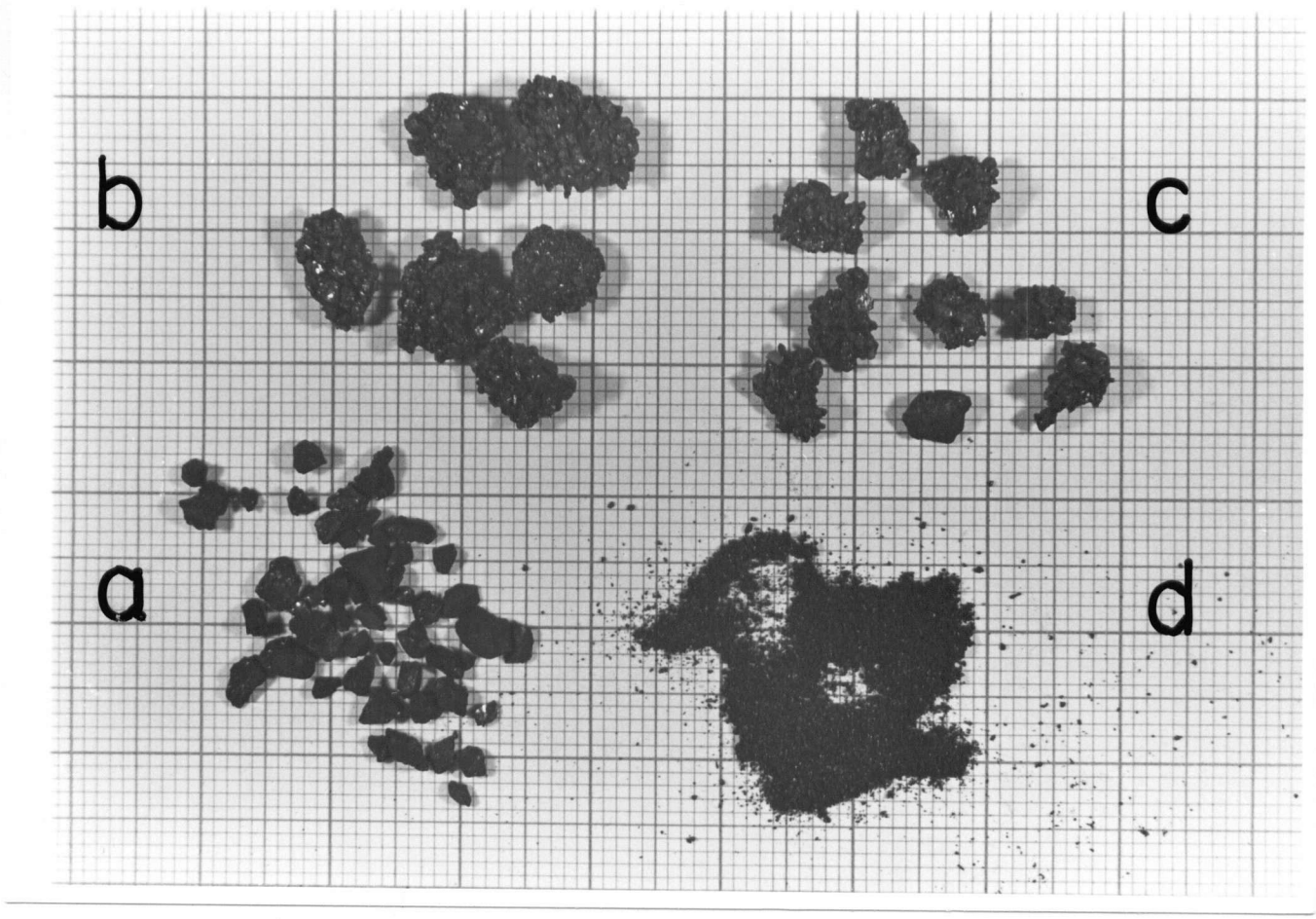

Figure 9 - Photograph of (a) Fresh coal feed, (b) and (c) char agglomerates, (d) cyclone catch

Table 12 - Properties of coals tested

Ultimate Analysis (% wt MAF)	Forestburg	Sukunka	Balmer A	Balmer B
C	76.4	89.98	91.77	89.38
H	4.02	4.53	4.73	4.8
S	0.58	0.69	0.28	0.25
N	1.71	1.75	1.25	1.14
O	17.3	3.05	1.97	4.43
Proximate Analysis				
% Moisture	23.17	1.08	1.2	1.47
% Volatiles	32.96	20.60	16.9	20.07
% Fixed carbon	37.18	65.14	53.43	66.95
% Ash*	6.69	13.18	28.47	11.51
Free Swelling Index	1	7	-	1.5
Atomic H/C Ratio	0.63	0.6	0.62	0.62
Maceral Analysis (% Volume)				
Vitrinite	92.5	65.3	51	40.3
Inertinite	5.8	27.7	48	58.5
Exinite	1.7	6.9	1.0	1.2

*Ash Analysis in Appendix B

yields increased as the feed rate was increased as noted from Figure 10.* However since the char accumulates in the bed with time, and the experiments were run for the same length of time, the high feed rate runs are characterized by larger weights of char being present in the bed (Figure 11). It is known that secondary cracking and polymerization of tar are catalysed and enhanced by the presence of hot char. Thus the drop in tar yield may be associated with the larger weight of char in the bed rather than being an effect of feed rate itself (Figure 12). Tyler[34] reported tar yields of 29% in a fluidized bed of sand, which dropped to 25% in a bed of petroleum coke, and to 3% in a bed of activated char of high surface area. Durai-Swamy et al.[56] also noted that tar yield decreased significantly with the presence of char. Experiments were therefore run in a bed consisting solely of char as shown in Table 13. The tar yield is significantly less for the char bed runs. The possibility of temperature gradients within the bed or coal particle resulting from higher feed rate and consequently reducing tar yield should be ruled out given the high residence time of coal particles in the bed (on average about 33 minutes). A substantial drop in bed temperture was noted with high coal feed rate runs, but, the bed was heated to a much higher temperature before starting coal feeding to compensate for this temperature drop. The tar collection was not started until after a stable temperature is reached. Thus, the conclusion to be drawn here is that the decrease in tar yield is more likely a result of char accumulation in the bed which must be avoided if maximum tar yield is sought. Therefore, care must be taken in the

* Normalized tar yield = 100 - (% gas yield + % char yield)

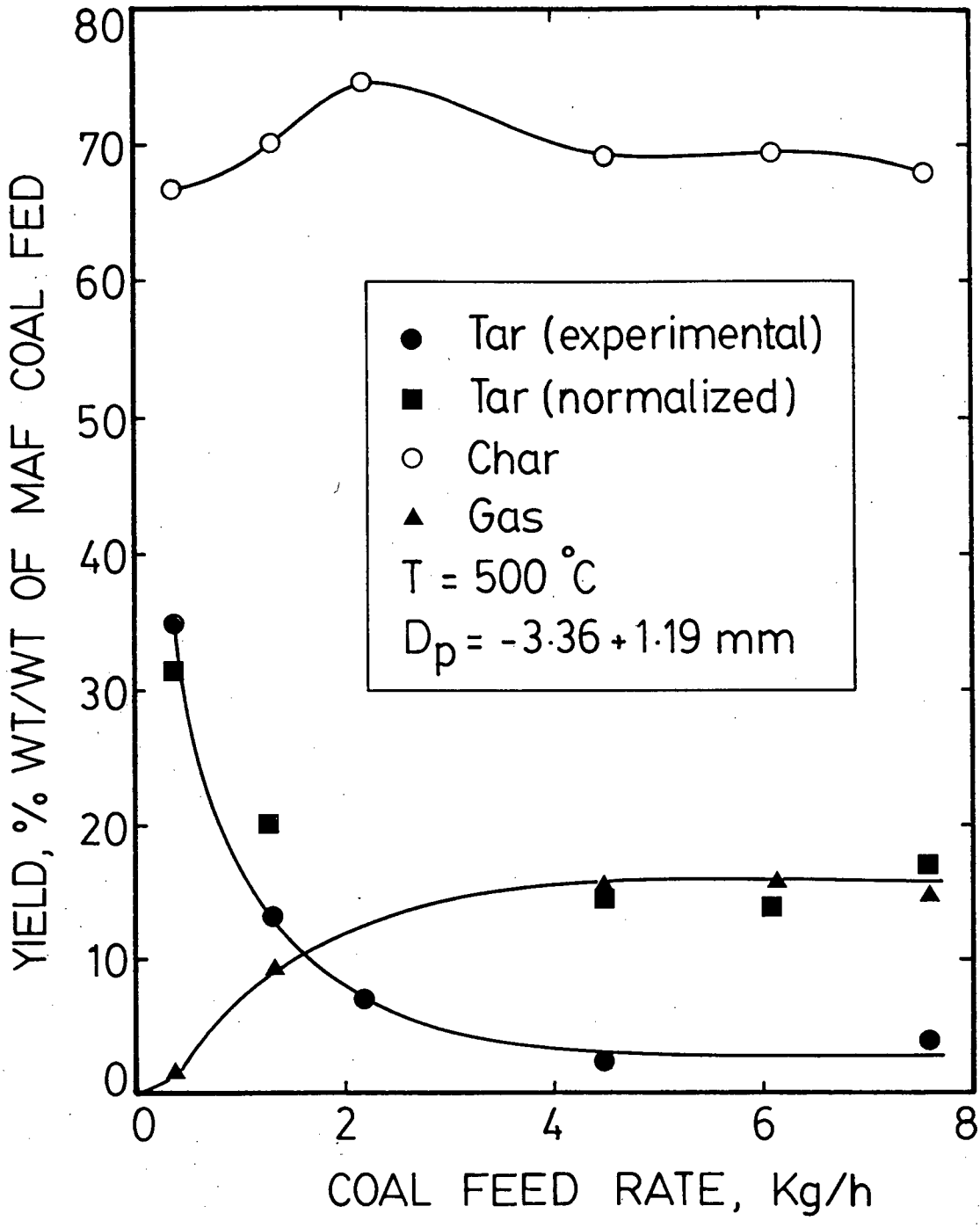

Figure 10 - Effect of coal feed rate on pyrolysis product yield - Forestburg coal.

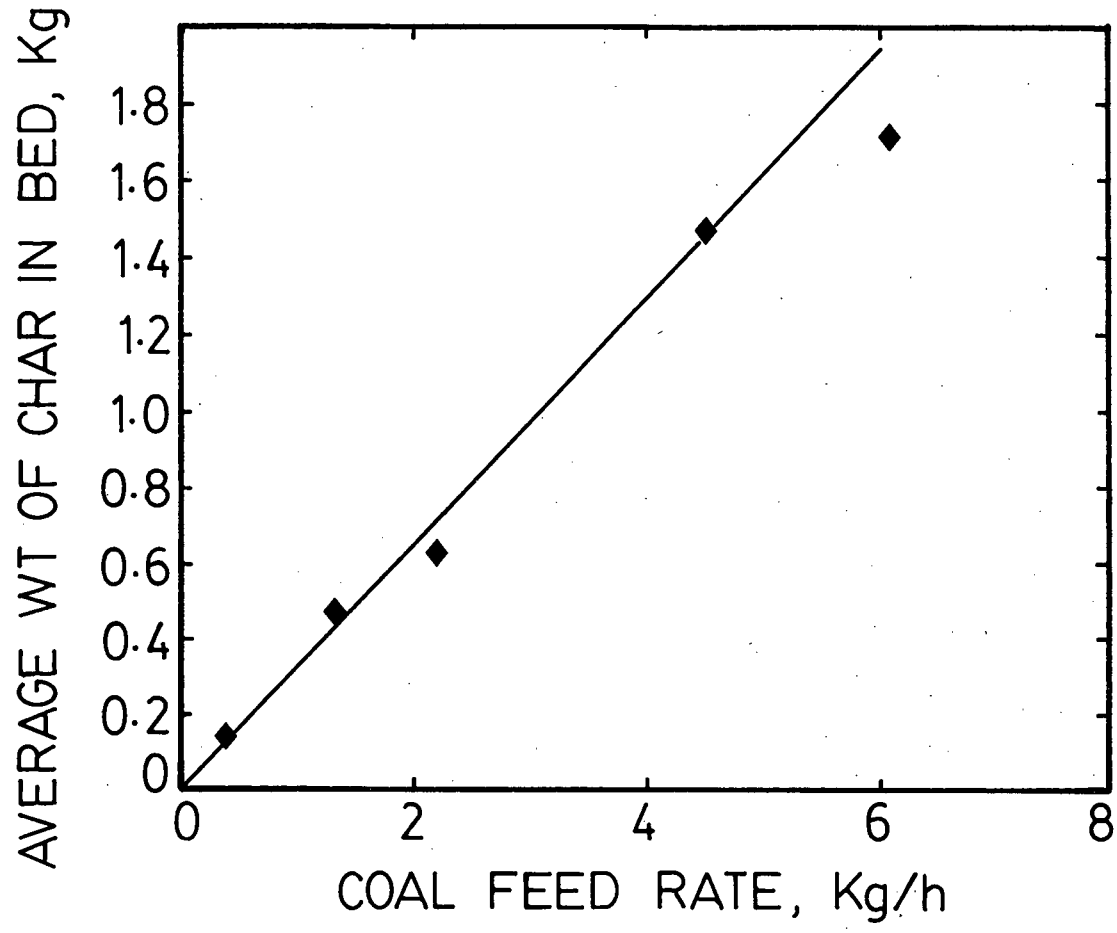

Figure 11 - Effect of coal feed rate on char accumulation in bed - Forestburg coal.

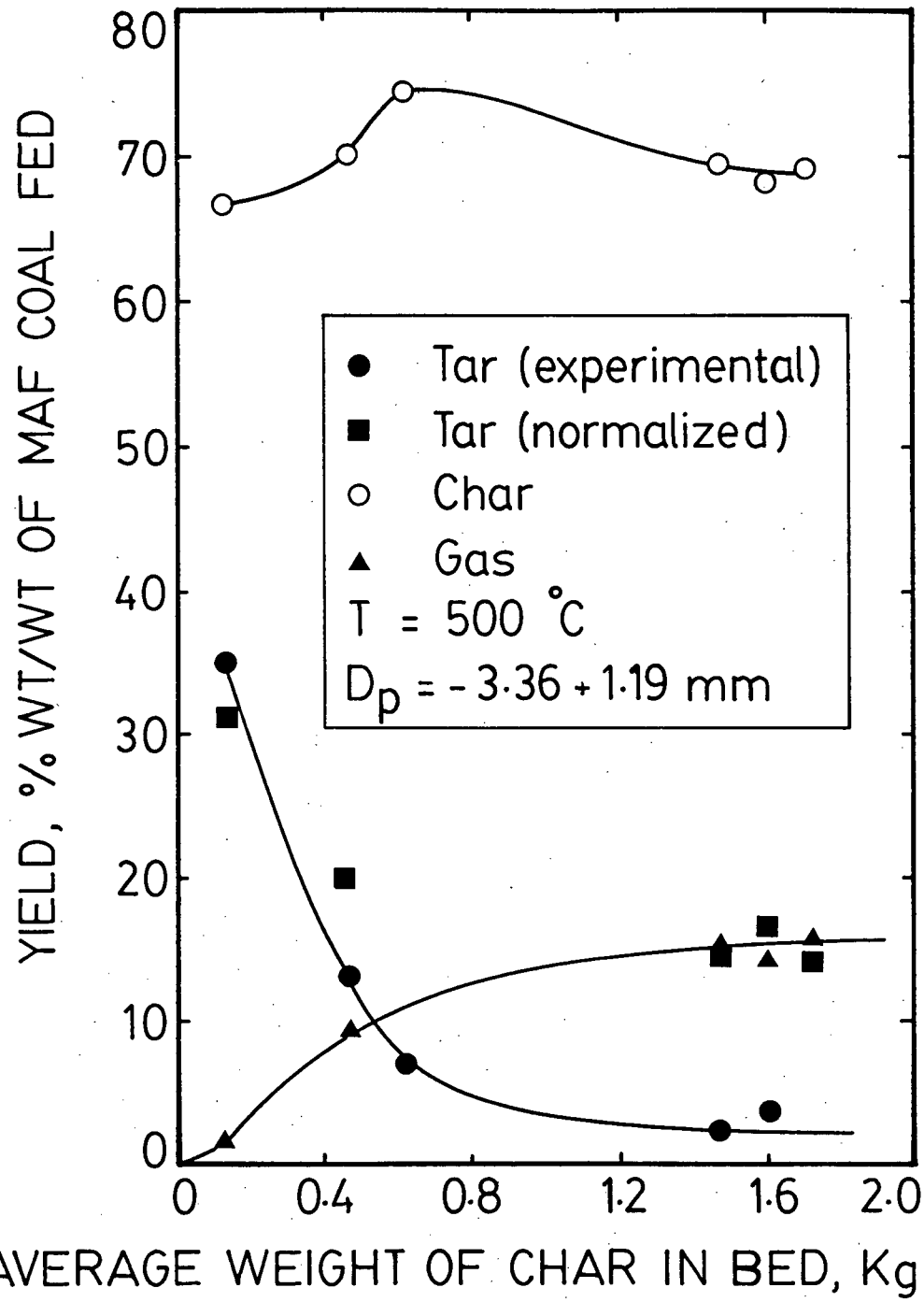

Figure 12 - Effect of char accumulation in bed on product yield - Forestburg coal.

Table 13 - Comparison of tar yields in bed of sand and of char

Temperature °C	Char Bed*			Sand Bed**			Final Wt (kg) of char in bed
	wt. % yield (MAF)						
	Run No.	Tar	Gas	Run No.	Tar	Gas	
500	85	5.14	14.2	35	13.2	13.8	0.752
530	86	12.5	14.2	33	21	15.7	0.953

*Run started with 5 kg char

**Run started with no char

Table 14 - Screen analysis of char sample from Run 59 on Sukunka coal

Tyler Mesh Size	Diameter, mm	Weight, g	Weight Fraction
-3 + 4	-6.73 + 4.76	2.7	4.7
-4 + 5	-4.76 + 4	7.3	12.6
-5 + 6	-4 + 3.36	3.1	5.3
-6 + 14	-3.36 + 1.19	44.9	77.4

design of commercial reactors where the particle residence time should be kept to the minimum needed for decomposition and provision for char discharge is provided accordingly.

The coal feed rate for subsequent runs in which other variables were studied was held constant at about 1.2 kg/h, and the char load in the bed was roughly 1 kg at the end of each experiment.

5.4.2 Effect of temperature

Temperature is the most important variable affecting the composition of pyrolysis products from coal. It affects the extent of coal decomposition and the secondary reactions of the volatiles. In general, the tar yield increases with temperature to a maximum value, but tar destruction by the secondary reactions also increases with temperature. Above the temperature of maximum tar yield, the rate of tar destruction is higher than tar generation leading to increase in gas yield and a decrease in tar yield.

The temperature range studied for Forestburg coal was between 450-600°C, which is a fairly low temperature range compared with most of the published studies on pyrolysis. However, it is clear that the temperature of maximum tar yield is below 600°C for this coal and higher temperatures are not warranted.

The effect of temperature on tar and char yield from Forestburg coal is shown in Figure 13. The maximum tar yield of 21% was obtained at a fairly low temperature of 530°C. The char yield decreased steadily with temperature as expected. About 66% char yield was obtained at the temperature of maximum tar yield of 530°C. The total

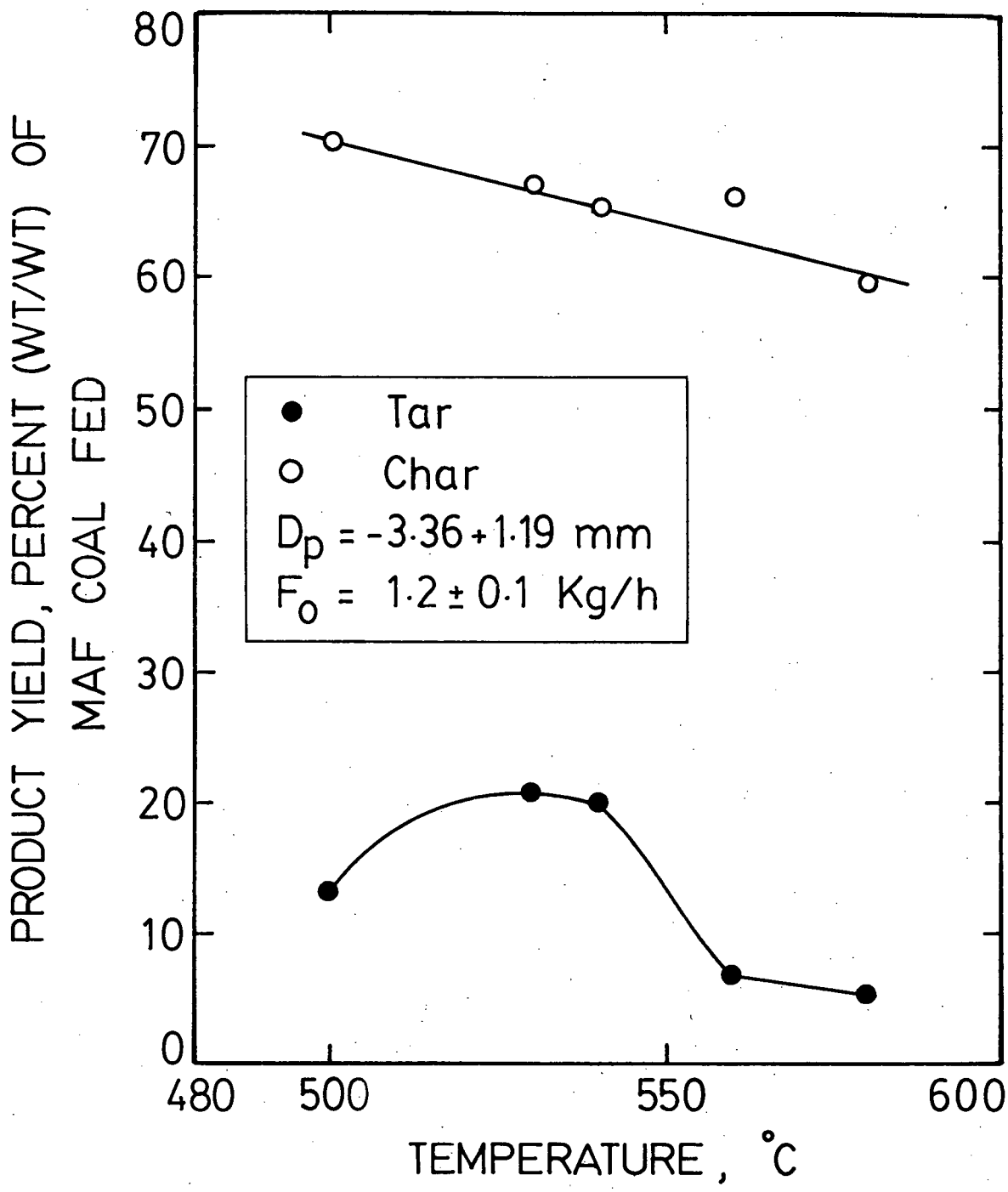

Figure 13 - Effect of temperature on tar and char yield - Forestburg coal

volatiles yield (100 - char yield), on the other hand, increases with temperature reaching about 40% at 580°C. The volatile matter content of this coal by proximate analysis which is obtained at about 950°C is 47% (MAF) as shown in Table 12. Therefore, it seems that most likely the total volatile yield in the spouted bed will be higher than that from the proximate analysis method as is commonly observed in rapid pyrolysis because of a reduction in secondary reactions.

The effect of temperature on the yields of hydrogen and methane is shown in Figure 14. The yields of both gases increased with temperature. At 600°C a yield of 3.7% was obtained for methane and 1.3% for hydrogen. As is generally the case,[4] methane which comes from dealkylation is evolved at lower temperature than hydrogen which comes from aromatization reactions. The effect of temperature on the yields of carbon oxides is shown in Figure 15. A large amount of carbon oxides was formed. These consist primarily of CO_2 which reached a yield of 15% at 600°C due to the high oxygen content of the coal. Carbon dioxide begins to evolve at low temperature due to the low activation energy of the decarboxylation reaction. The yield of carbon dioxide increased with temperature to an asympototic value. This trend was also observed by Suuberg[30] during the pyrolysis of Montana Lignite on an electrically heated grid.

Forestburg coal used in this study has a high (> 23%) moisture content. Therefore, some steam will be generated in the reactor. The steam-char reaction should not be expected to take place in the temperature range studied because this reaction normally starts

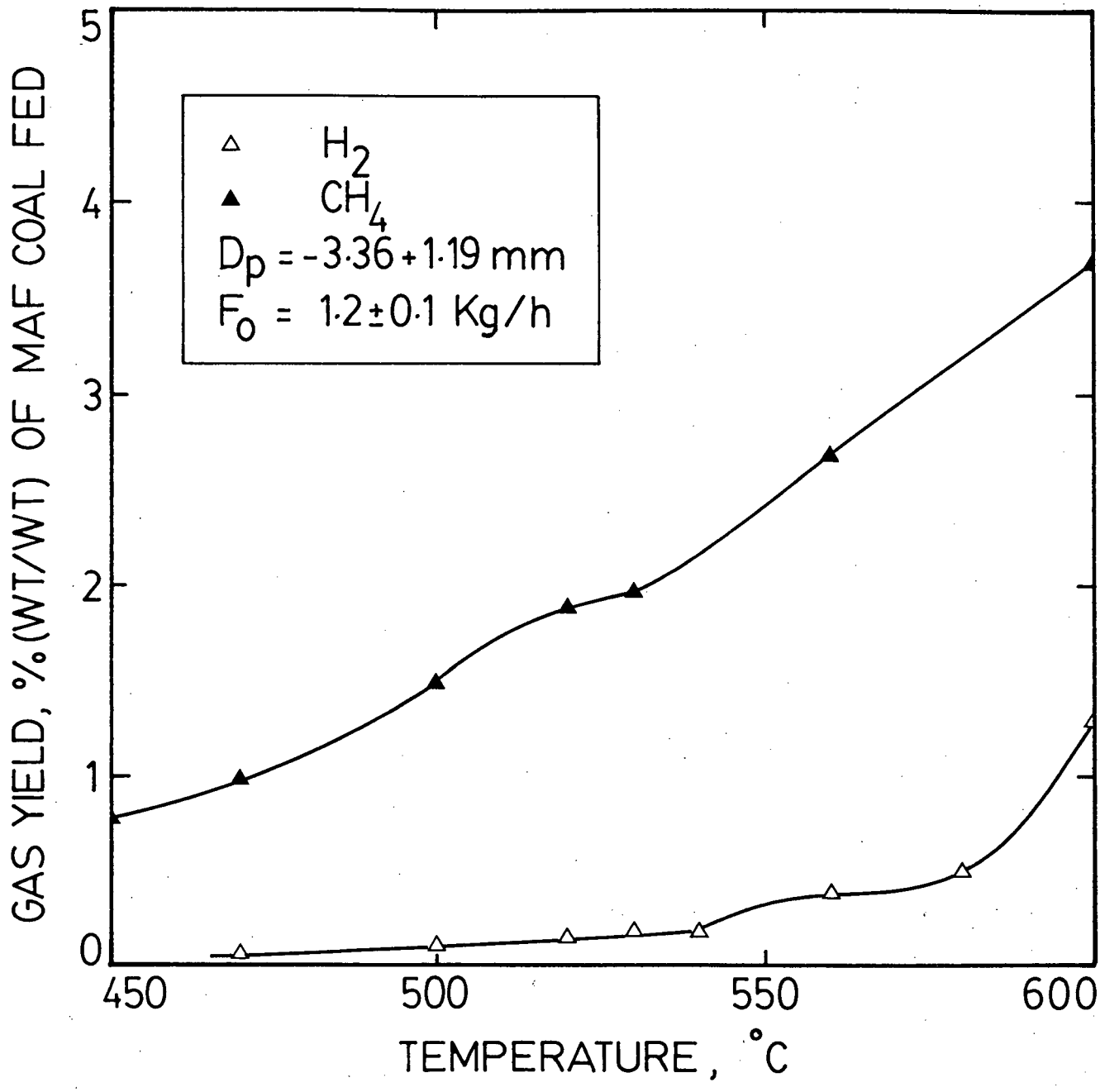

Figure 14 - Effect of temperature on hydrogen and methaneyield - Forestburg coal.

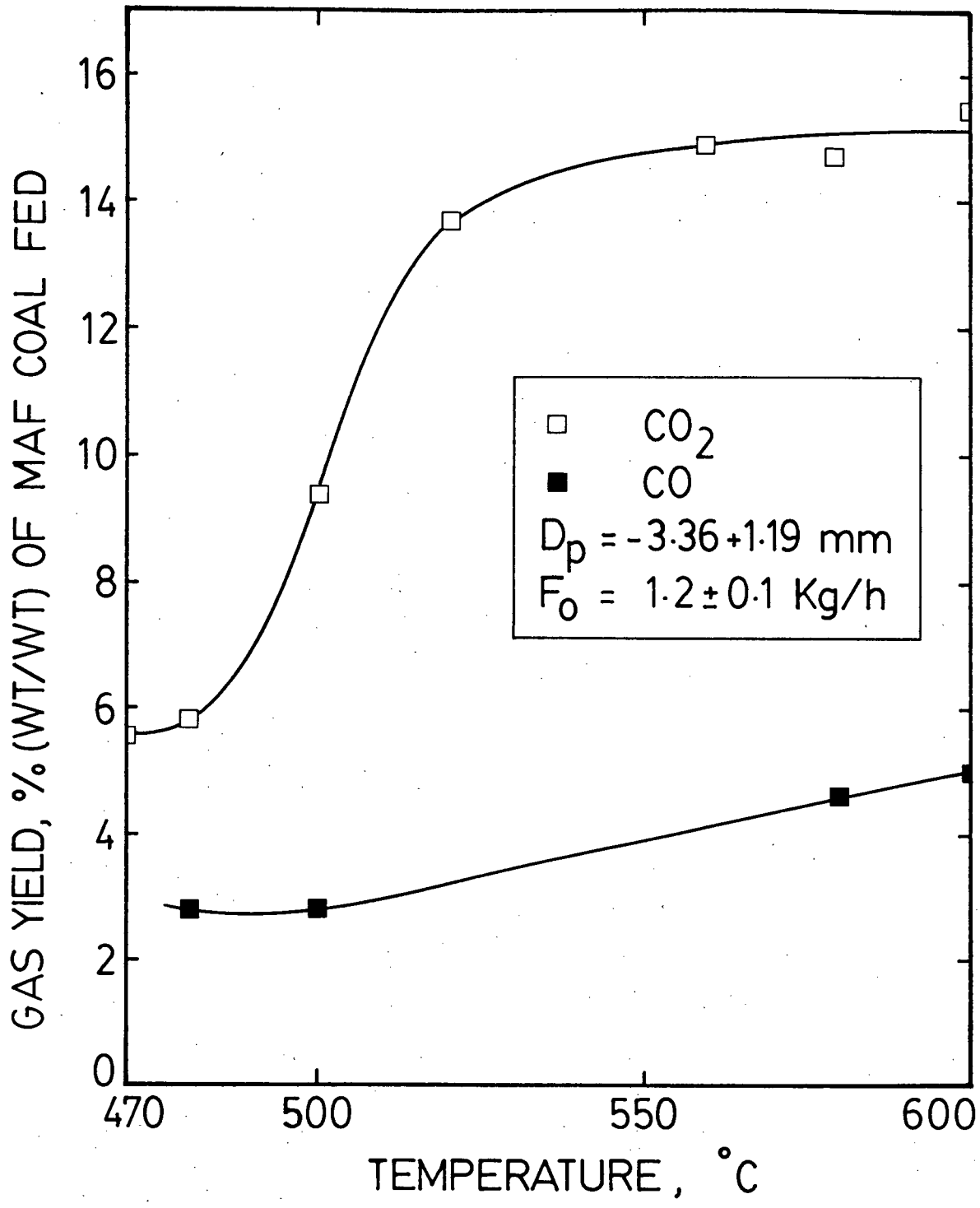

Figure 15 - Effect of temperature on yields of carbon oxides - Forestburg coal.

at temperatures higher than 700°C. Therefore, the hydrogen and carbon monoxide generated is not likely a result of this reaction.

No pyrolytic water was found in the temperature range studied. Attempts were made to measure pyrolytic water by the following method. The water content of the first two impingers (see Section 4.2.2 and P. 146) was measured before and after tar collection for each run but no pyrolytic water was detected. The gases leave the second impinger at a temperature of less than 20°C, also the water formed in the main condenser was measured but no indication of pyrolytic water was found. No pyrolytic water was obtained from other coals studied in the temperature range indicated. Suuberg et al.[30] noticed that pyrolytic water was only evolved from the pyrolysis of Montana lignite at temperatures higher than 600°C.

There has been no coal pyrolysis work reported in North America using the spouted bed for direct comparison. The work done in Australia[1,2] and India[39] using the spouted bed was not aimed at investigating conditions for maximum liquid yield and no tar was collected. Most of the work in the literature reports tar yield by difference and normalizes the results to 100%. The study perhaps most comparable to the present work was that done by Scott et al.[37], who pyrolysed Forestburg coal of particle diameter 74-149 μm in a 2 cm diameter miniature fluidized bed. Their coal sample had an atomic H/C ratio of 0.76 and 10% moisture content compared to 0.63 and 23.17% respectively for the coal sample used in the present study. They reported tar yields reaching a maximum of only 10% at about 650°C and a

normalized tar yield of 19% at 700°C, which compare with 21% at 530°C in the present work. At 650°C their CO_2, CO and CH_4 yields were 11%, 5% and 1% which compare with 14.8%, 3.5% and 2% at 530°C in this work. Difference in apparatus, technique, and coal samples probably contribute to the disparities in yields.

5.5 Sukunka coal

Sukunka coal is a bituminous coal from the Peace River coal field in north eastern British Columbia. Its proximate and ultimate analyses as well as its maceral composition are given in Table 12, its relatively high exinite content is notable from this table. This is a strongly agglomerating coal with a free swelling index of 7.

5.5.1 Effect of char accumulation

To confirm the effects which result from coal feed rate variation on product yield from Forestburg coal, some further tests were performed on Sukunka coal. The results are shown in Figure 16. The average content of the char in bed (final weight of char in reactor/2) for the two runs on the right in Figure 16 was 0.346 and 0.568 kg. Here, also as in the case of Forestburg coal, the tar yield decreases with incresing content of char in the bed because of the catalytic effect of the char on the secondary cracking and polymerization reactions as evidenced by the increase of gas and char yields.

5.5.2 Effect of temperature

The temperature range studied for Sukunka coal was 480-650°C. The effect of temperatue on tar and char yield is shown in Figure 17. A maximum tar yield of 30.6% was obtained at 600°C. This is

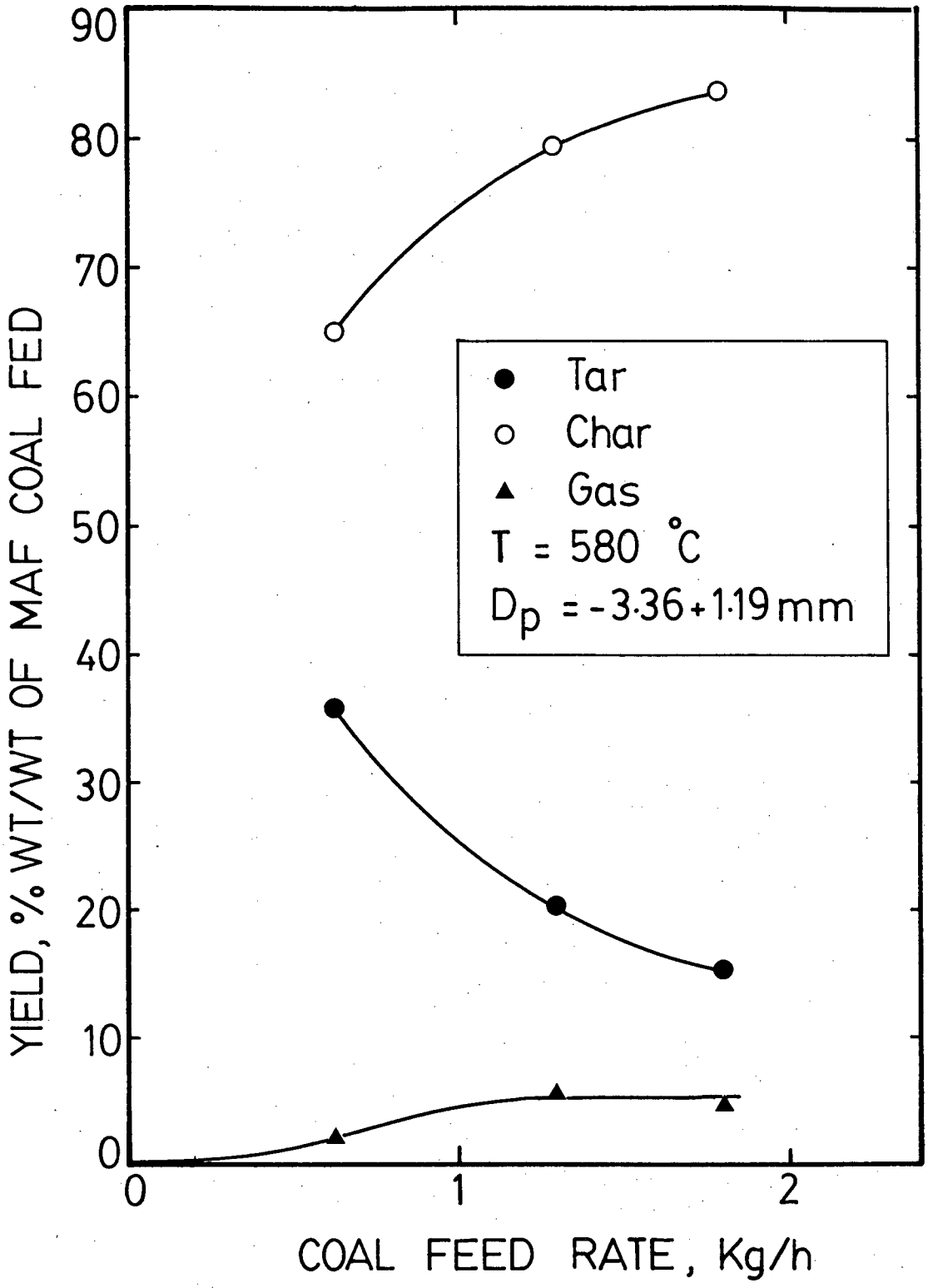

Figure 16 - Effect of coal feed rate on product yield - Sukunka coal.

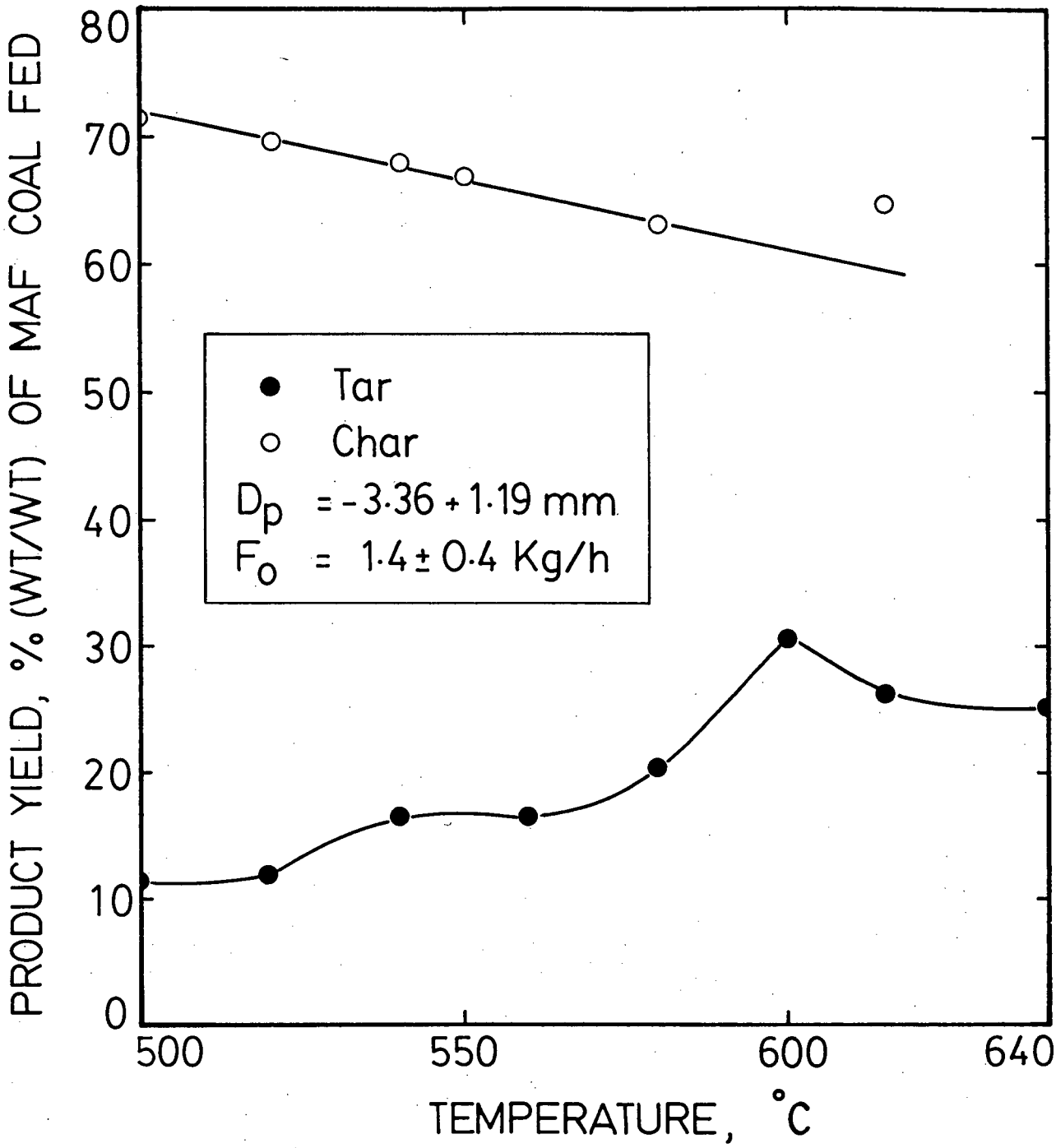

Figure 17 - Effect of temperature on tar and char yield - Sukunka coal.

a promising yield of tar and suggests that Sukunka coal might be a good pyrolysis feedstock. One possible reason for the high tar yield is the high exinite content of this coal as noted in Table 12. The char yield at the temperature of maximum tar yield (600°C) is 61%, and the corresponding gas yield (Figure 18) is 0.6% for hydrogen and 3% for methane. A low yield of carbon oxides was obtained because of the low oxygen content of the Sukunka coal. Small amounts of ethane and ethylene were obtained. The total volatile yield at 600°C (tar + gas) is about 36% which is significantly higher than the 24% volatiles by the proximate volatile matter method obtained at 950°C. As the total volatile yield increases with temperature, an even higher volatiles yield will be produced under rapid pyrolysis conditions at higher temperature.

Scott et al.[37] obtained about 20% maximum tar yield from a bituminous coal (DEVCO) at a relatively high temperature of 750°C. They obtained a total gas yield of 8.8% and a char yield of 56% at this temperature. Tyler[34] and Edwards and Smith[35] pyrolysed a variety of bituminous Australian coals in a 3 cm and 15 cm diameter fluidized bed reactors respectively. They obtained similar results from the above two reactors with Millmerran coal giving as high as 35 wt% tar yield at 600°C.

It is important to note that no serious operating problems with the spouted bed occurred during the runs with this strongly agglomerating coal which has a free swelling index of 7. Relatively small pieces of agglomerating char and sand particles were noted after

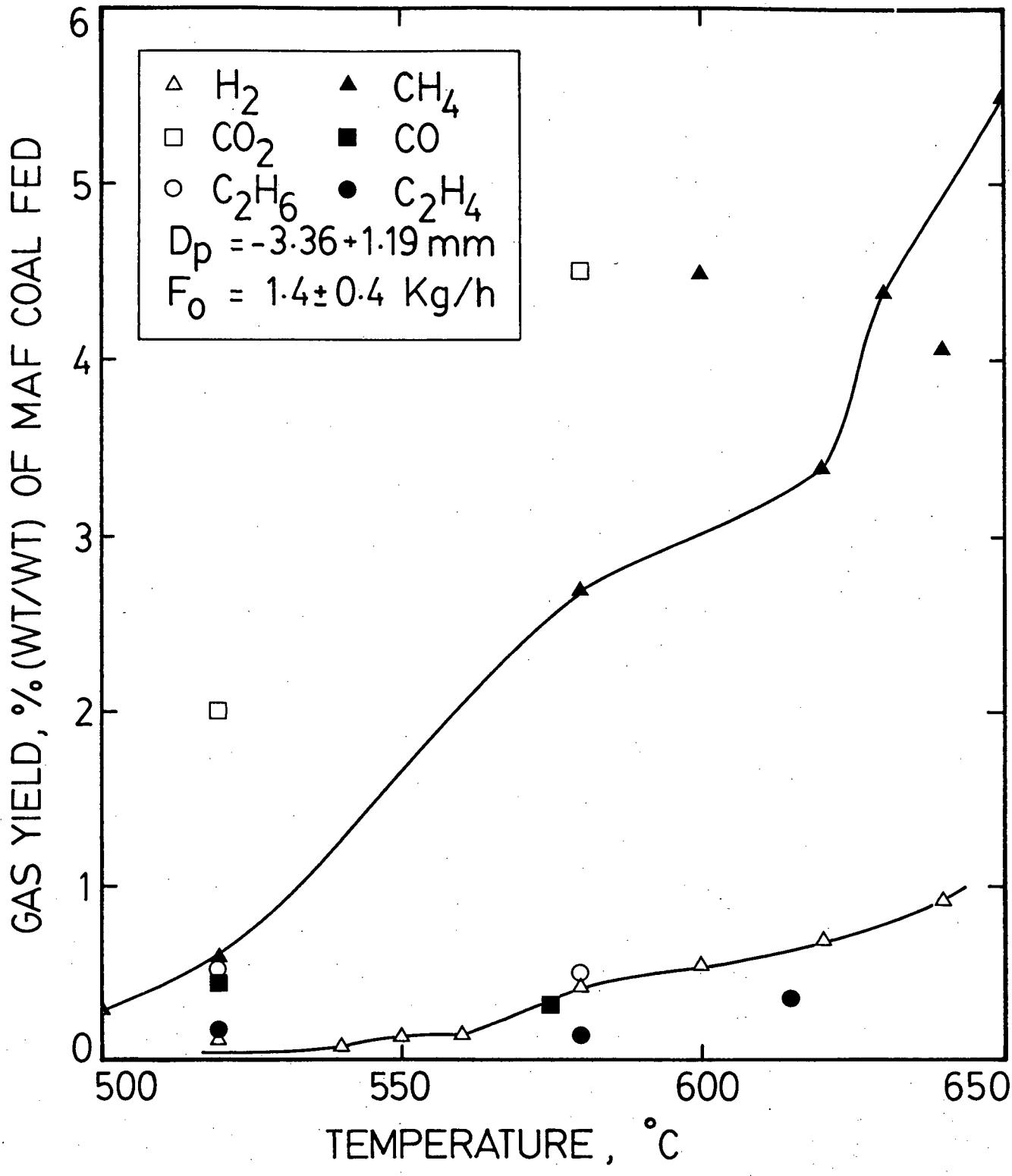

Figure 18 - Effect of temperature on yield of gaseous species - Sukunka coal.

emptying the reactor as shown in Figure 9. Agglomerates shown in Figure 9b and 9c represent a small fraction of the total char. Screen analysis of this sample is shown in Table 14. The -6.73 + 3.36 mm fraction which is larger than fresh coal feed of -3.36 + 1.19 mm represents 22.6% of the total sample. Each small division in Figure 9 represents 1mm. By examining this sample and other char samples from Sukunka coal, it is noticed that the larger size fraction of the coal feed (roughly the -3.36 + 2 mm fraction) did not agglomerate but rather it was the smaller fraction (roughly the -2 + 1.19 mm fraction) which agglomerated and lumped together as shown in Figure 9b and 9c. This observation is of a potential importance with regard to agglomeration control in commercial plants, and may indicate an advantage of the spouted bed because of its ability to handle larger particles. However, more work in this area is needed to confirm this observation. It was necessary to quench the bed after each run; otherwise as was noticed in the early runs, the bed of sand and char would solidify into big lumps of clinker after shut down. In the early runs the bottom part of the reactor had to be dismantled and the clinkers had to be broken down in order to empty the reactor. Edwards and Smith[35] also reported no operating problems with the pyrolysis of some agglomerating Australian coals in a fluidized bed. McCarthy[57] studied the effects of pre-oxidation and of oxygen in the inlet gases on formation of agglomerated material during the pyrolysis of some Australian coals. He found that addition of oxygen to nitrogen (oxygen concentration 2.6 - 10.5% v/v) in the inlet gas during flash pyrolysis at 600°C significantly reduced the amount of char agglomerate

formed from a relatively strongly caking Liddel coal and a weakly caking Millmerran coal. He also subjected Liddel coal to preoxidation at 400°C and found that this treatment effectively reduced agglomeration of this coal. He did not report the effect on tar yield from this kind of treatment. However, it is known[58] that preoxidation of coal causes a significant decrease in tar yield. Many other methods to control agglomeration have been investigated. These include the bed recirculation procedures adopted by Westinghouse[59] in their gasification process. Heat treatment of the coal feed or staged operation with successively increased temperatures has also been used as in COED[60] process. Chemical treatment of the feed will require consumption or recycling of chemicals such as sodium or calcium hydroxide[61].

5.5.3 Effect of Bed Height

The effect of sand bed height on product yield from Sukunka and Forestburg coals is shown in Table 15. It seems that bed height has no clear effect on tar yield over the narrow range tested. If the height of the bed is less than the height of the heated section (38 cm) of the reactor, then the hot reactor wall just above the bed of sand could lead to some tar cracking. This may explain the decrease in gas yield at essentially equal char yield from Forestburg coal as the bed height was raised from 20 cm to 34 cm.

5.5.4 Effect of vapour residence time

The effect of mean vapour residence time is shown in Table 16. The vapour residence time was estimated from the spouting gas

Table 15 - Effect of Sand Bed Height

Coal	Temperature °C	Run No.	Bed Height* (cm)	Yield wt. % MAF Coal		
				Tar	Gas	Char
Sukunka	560	49	34	15.9	7.3	72
		56	38	16.5	5.8	65.5
		64	45	15.5	7.4	-
Sukunka	580	58	38	20.4	5.7	63.3
		60	45	17.5	7.5	64.8
Forestburg	480	11	20	-	12.4	69.9
		31	34	-	8.3	69.6

*static bed height

Table 16 - Effect of Vapour Residence Time

Coal	Temperature °C	Run No.	Gas Velocity (m/s)	Vapour Residence Time*(s)	Yield wt. % MAF Coal		
					Tar	Gas	Char
Sukunka	560	56	0.86	1.15	16.5	5.8	65.5
		64	1.01	0.98	15.5	7.4	-
		65	1.45	0.68	16.7	7.0	-

*calculated from spouting gas velocity at temperature

velocity and the distance the vapours travel from the bottom of the reactor to the inlet of the impingers. It was varied by changing the spouting velocity, although there is little flexibility to vary this parameter over a wide range. In a spouted bed the gas residence time distribution is intermediate between that of a packed bed and a perfectly mixed tank.[26] Thus the mean residence time is only a rough indication of the time the vapour has for reaction. The time the vapour spends in the bed of sand is less than half the total shown in the table. There seems to be no marked effect on tar yield of vapour residence time over the range shown. It must be emphasized here that this conclusion is only valid over the narrow time range shown. It is known that holding hot organic vapours over longer times will probably lead to some cracking or polymerization of the unstable radicals leading to reduction in tar yield which must be avoided in a plant aiming at maximizing liquid yield. Nevertheless, in a commercial plant, the vapour residence time in a reactor is expected to be of the order shown. The effect of vapour residence time will be studied further by McCafferty[62] who has designed a reactor where a large range in times can be accommodated to permit more definitive results to be achieved.

Edwards et al.[35] measured tar yields simultaneously at two points in their apparatus with a vapour residence time of 0.7 s to 1 s and noticed a slight decrease in tar yield (e.g. 31.5 wt% vs. 30 wt/%) at the position with longer residence time.

5.5.5 Effect of Particle Size

The effect of coal particle diameter on tar yield is shown in Figure 19. The tar yield decreases with increasing particle size.

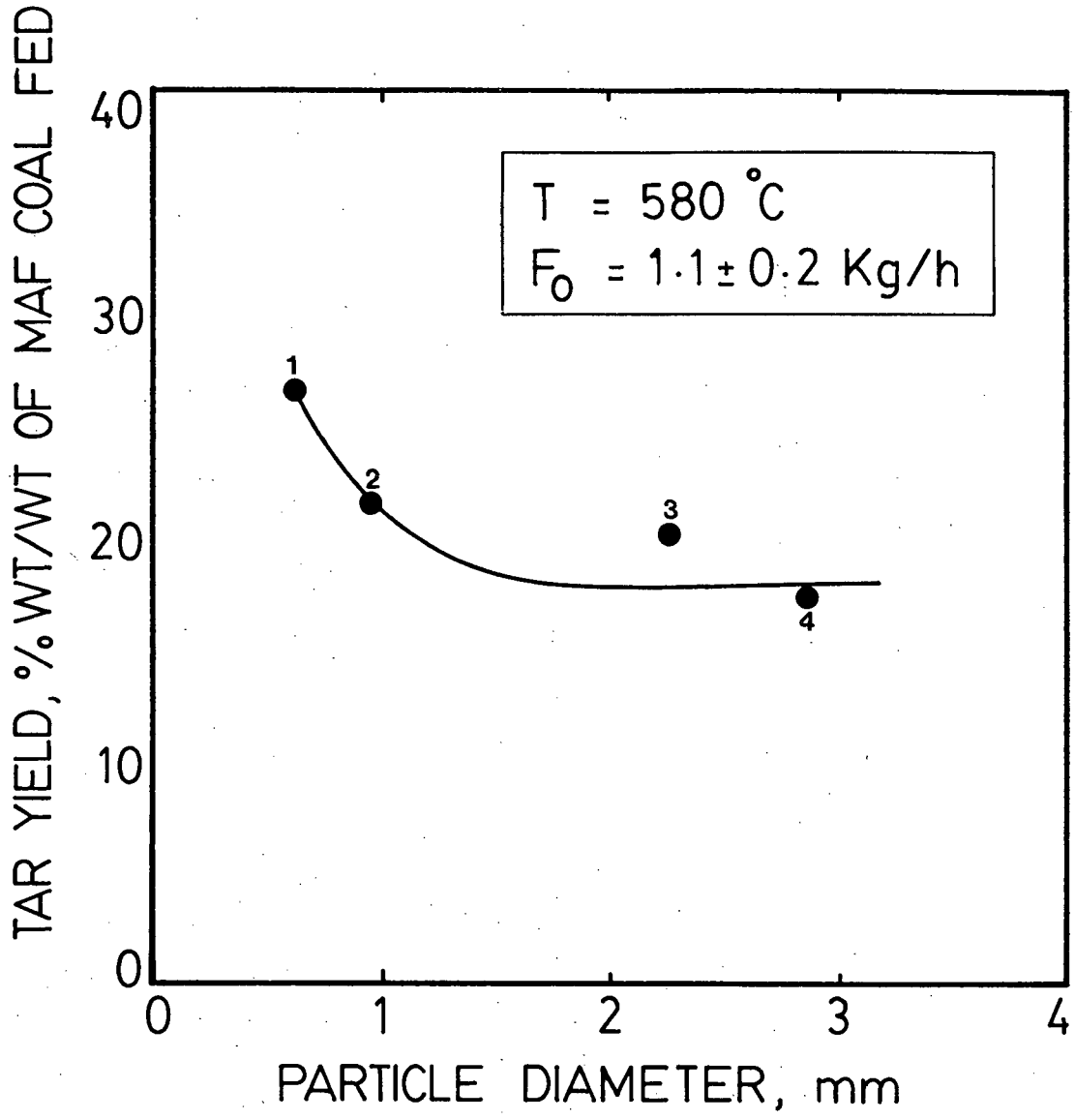

Figure 19 - Effect of coal particle size on tar yield - Sukunka coal. Size range is for (1) - 0.707 + 0.595 mm, (2) - 1.19 + 0.707 mm, (3) - 3.36 + 1.19 mm, (4) -3.36 + 2.38 mm.

The decrease is rather large at first then goes to an asymptotic value. The coal feed rate and the duration of the run was approximately constant for all these runs. The decrease in tar yield reflects an increased extent of secondary reactions for larger particles which offer more resistance to the escape of volatiles. The asymptotic behavior, apparently reflects the depletion of the tarry species susceptible to these secondary reactions. It was not possible to test smaller particle sizes than the smallest one shown in this figure because of the difficulty encountered with feeding these smaller sizes using the vibratory feeder. However, it would be expected that the increase in tar yield with decreasing particle size would level off at the critical diameter (see section 2.3.2) where the mass transfer effect is diminished and the pyrolysis process becomes chemically controlled.

Anthony[63] varied particle size over the range 53-1,000 μm of Pittsburgh bituminous coal in pyrolysis experiments with a wire mesh heater. He noticed 3 wt% (as received) decrease in weight loss over the above particle size range. Tar yield was not measured. Suuburg[30] studied the effect of partice size on pyrolysis products from the same coal and over the same particle size. He observed that tar yield decreased from 23% to 18% with increasing particle size over the above size range.

5.5.6 Effect of pyrolysis atmosphere

In a commercial pyrolysis process heat for the pyrolysis reaction could be provided by hot flue gases arising from combustion of part of the solid char. It was of interest to determine if the presence of CO_2 in the nitrogen used would result in any changes during pyrolysis. Thus CO_2 was mixed with nitrogen in the spouting gas. From

Table 17 - Pyrolysis of Sukunka Coal in CO_2 - N_2 Mixture

Temperature °C	Yield in N_2 Wt. % MAF Coal				Yield in 15% CO_2 - 85% N_2 Wt. % MAF Coal			
	Run No.	Tar	Gas	Char	Run No.	Tar	Gas	Char
500	21	11.2	3.4	72.0	75	10.7	4.8	77.4
500	48	11.9	4.1	69.7	73	11.0	6.0	74.5
580	58	20.4	5.7	63.3	76	17.6	5.4	68.3

Table 17, a small decrease in tar yield is noticed from the runs with CO_2 while the char yield increased. These effects appear significant compared to the reproducibility of the experiments (p. 150).

5.6 Balmer coal

Balmer coal is a medium volatile bituminous coal from the Crowsnest coal field in south eastern British Columbia. Two different coal samples, labelled Balmer A and Balmer B were used. Their proximate, ultimate, and maceral analyses are given in Table 12. Balmer A shows a high ash content compared to Balmer B. The low sulphur content of both Balmer coals is also noted from this table.

5.6.1 Effect of temperature

The effect of temperature on tar and char yield from Balmer A coal is shown in Figure 20. The maximum tar yield of 12.1% was obtained at 620° C. The behavior of this coal is different from the others as evidenced from the char yield in Figure 20 and the methane yield in Figure 21. The char yield does not steadily decrease with temperature as would normally be expected, but shows a fluctuating behavior. This perhaps reflects the importance of polymerization reactions increasing in certain temperature ranges. It is speculated that the high ash content of Balmer A coal catalyses these polymerization reactions resulting in a relatively low tar yield and high char yield. Surface oxidation could produce the same effect. The char yield at the temperature of maximum tar yield is about 76%. The effect of temperature on the yield of hydrogen and methane is shown in Figure 21. The hydrogen yield at 620° C is 0.5% and the methane yield is 3%. The methane yield shows an interesting fluctuating behavior.

The effect of temperature on tar and char yield for Balmer B

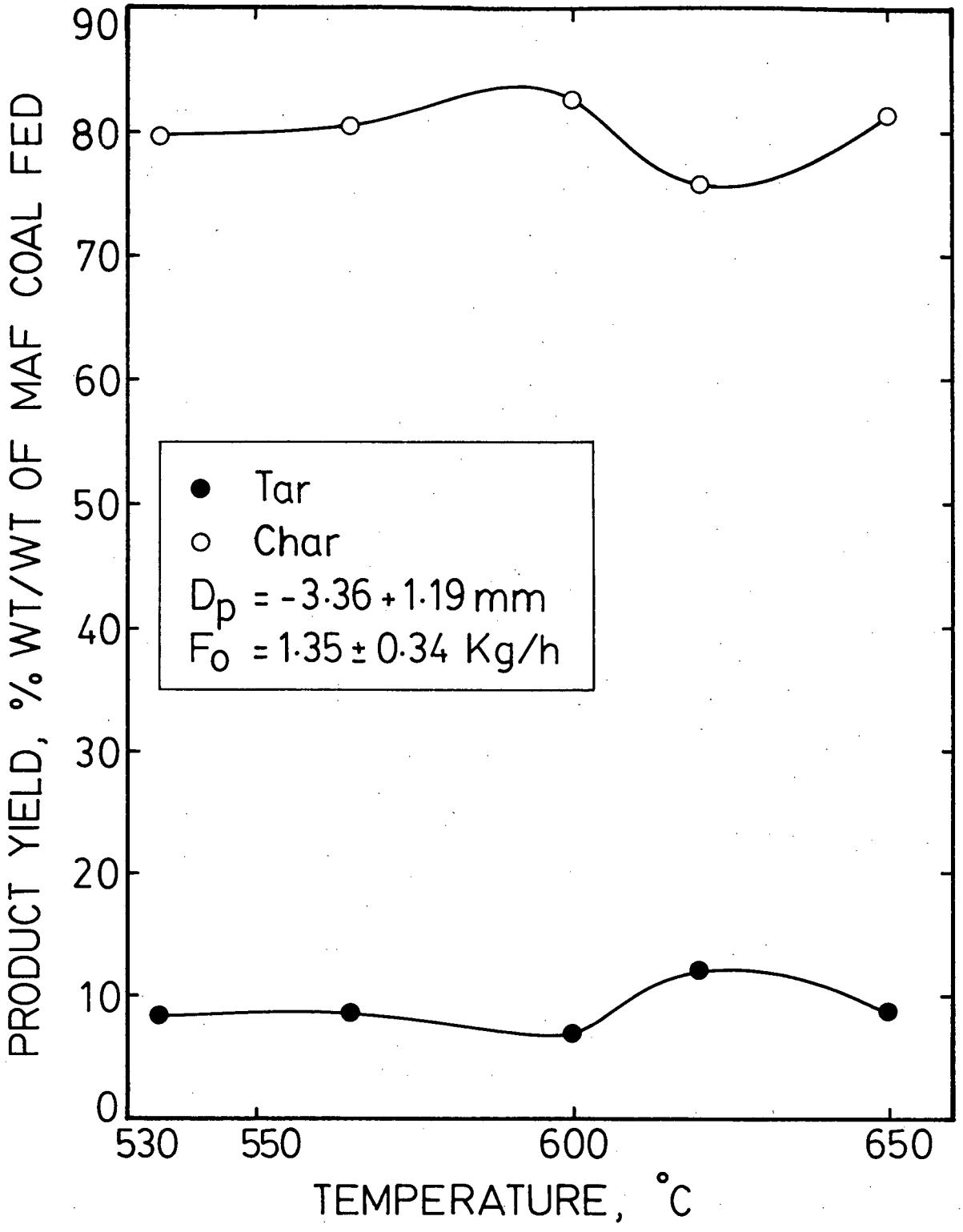

Figure 20 - Effect of temperature on tar and char yield - Balmer A coal.

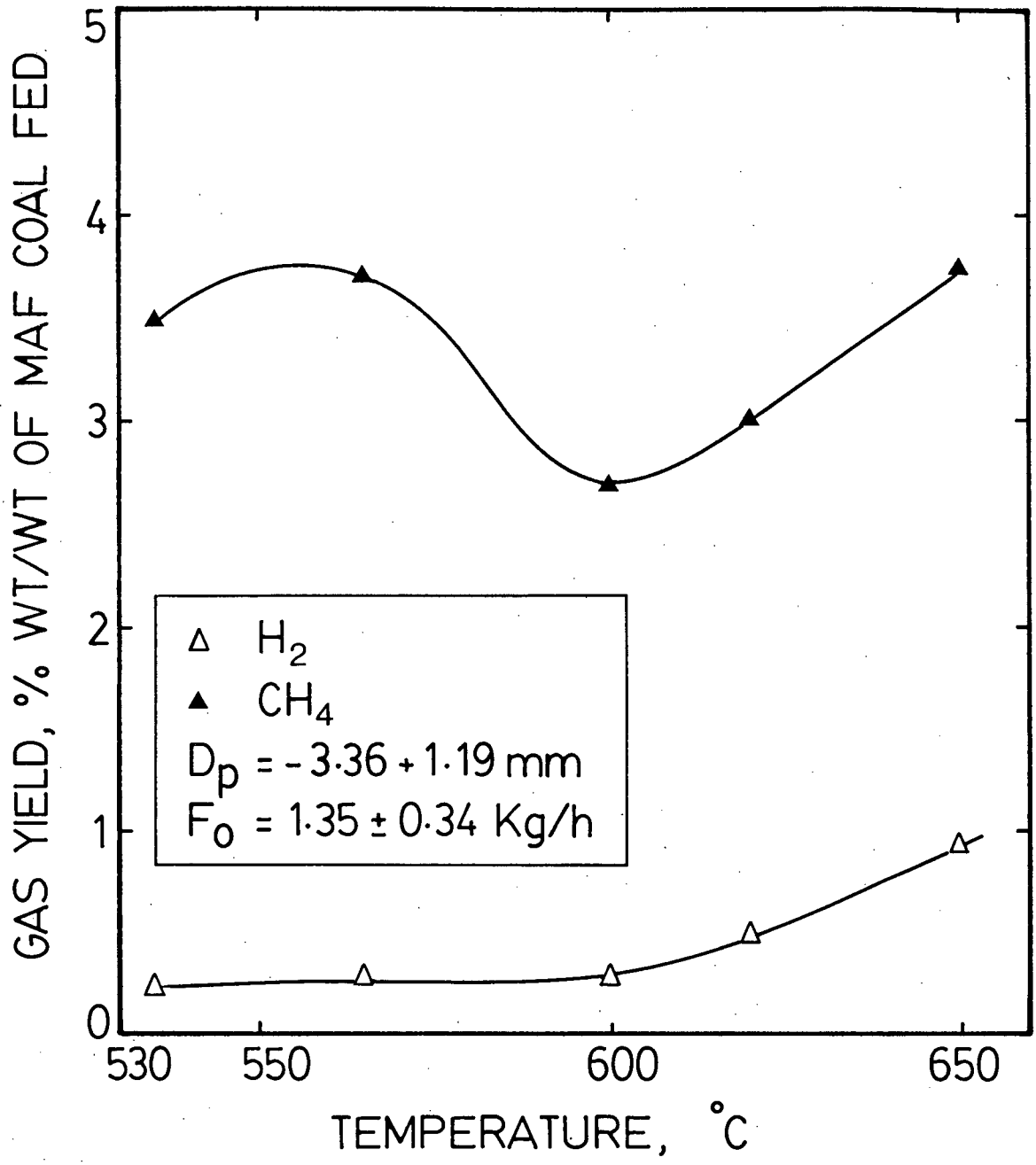

Figure 21 - Effect of temperature on hydrogen and methane yield - Balmer A coal.

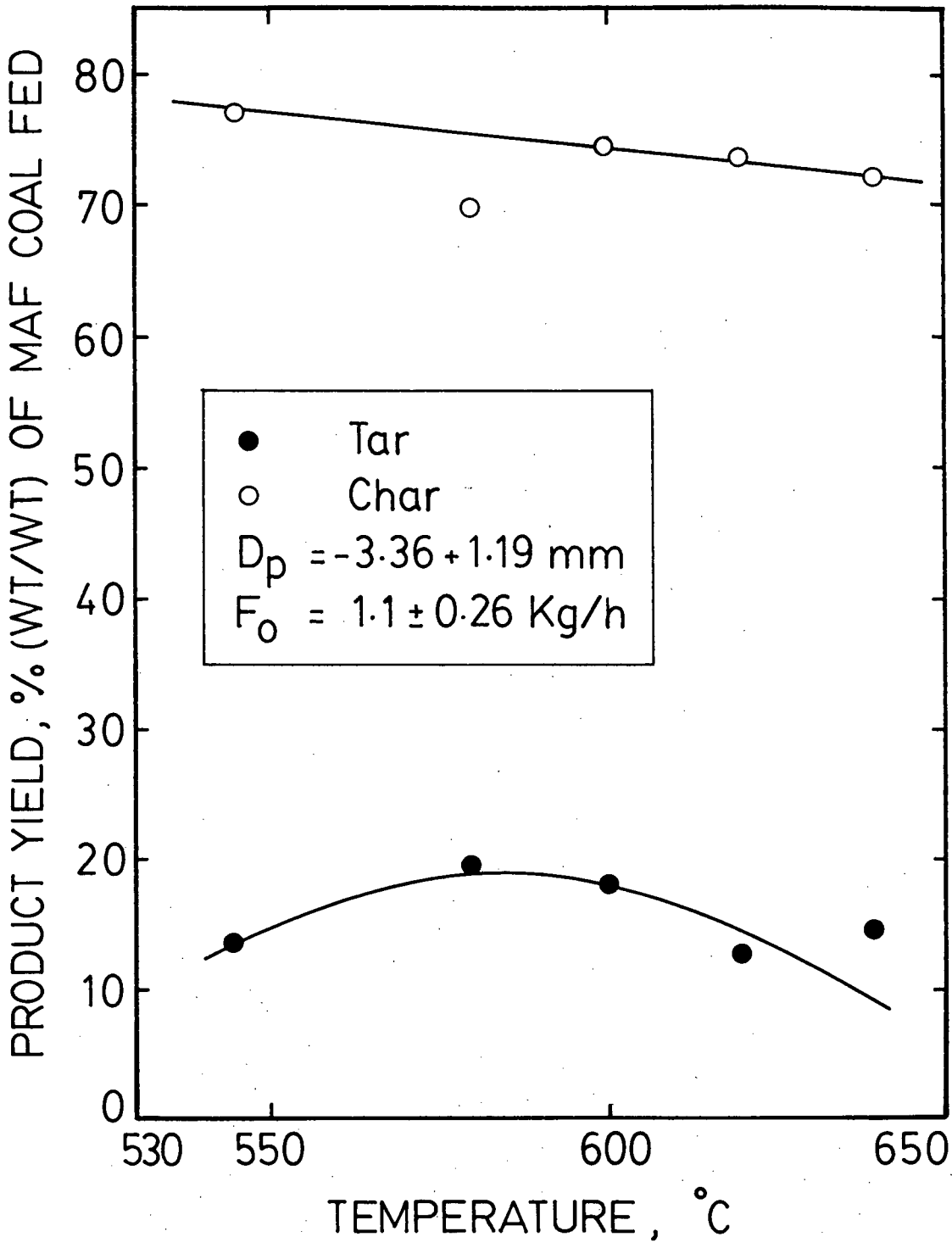

Figure 22 - Effect of temperature on tar and char yield - Balmer B coal.

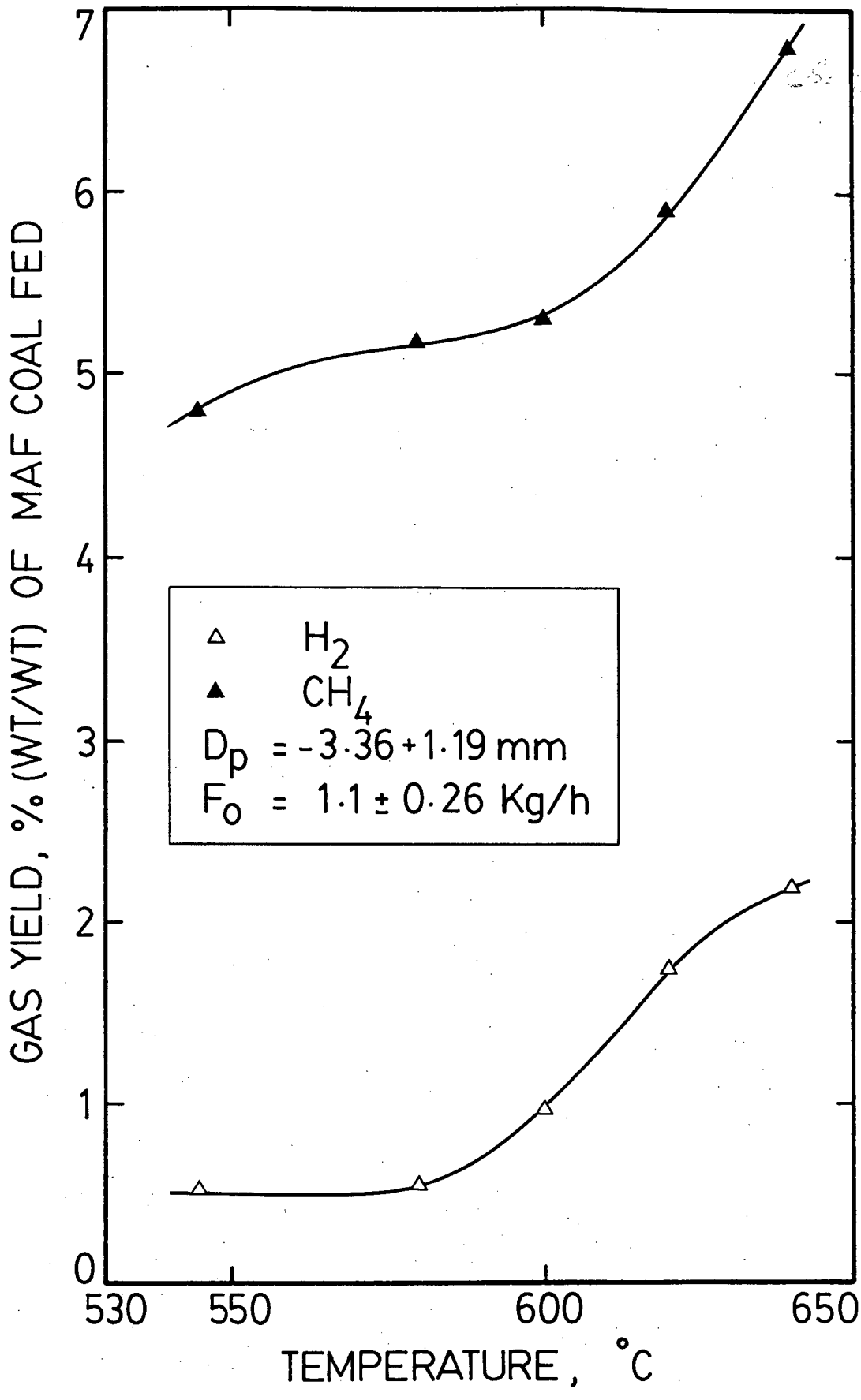

Figure 23 - Effect of temperature on hydrogen and methane yield - Balmer B coal.

coal shown in Figure 22, both exhibit behaviour typical of most other coals. The maximum tar yield of 19.4% was obtained at 580° C. The char yield at this temperature is about 70%. The hydrogen and methane yields are shown in Figure 23. They also behave as generally expected. A hydrogen yield of about 0.6% and a methane yield of about 5% were obtained at the temperature of maximum tar yield. Here again no carbon oxides were detected because of the low oxygen content of the coal. Here also a higher volatiles yield than from the proximate analysis (23%) is expected. At 580°C the tar + gas yield was 25.2%.

5.7 Char and tar compositions and total and elemental material balances

Analysis of the product char provides a means to determine the amount of hydrogen left in it and consequently the feasibility of a second degasification of this char at higher temperatures to recover further useful volatile products. It may also give clues to its combustion behaviour. The partitioning of the sulphur and nitrogen of the coal between the solid and volatile products of pyrolysis is important for tar upgrading as well as in pollution control in the pyrolysis process.

The composition of char from Forestburg coal is shown in Figure 24 as a function of pyrolysis temperture. As expected the carbon content of the char increased with temperature while that of the hydrogen decreased. The oxygen content also decreased while the nitrogen exhibited a slight increase. In this figure the oxygen plus sulphur content is given by difference which will increase its potential

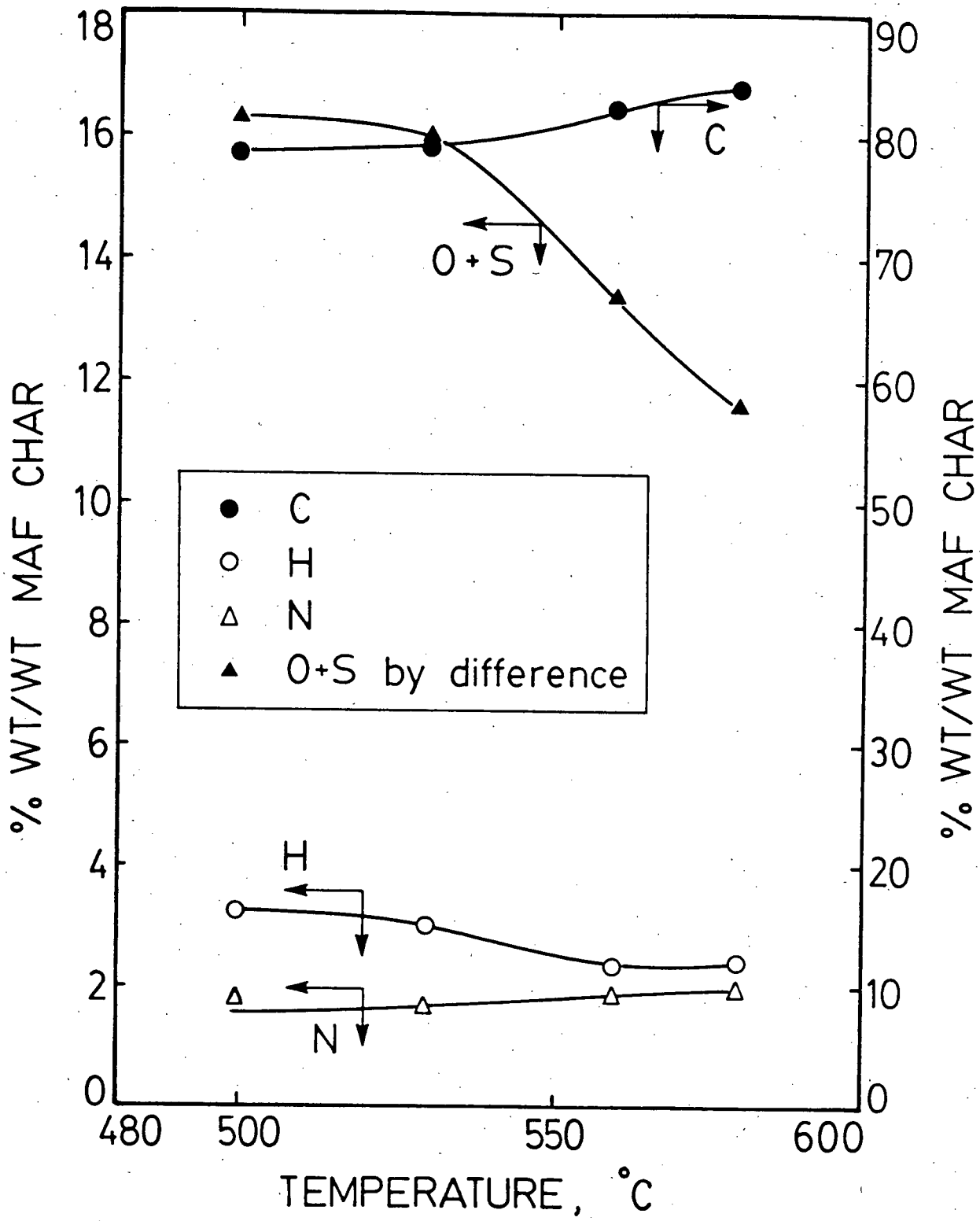

Figure 24 - Composition of char from Forestburg coal.

uncertainity. The sulphur content alone was determined for tar and char only at the conditions of maximum tar yield. Total and elemental material balances for runs for which tar and char analysis was performed are given in Table 18. Total material balances closed within about 3% for temperatures equal or less than 540°C while for temperatures of 560 and 580°C, the closure was within about 9% and 14% respectively. These two runs were repeated twice and similar results were obtained. One reason for the loss of material at these higher temperatures might be that some of the tar fraction cracked to lighter liquid hydrocarbons which have a boiling point lower than 100°C and which would have been lost during the solvent evaporation procedure (see Section 4.2.2). Elemental balances obviously are related to the total material balances. Hydrogen balances give the poorest closure, probably because of the low weight % in the coal, and the char and possibly because of the loss of volatiles mentioned above. At the temperature of maximum tar yield (530°C) about 27% of the carbon and 53% of the hydrogen is devolatilized. At this temperature about 80% of the original nitrogen remains in the char. Also at this temperature, the percentage of sulphur in the char is 0.7 wt% (MAF) while that in the parent coal is 0.58%. Hence about 80.7% of the original sulphur remains in the char. In general the sulphur content of the Western Canadian coals, especially the Balmer coal, (Table 12) is low compared to Eastern coals which give them a certain advantage. Torrest et al.[64] used steam for the pyrolysis and desulphurization of a Texas lignite (Alco D) of particle size 550 μm in a free fall reactor and managed to reduce the organic

Table 18 - Forestburg Coal; Product yield (Wt. %) MAF coal fed and total and elemental material balances

Run No.	35			33				34	40			32
Temperature °C	500			530				540	560			580
	Total	C	H	Total	C	H	S	Total	Total	C	H	Total
H_2	0.13	-	0.13	0.17	-	0.17	-	0.18	0.37	-	0.37	0.48
CH_4	1.46	1.1	0.37	1.95	1.46	0.49	-	2.2	2.7	2.02	0.68	3.2
CO_2	9.4	2.56	-	13.6	3.7	-	-	14.5	14.9	4.06	-	15.1
CO	2.8	1.2	-	-	-	-	-	-	-	-	-	4.6
Tar	13.2	9.54	0.85	21	15.66	1.59	0.124	19.9	6.8	5.16	0.51	5.22
Char	70.4	55.33	2.25	66.9	53.12	2	0.468	65.5	66	54.36	1.56	59.6
Total	97.4	69.73	3.6	103.6	74.13	4.25	0.592	102.3	90.8	65.6	3.12	86.6
Closure	97.4	91.3	90	103.6	97	105	102	102.3	90.8	86	77.6	86.6

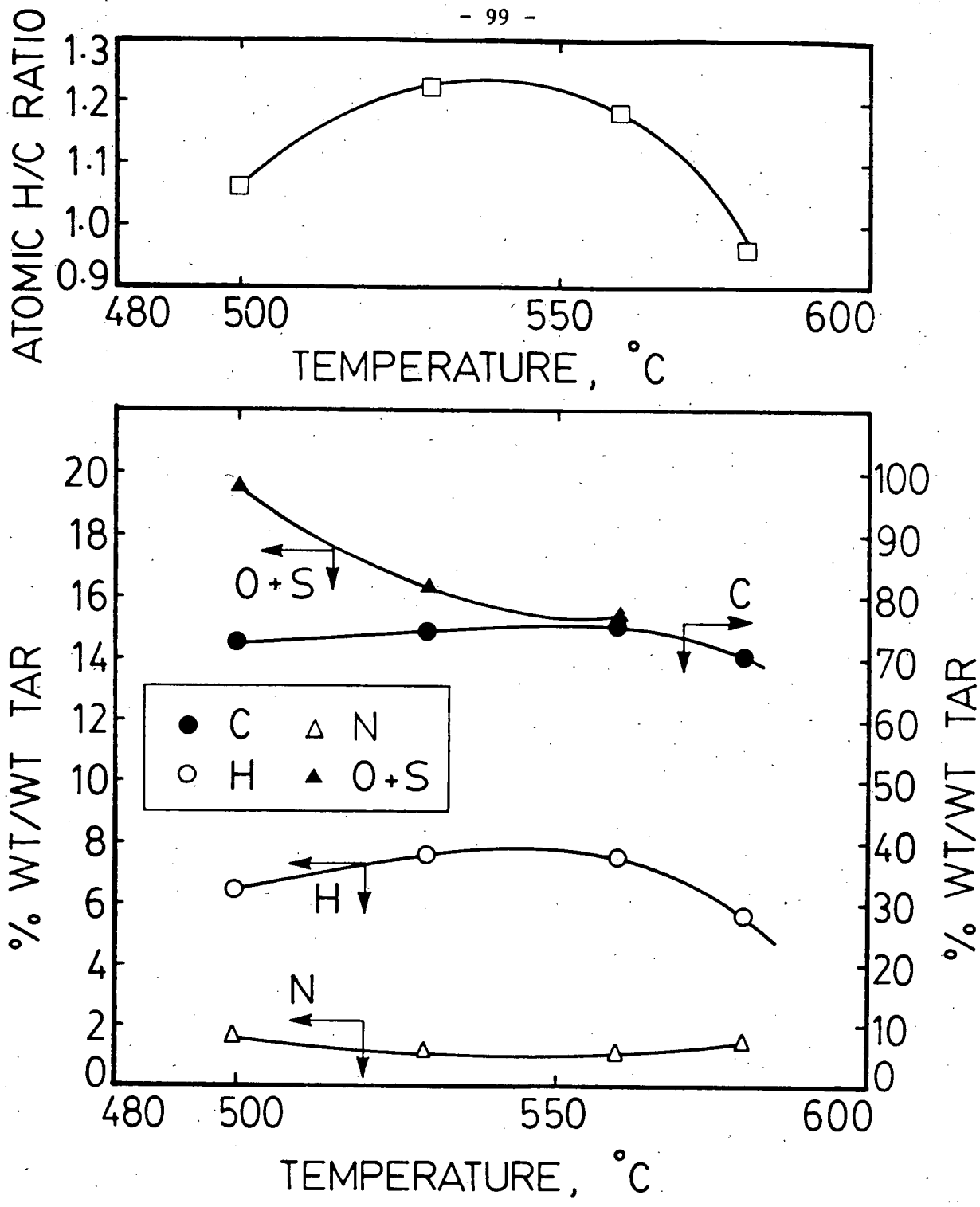

Figure 25 - Composition of tar from Forestburg coal.

sulphur of the lignite from $\geq$ 1.3 wt% to $\leq$ 0.8 wt% over a temperature range of 700 - 800°C. Tables showing the ash content of some char samples obtained from all the coals tested at different temperatures are shown in Appendix B. The heating value of Forestburg char produced at the temperature of maximum tar yield (530°C) is 28.7 MJ/Kg.*

The composition of tar from Forestburg coal and the H/C atomic ratio are shown in Figure 25. The tar is more enriched in hydrogen compared to the parent coal as would be expected. The hydrogen content of the tar is important in that it affects the amount of additional hydrogen required when the tar is upgraded to liquid fuel. The H/C atomic ratio of Forestburg tar goes through a maximum value of 1.22 at the temperature of maximum tar yield which is a fortunate circumstance. The sulphur content of the tar at this temperature is 0.59 wt%.

The composition of char from Sukunka coal is shown in Figure 26. It generally exhibited behaviour similar to that of Forestburg coal. Total and elemental material balances for runs for which tar and char analyses were performed are given in Table 19. Material balances closed within about 10%. At 600°C, the temperature of maximum tar yield the sulphur content of the MAF char is 0.69 wt%, and the heating value of the char produced at this temperature is 34.9 MJ/Kg.*

The composition of tar from Sukunka coal is shown in Figure 27. Here also the tars appear to be more enriched in hydrogen compared to the parent coal but the H/C atomic ratio steadily falls with temperature. At 600°C, the temperature of maximum tar yield, the H/C atomic ratio of the tar is 0.99 which is significantly higher than the value of 0.6 for the parent coal. However, in a commercial plant both

*Estimated using the Dulong formula

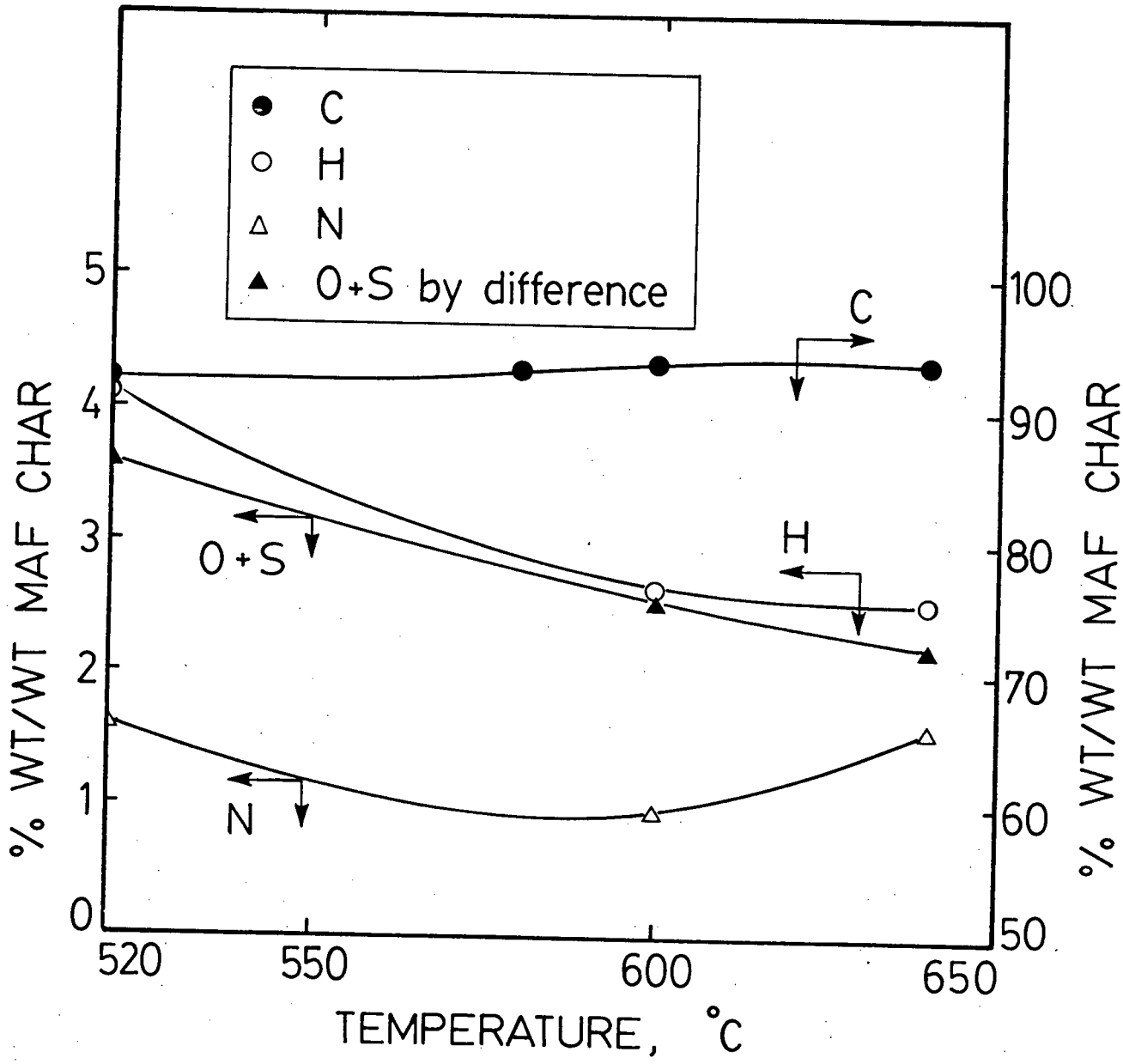

Figure 26 - Composition of char from Sukunka coal.

Table 19 - Sukunka Coal; Product yield (Wt. % MAF coal fed) and total and elemental material balances

Run No.	48			59	58			45			61		
Temperature °C	520			540	580			600			640		
	Total	C	H	Total	Total	C	H	Total	C	H	Total	C	H
H_2	0.14	-	.14	0.1	0.44	-	0.44	0.57	-	0.57	0.93	-	0.93
CH_4	0.6	0.45	0.15	1.3	2.72	2.04	0.68	3	2.25	0.75	4.07	3.05	1.02
C_2H_4	0.17	0.15	0.02	0.16	0.15	0.13	0.02	-	-	-	-	-	-
C_2H_6	0.52	0.42	0.1	0.5	0.46	0.37	0.09	-	-	-	-	-	-
CO	0.67	0.29	-	-	0.67	0.29	-	-	-	-	1.7	0.73	-
CO_2	2	0.55	-	2.8	1.3	0.35	-	-	-	-	3.4	0.93	-
Tar	11.9	9.6	0.91	16.5	20.4	17	1.17	30.6	25.33	1.87	25.3	21.3	1.49
Char	69.7	64.3	2.86	67	63.3	58.9	1.63	61	57.18	1.6	57	53.4	1.46
Total	85.7	75.76	4.18	88.4	89.5	79.1	4.03	97.2	84.76	4.79	92.4	79.4	4.9
Closure	85.7	84.2	92.3	88.4	89.5	88	89	97.2	94.2	105	92.4	88.2	108

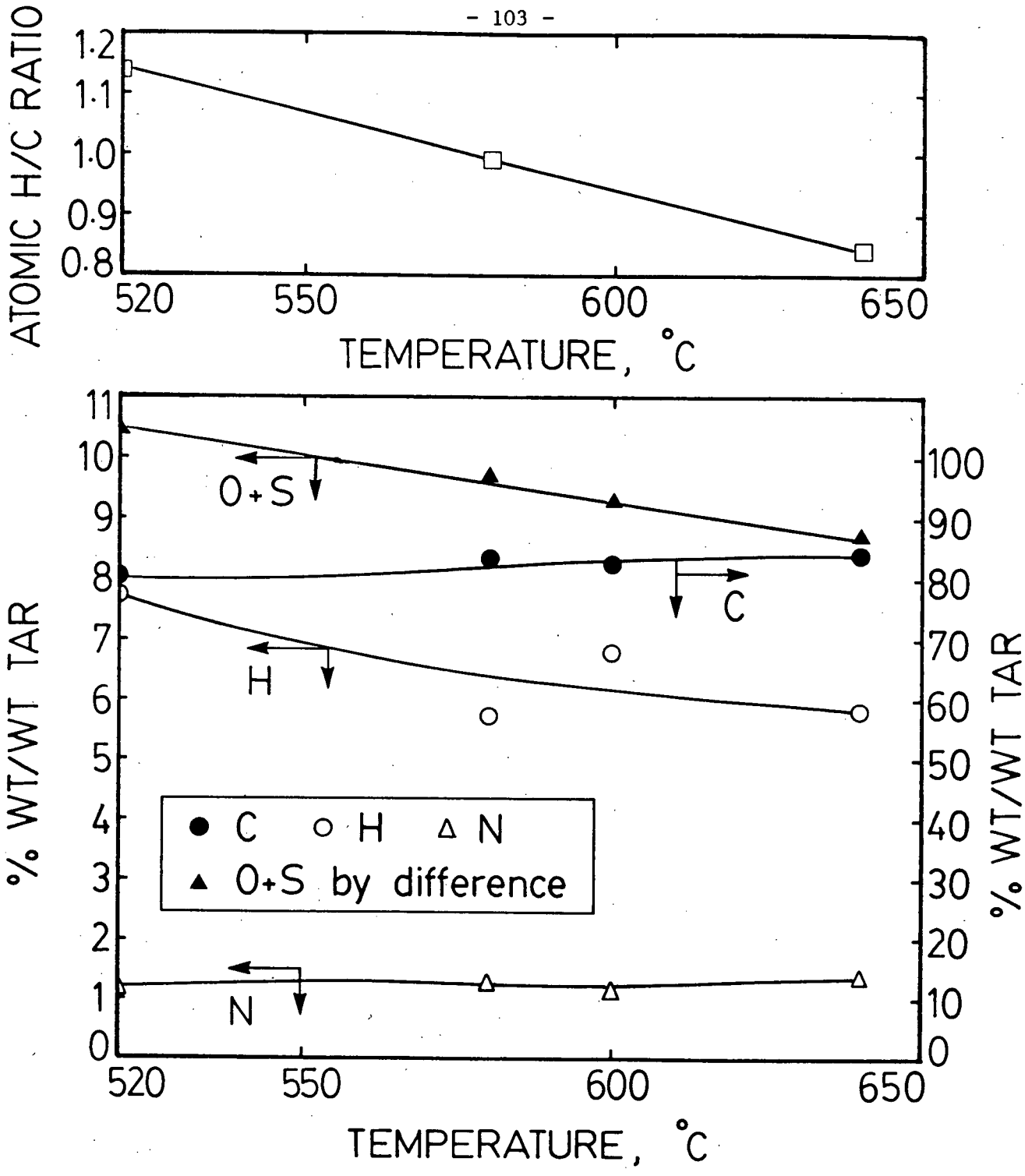

Figure 27 - Composition of tar from Sukunka coal.

the quantity and quality of tar will have to be optimized depending on the requirements of upgrading. The sulphur content of the tar at the temperature of maximum tar yield is 0.7%.

The composition of char from Balmer B coal is shown in Figure 28. This also shows expected behaviour of increasing carbon and decreasing hydrogen and oxygen content while nitrogen shows a very slight change with temperature. Total and elemental balances are shown in Table 20. Material balances closed within less than 5% which is better than balances for the other coals. This may result from less material (tar) lost due to a smaller fraction of lighter liquid hydrocarbons in the tar.

The composition of tar from Balmer B coal is shown in Figure 29. The H/C atomic ratio of this tar goes through a maximum as with Forestburg coal tar. Fortunately, the highest H/C ratio of 0.97 is obtained at the temperature of maximum tar yield (580°C).

Total material balances for Balmer A coal are shown in Table 21. They closed within 7%.

5.8 Comparison of results for the various coals

A comparison between the maximum tar yields for the various coals is given in Table 22. The compositions of tars and chars at the temperature of maximum tar yield is shown in Table 23. The highest tar yield of 30.6% was obtained from Sukunka bituminous coal at 600°C. The sub-bituminous Forestburg coal gave 21% tar yield at 530°C while that from the bituminous Balmer (B) coal was 19.4% at 580°C. The lowest maximum tar yield of 12.1% was obtained from Balmer A coal at 620°C.

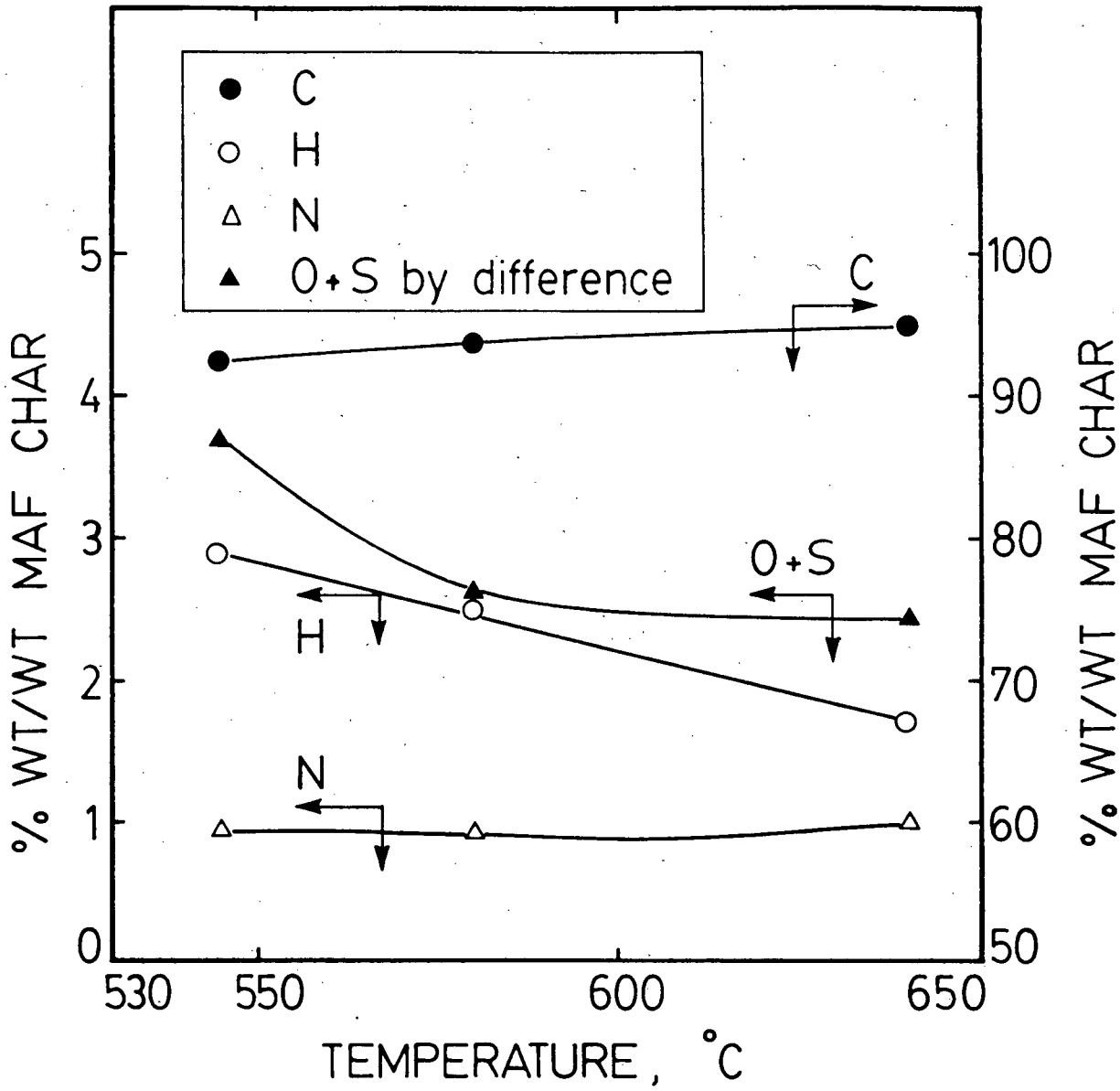

Figure 28 - Composition of char from Balmer B coal.

Table 20 - Balmer B Coal; Product yield (Wt. %) MAF coal fed) and total and elemental material balances

Run No.	84			80			82	79	83
Temperature °C	545			580			600	620	640
	Total	C	H	Total	C	H	Total	Total	Total
H_2	0.57	-	0.57	0.56	-	0.56	0.98	1.75	2.18
CH_4	4.8	3.6	1.2	5.2	3.9	1.3	5.3	5.9	6.8
Tar	13.6	11.4	.84	19.4	16.2	1.3	18.1	12.9	14.7
Char	77.2	71.33	2.24	69.9	65.7	1.75	74.4	73.6	71.9
Total	96.2	86.33	4.85	95.1	85.8	4.91	98.8	94.2	95.6
Closure	96.2	96.6	100	95.1	96	102	98.8	94.2	95.6

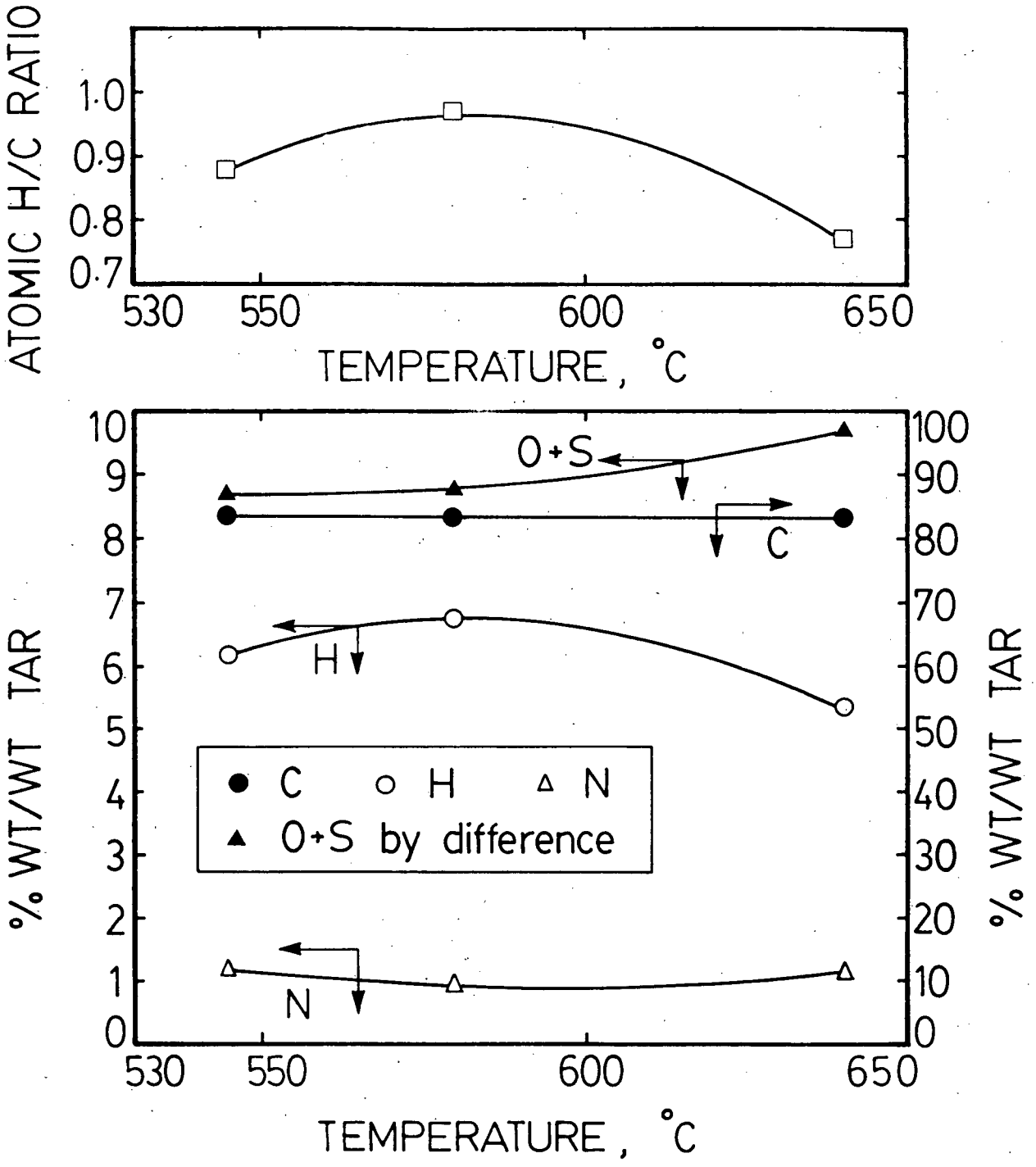

Figure 29 - Composition of tar from Balmer B coal.

Table 21 - Balmer A Coal; Product yield (Wt. %) MAF coal fed and total material balances

Run No.	72	68	69	70	78
Temperature °C	535	565	600	620	650
H_2	0.25	0.29	0.29	0.5	0.93
CH_4	3.5	3.7	2.7	3.02	3.74
Tar	8.4	8.6	7.1	12.1	8.9
Char	79.7	80.3	82.9	76	81.1
Total	91.9	92.9	93	91.6	94.7
Closure	91.9	92.9	93	91.6	94.7

Table 22 - Comparison of optimum product yields from various coals

Coal Type	Temperature of Maximum Tar Yield, °C	Yield as wt. % of MAF Coal Fed			
		Tar	Char	H_2	CH_4
Forestburg	530	21	66.9	0.17	1.95
Sukunka	600	30.6	61	0.57	3
Balmer A	620	12.1	76	0.5	3
Balmer B	580	19.4	69.9	0.56	5.2

Table 23 - Elemental composition of tars and chars at temperature of maximum tar yield

Coal Type	Temperature of Maximum Tar Yield, °C	Product Type	Elemental Composition, Wt. %				
			C	H	N	S	O
Forestburg	530	Tar	74.58	7.59	1.31	0.59	15.93
		Char	79.4	3	1.7	0.7	15.2
Sukunka	600	Tar	82.77	6.86	1.1	0.7	8.57
		Char	93.73	2.64	0.96	0.69	1.91
Balmer B	580	Tar	83.53	6.75	0.96	-	-
		Char	93.94	2.5	0.94	-	-

The temperature of maximum tar yield decreases with decreasing rank as is generally known. In terms of tar quality as indicated by the H/C ratio, Forestburg tar has the best quality. Its sulphur content is 0.59% compared to 0.7% for Sukunka tar. The effect of temperature on the yield of tar (Figure 30) from the bituminous coals is less profound than that from the sub-bituminous coal. This suggests that the tar from the sub-bituminous coal is more susceptible to cracking at higher temperatures. By examining the proximate and ultimate analyses of Sukunka and Balmer (B) coals in Table 12, it is seen that they have almost identical composition, yet, they gave markedly different tar yields. Thus, these analyses alone might not be sufficient to predict and compare tar yields and knowledge of the maceral composition is important. A large quantity of carbon oxides was obtained from the sub-bituminous Forestburg coal because of its large oxygen content. The highest methane yield was obtained from Balmer (B) coal and the lowest from Forestburg coal. Balmer (B) coal also gave the highest hydrogen yield while the lowest was obtained from Sukunka.

For Forestburg coal, the distribution of heating value among products produced at the temperature of maximum tar yield is: 66.4% of the heating value of the coal ends up in the char, 24.3% in the tar, and 4.7% in the gas. While for Sukunka, 59% of the heating value of the coal ends up in the char, 30.7% in the tar, and 7% in the gas.

In terms of tar quantity Sukunka coal stands to be an excellent potential for a commercial pyrolysis venture.

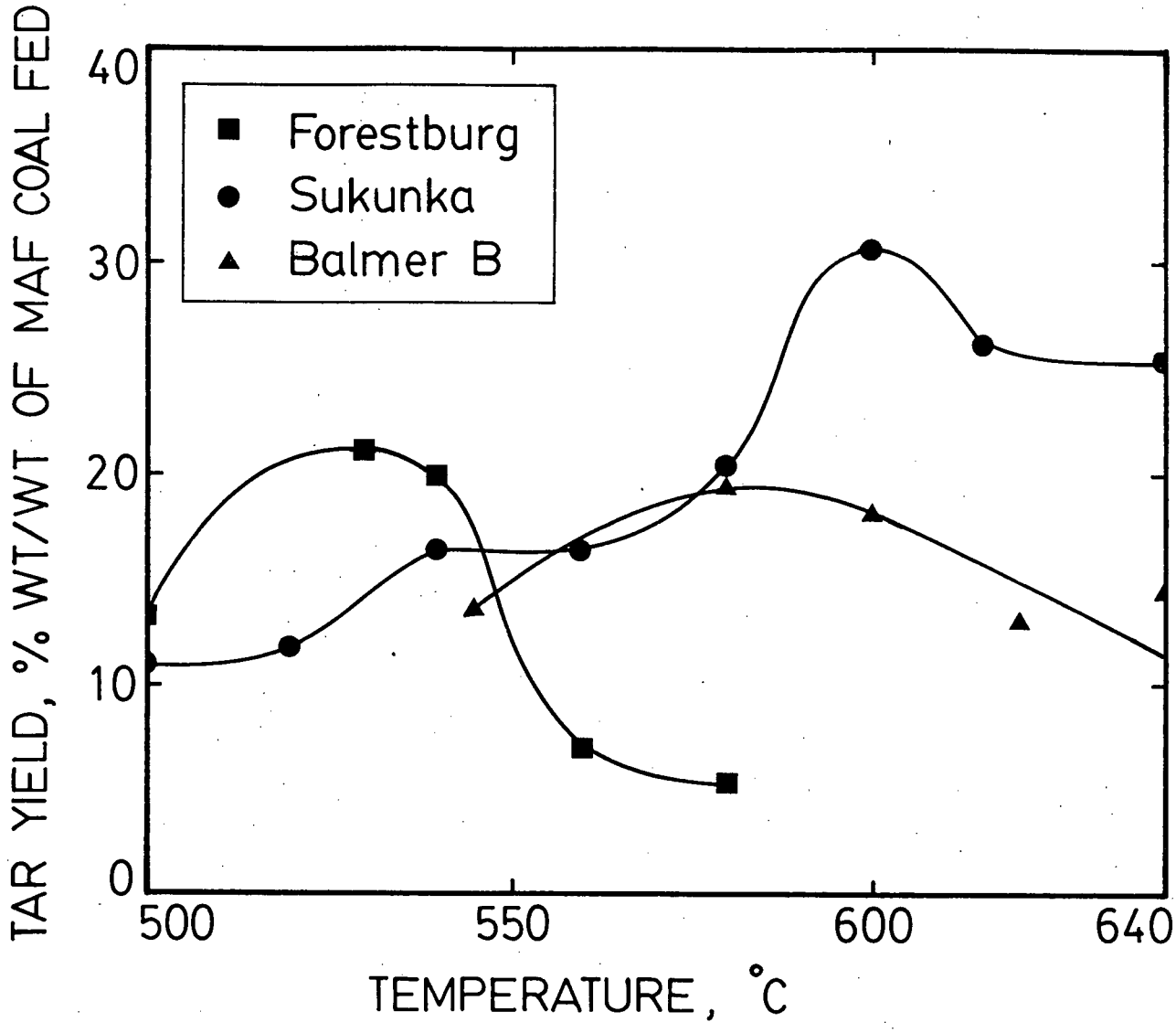

Figure 30 - Comparision of tar yields from various coals.

6. KINETIC MODEL FOR THE SEMI-BATCH COAL PYROLYSER

A simplified model was derived to predict the volatile matter content of the product char from which the volatiles yield (weight loss) can be calculated. In this model, the structure of the spouted bed is not taken into account and both the gas and the solids are considered to be backmixed. Because the char accumulates in the reactor with time, the reactor was considered to be a semi-batch variable mass reactor. The major assumption used to derive the kinetic model below is that the decomposition of the coal particle takes place isothermally. In Section 2.5, the time to heat up a typical particle was estimated to be 11 seconds. Since the average holding time of a particle is more than half an hour and the decomposition time ranges from 500 to about 2,000 seconds (Figures 34 and 35), then the above assumption of isothermality is justified. The configuration of the model is shown below:

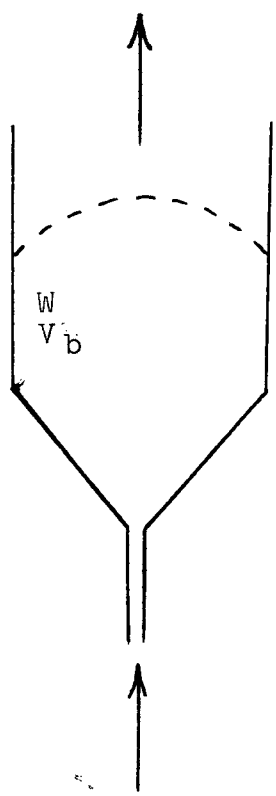

F_1 entrainment rate (g/s)

V_1 volatile fraction in the entrained char (MAF)

G_2 total gas rate out of reactor g/s

W is the weight of char in bed (g).

V_b is the volatiles fraction in char in bed (MAF)

F_o coal feed rate (g/s)

V_o volatiles fraction in the coal fed (MAF)

G_1 spouting gas rate (g/s).

Mass balance on volatiles

Volatiles entering Reactor with Coal	— Volatiles released by reaction and leaving in gas phase	— Volatiles carried out with entrained char	= Accumulation of volatiles in the reactor

$$F_o V_o - rW - F_1 V_1 = \frac{d(V_b W)}{dt} \qquad (6.1)$$

The rate of volatiles release is proportional to the remaining (yet to be released) volatiles content of the coal/char. This rate is assumed to be first order.

$$r = kV_b$$

Assuming a well mixed reactor: $V_1 = V_b$

$$\therefore \quad F_o V_o - k V_b W - F_1 V_b = \frac{d(WV_b)}{dt} \qquad (6.2)$$

Since the char is accumulating in bed, then W is a function of time. If we take $W_{average} = \overline{W} = W_{final}/2$ and treat $\overline{W}$ = constant, then equation 6.2 can be written as below. This simplification seems justified in that the average values of the tar yield and gas composition are measured in the experiment. It should be mentioned here that a model can readily be derived for the case where W is not constant as in Appendix C. While this model is more realistic, difficulties in solving for the rate constant precluded its use.

$$F_o V_o - k V_b \bar{W} - F_1 V_b = \bar{W} \frac{dV_b}{dt} \tag{6.3}$$

$$\frac{F_o V_o}{\bar{W}} - (k + \frac{F_1}{\bar{W}})V_b = \frac{d V_b}{dt} \tag{6.4}$$

let $\frac{F_o V_o}{\bar{W}} = A$, $k + \frac{F_1}{\bar{W}} = B$

then equation (6.4) becomes:

$$A - B V_b = \frac{d V_b}{dt} \tag{6.5}$$

integrate

$$\int_{V_o}^{V_b} \frac{d V_b}{A-B V_b} = \int_o^t dt$$

since we have continuous coal feeding into the reactor, and char accumulates in the reactor, an average holding time $\bar{t}$ should be used for the upper limit of the above integration.

$$\ln \frac{A - BV_b}{A - B V_o} = - B\bar{t}$$

or

$$\frac{F_o V_o}{\bar{W}} - (k + \frac{F_1}{\bar{W}})V_b = e^{-\bar{t}} (k + \frac{F_1}{\bar{W}}) (\frac{F_o V_o}{\bar{W}} - V_o (k + \frac{F_1}{\bar{W}})) \tag{6.6}$$

where $$\bar{t} = \frac{\bar{W}(1 - Q\,V_b)}{F_o\,(1 - Q\,V_o)}$$

The proximate volatiles are dependent on the particular heating conditions of the proximate analysis method. For example, if more rapid heating is used, the actual volatile matter may exceed that of the proximate analysis, we therefore define Q as the factor to correct proximate volatile matter to actual volatile matter.

$$Q = \frac{\text{Volatiles content under rapid heating conditions}}{\text{Volatiles content under standard (slow) heating conditions}} .$$

Note that $1 - QV_o$ and $1 - QV_b$ represent the corrected fixed carbon fraction in the coal and char respectively.

Rearranging and dividing by $\frac{F_o\,V_o}{\bar{W}}$, equation (6.6) becomes:

$$1 - \frac{V_b}{F_o\,V_o}(k\bar{W} + F_1) - e^{-\bar{t}(k + \frac{F_1}{\bar{W}})}\left[1 - \frac{k\bar{W} + F_1}{F_o}\right] = 0 \qquad (6.7)$$

From this equation, k can be calculated for each experimental run knowing F_o, F_1, $\bar{W}$, and $\bar{t}$. V_o is known from the coal analysis. V_b can be calculated from equation 6.13 below or by analysing the char sample collected from the experiment.

For the case when k is known, the above equation can be written explicitly in V_b for design purposes.

$$V_b = \frac{F_o\,V_o}{k\bar{W} + F_1}\left(1 - e^{-\bar{t}(k + \frac{F_1}{\bar{W}})}\right) + V_o\, e^{-\bar{t}(k + \frac{F_1}{\bar{W}})} \qquad (6.8)$$

A Correlation Between Char Volatile Matter and Volatiles Yield

The total volatiles yield can be calculated from the char volatile matter content by the correlation derived below: If we consider a single particle undergoing pyrolysis which results in a fractional weight loss ΔW, which represents the volatile yield, i.e. ΔW = fractional weight loss = volatiles yield as fraction of MAF coal fed. When the coal and char are analysed by the proximate method, we obtain:

V_o = proximate volatile matter fraction of MAF coal fed.

V_b = proximate volatile matter fraction of MAF char.

To compute the yield we require V_b based upon the weight of coal rather than char.

V_2 = proximate volatile matter in char expressed as fraction of the MAF coal fed.

In terms of proximate analysis, the volatiles released are:

$$\Delta V = V_o - V_2 \tag{6.9}$$

But for the corrected analysis, the volatiles released are:

$$\Delta W = Q\Delta V = Q(V_o - V_2) \tag{6.10}$$

To calculate V_2 in equation (6.10), note that

Weight of Char = (1 - ΔW) x Weight of Coal

$$\therefore V_b = \frac{V_2}{1 - \Delta W} \tag{6.11}$$

Substituting (6.11) into (6.10) gives

$$\Delta W = Q(V_o - V_b)/(1 - QV_b) \tag{6.12}$$

or

$$V_b = \frac{1}{1 - \Delta W}\left(V_o - \frac{\Delta W}{Q}\right) \tag{6.13}$$

Q can be estimated using the empirical formula given by Wen et al[6] which they obtained by regression analysis of the curves given by Badzioch and Hawksley.[23] For the coals studies in this work, Q was estimated from this formula to be 1.3, 1.41, and 1.7 for Forestburg, Balmer (B), and Sukunka coals respectively.

To predict volatiles yield at any temperature for a certain coal, the following steps are followed:

1. By using the experimental data, k can be obtained from equation (6.7) for different temperatures and an Arrhenius relationship between k and 1/T can be obtained.
2. Then, from this Arrhenius relationship, k can be calculated at any temperature.
3. From equation (6.8), V_b can be calculated since k and all other parameters are known.
4. Once V_b is known, then the volatiles yield (ΔW) can be calculated from equation (6.12).

6.1 Model results and Discussion

The reaction rate constant was calculated for each coal from experimental runs at different temperatures using equation 6.7. A sample calculation is given in Appendix A. The dependence of this rate constant on temperature is well represented by an Arrhenius equation (Figure 31) of the form.

$$k = k_o \, e^{-E/RT}$$

which when plotted on a semi-log graph paper gives the frequency factor as the intercept and -E/R as the slope. By examining the scatter of data from both Sukunka and Balmer (B) coals in Figure 31, it seems that they can be fitted with one line yielding one activation energy and frequency factor for the two bituminous coals as given below:

Coal	Rank	k_o, s^{-1}	E, Kcal/Mole	Correlation factor
Forestburg	sub-bituminous	1.89×10^{-2}	4.71	- 0.91
Sukunka and Balmer (B)	bituminous	16.85	14.1	- 0.97

The activation energy of the sub-bituminous Forestburg coal is lower than that of the bituminous coals presumably because of the differences in mechanism. In Figure 4 and Table 6 some examples are shown of the values of the rate constants and activation energies obtained by other workers. It is seen that the values obtained here are within the range of values obtained by these workers. Differences in

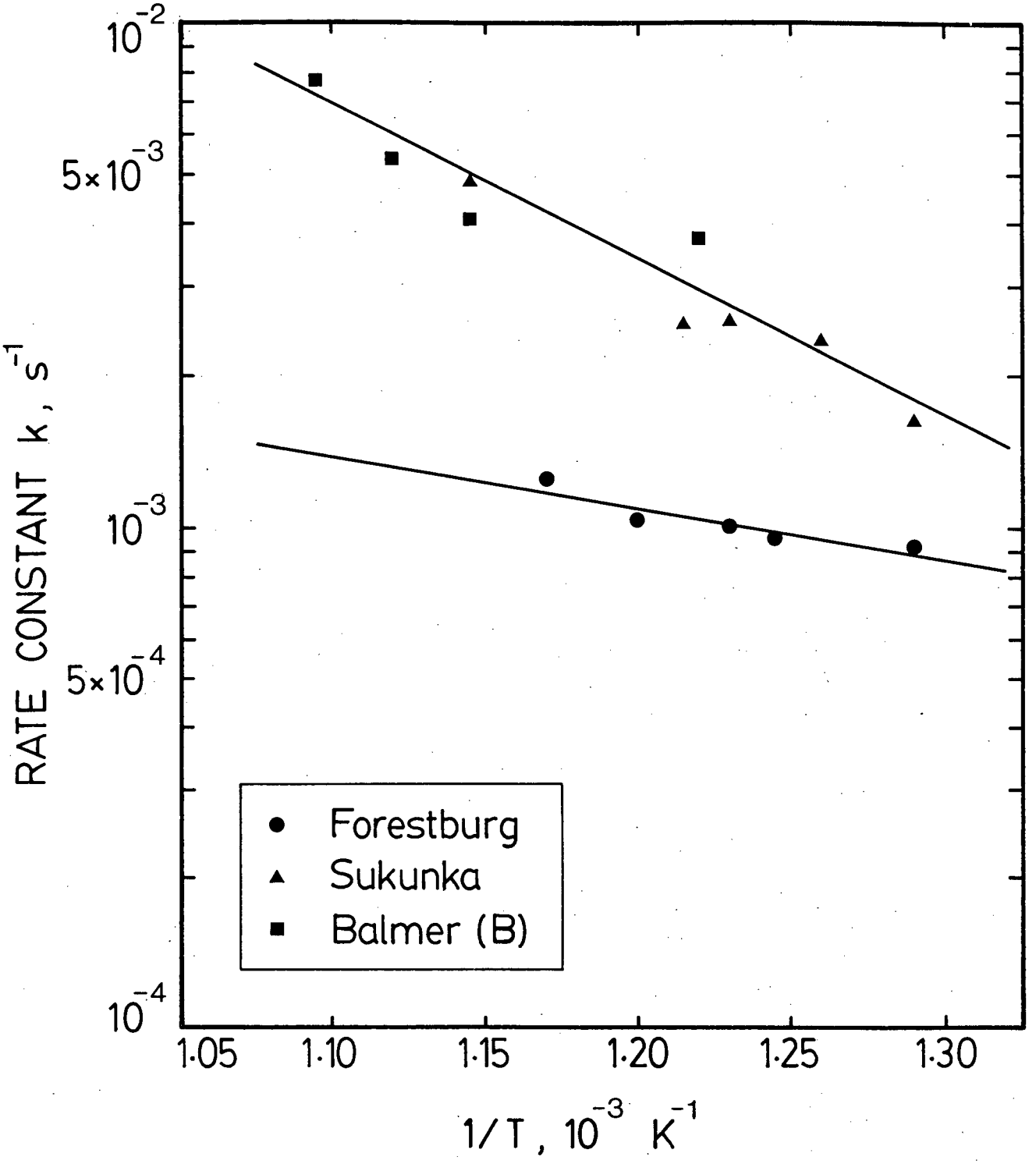

Figure 31 - Effect of temperature on pyrolysis rate constant.

coal type, equipment and experimental procedure contribute to the disagreement between these values. The activation energy for Forestburg coal is of a magnitude which implies a physical rather than a chemical process may be important. The value of the activation energy for the bituminous coals is more in the range typical of a chemical process but the data is rather scattered.

The reaction rate constant has been evaluated for runs on Forestburg coal with different coal feed rates at a constant temperature of 500°C. The effect of coal feed rate or bed char content on the reaction rate constant is shown in Figure 32. The reaction rate constant fluctuates around a constant value of about 0.001 s^{-1}; hence the reaction rate constant is independent of the coal feed rate and char accumulation in the bed. Thus in modelling the total volatiles yield, the char accumulation need not be included, however it has a strong effect on the fraction of volatiles which reports as liquid.

The effect of particle size on the rate constant for Sukunka coal is shown in Figure 33. From this figure it is seen that the rate constant increases with decreasing particle size. This indicates that the transport processes become more important as the particle size increases as would be expected. It should be pointed out here that the total volatile yields to calculate the rate constant here is taken as the sum of tar and gas yields rather than 1 - char yield because the char yield is not available for some of the runs.

The dependency of the extent of decomposition on time at fixed temperatures is shown in Figures 34 and 35. The solid lines are calculated by the following method: The reaction rate constant is

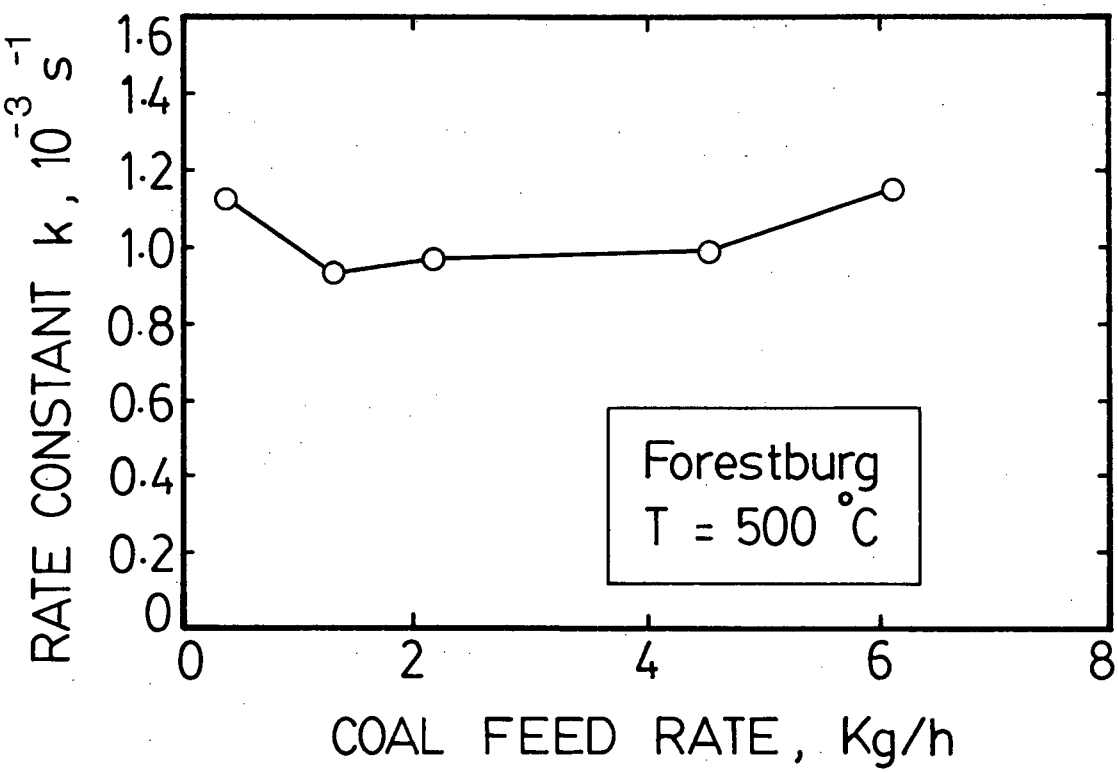

Figure 32 - Effect of coal feed rate on pyrolysis rate constant.

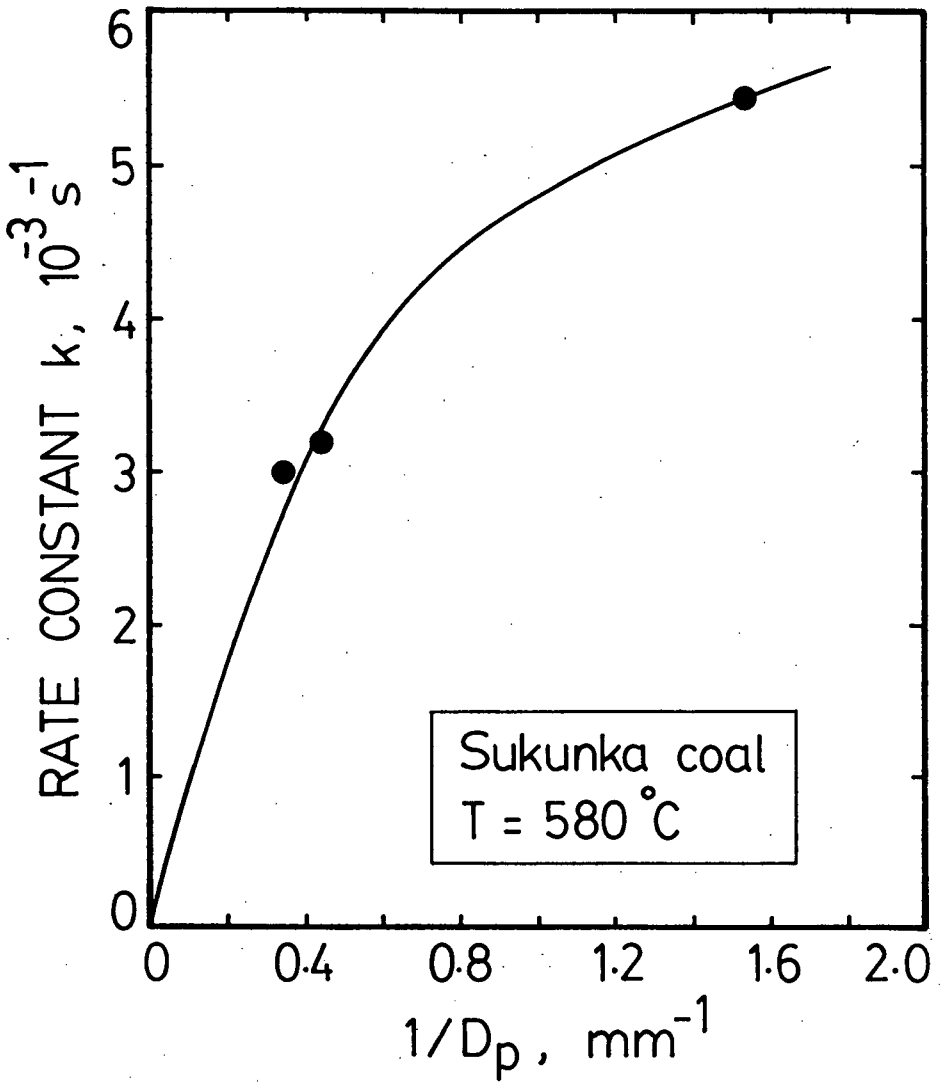

Figure 33 - Effect of coal particle size on pyrolysis rate constant.

evaluated at the given temperature from the Arrhenius correlation for that coal. Then this k value along with typical values for feed rate (F_o) etc. are used to calculate V_b at different values of average holding times. The calculated extent of decomposition for Forestburg coal is shown in Figure 34, along with experimental values. There seems to be good agreement between experimental and the calculated curve, although at longer holding times, the conversion is underestimated in spite of a good fit of k vs. 1/T in Figure 31. Figure 35 shows the decomposition for Sukunka coal predicted by the same method. Unfortunately, data were not available over a range of holding times for comparison. From these figures it is clear that the rate of decomposition depends on coal type and temperature. It also depends on heating rate which is essentially fixed here by the spouting conditions. The rate of decomposition increases with increases in temperature as would be expected. Sukunka coal decomposes faster than Forestburg because of the nature of the coal. For Sukunka coal at 600°C, almost complete decomposition was obtained in less than 500 seconds while for Forestburg coal at 580°C this took about 1,500 seconds. This type of calculation is useful for the design of scaled-up pyrolysis reactors to provide a mean residence time in the reactor sufficient for almost complete decomposition. The above discussion and figures quoted for time of decomposition are only valid for the particle size studied -3.36 + 1.19mm because smaller particle size results in faster heating rate where the decomposition is expected to be faster. Similar results (decomposition time) were obtained by Quinlan et al.[28], Pitt[21], and Ramakrishnan[41].

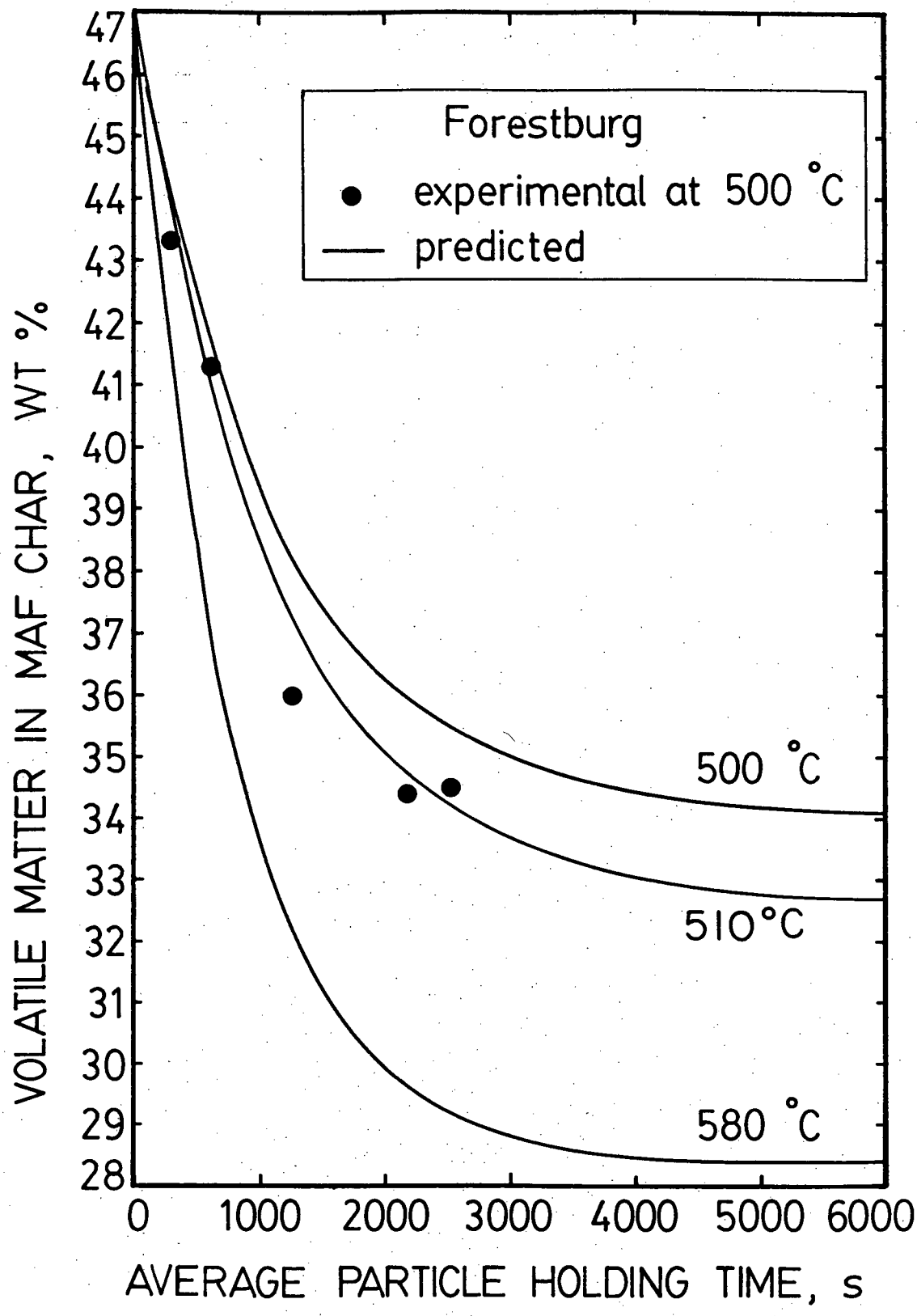

Figure 34 - Rate of decomposition of Forestburg coal.

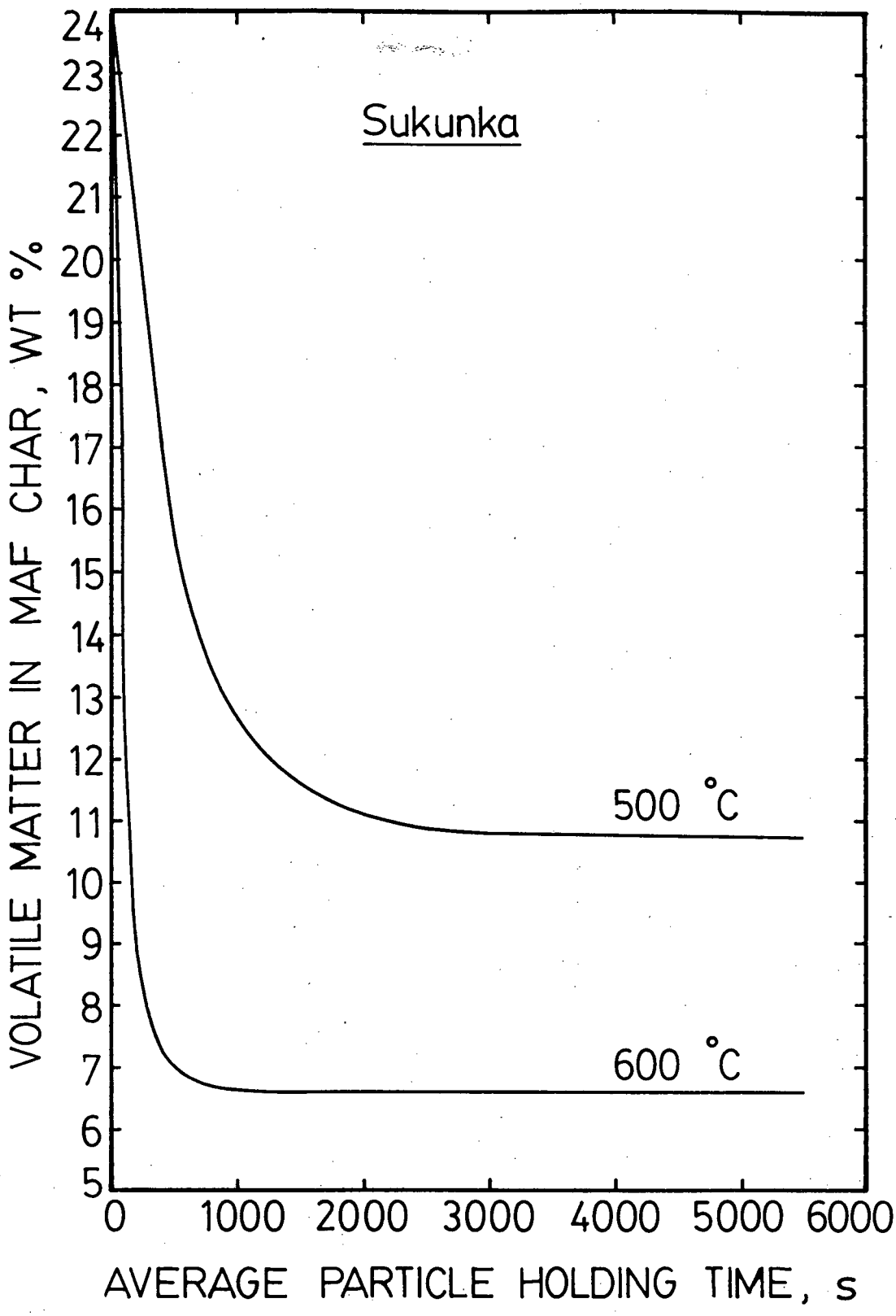

Figure 35 - Rate of decomposition of Sukunka coal.

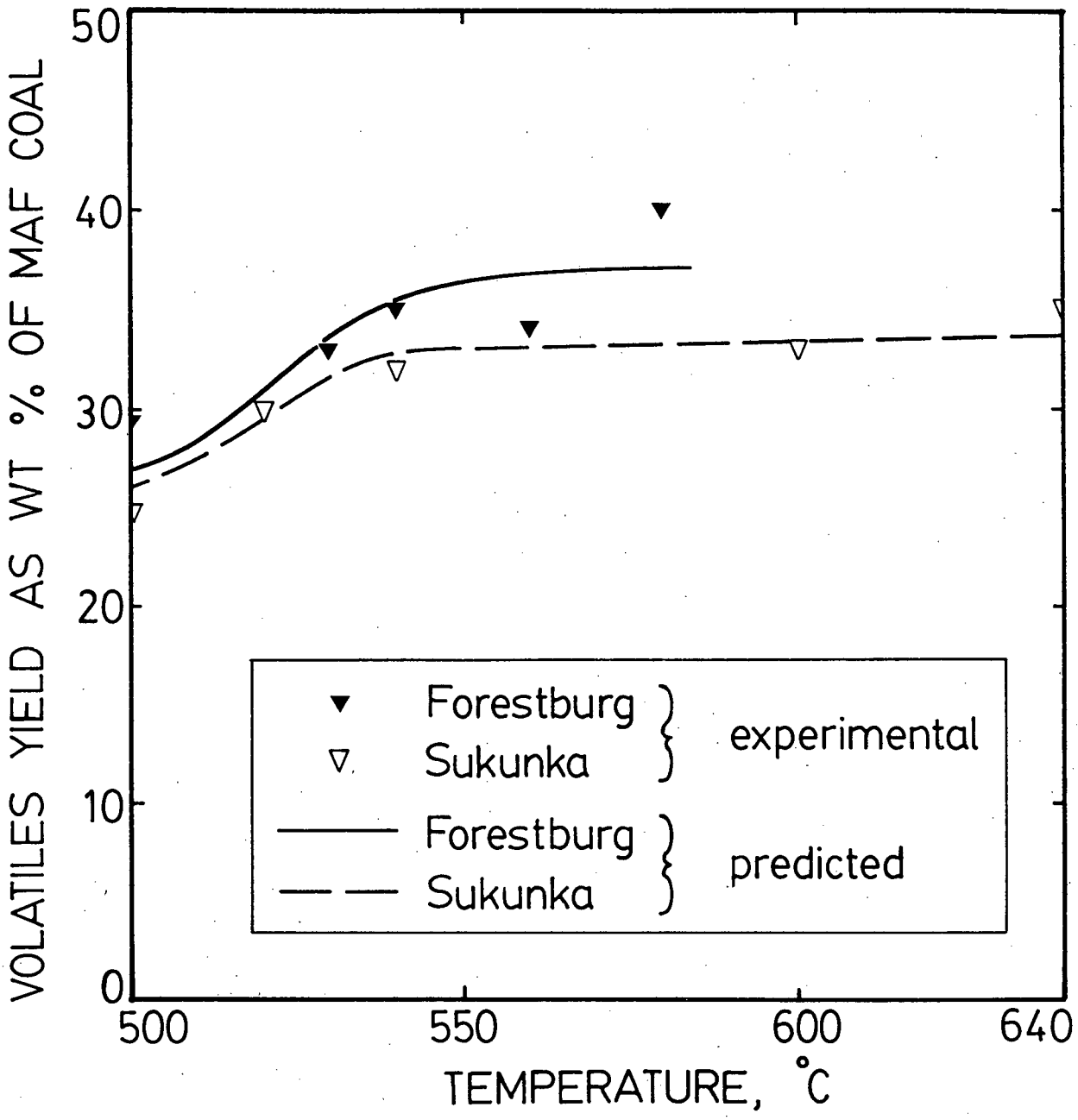

Figure 36 - Predicted and experimental volatiles yield with temperature.

The effect of temperature on the yield of volatiles (in this case 100 - % char yield) is shown in Figure 36. The predicted curves were calculated as follows: At a certain temperature, the reaction constant k is calculated from the Arrhenius correlation for that coal. By using the other data (F_o, F_1, t etc.) for that run at that temperature along with k value, V_b is calculated from equation 6.8. Then ΔW(weight loss = volatiles yield) is calculated from equation 6.12 using this V_b value. From Figure 36 it seems that a reasonable agreement exists between experimental and predicted values. From this and from the agreement between experimental and predicted volatile matter in char shown in Figure 33, the model derived here seems to be adequate to describe pyrolysis in semi-continuous pyrolysis reactor under the conditions used.

7. CONCLUSIONS

A spouted bed of sand appears to be a feasible reactor to pyrolyze caking bituminous coals as well as lower rank coals.

For a given type of coal, temperature is the most important variable affecting the tar yield. The effect of temperature on the tar yield for the Western Canadian bituminous coals tested is less profound than for the sub-bituminous coal. The temperature of maximum tar yield is lower for the sub-bituminous coal than for the bituminous coals.

An excellent tar yield of more than 30 wt% was obtained from the bituminous Sukunka coal in the 1-3 mm size range under optimal temperature conditions and coal feed rate. The sub-bituminous Forestburg coal gave a tar yield of 21% under optimal conditions. This coal also gave a large quantity of gas (mostly carbon oxides).

The presence of large amounts of char in the reactor is to be avoided, if maximum liquid yields are sought. While decreases in particle size increases liquid yield, bed depth, vapour residence time and the presence of CO_2 in the pyrolyzing atmosphere have little effect on tar yield.

High-ash bituminous Balmer coal gave low tar (12 wt%) and high char yields perhaps because of the catalytic effect of the ash mineral matter on the secondary polymerization reactions, whereas a clean Balmer coal yielded about fifty percent more tar.

Tar and char elemental compositions have been reported as a function of operating conditions. Tars are enriched in hydrogen with H/C atomic ratios up to twice that of the parent coal. Sulphur seems to

split equally between tar and char and its percentage is relatively low. The chars produced in the spouted bed still contain about 2% H, and should be an acceptable fuel.

It appears that the pyrolysis process in the spouted bed can be adequately described by a first - order kinetic model, which assumes back-mix flow of solids and constant holdup of char. The dependence of the reaction rate constant on temperature followed an Arrhenius equation. Good agreement between experimental volatile matter yield and model prediction was obtained. The activation energy is 4.71 kcal/mole for sub-bituminous Forestburg coal and 14.1 kcal/mole for both Sukunka and Balmer (B) bituminous coals.

8. RECOMMENDATIONS FOR FUTURE WORK

At present a miniature spouted bed pyrolysis apparatus is under development in this department to conduct further studies in characterization of coal liquids produced. Also a two reactor (15 cm diameter) spouted bed pyrolysis unit has been assembled where the heat for pyrolysis will be supplied by char combustion in the first reactor and flue gases sent for pyrolysis and spouting in the second reactor. In addition to these studies, future work should include:

* Further tests on the effect of coal particle size, especially below 0.65 mm, the smallest size used in this work.
* Further tests to confirm the effect of char accumulation in bed on tar yield. This can be done by using beds of char with different coal feed rates.
* Installation of an electrostatic precipitator downstream of the condenser to trap tar droplets which can be used for qualitative studies.
* More investigation of the catalytic effect of ash mineral matter on the polymerization reactions . The above mentioned small apparatus is easier to use for this since it requires small quantities of coal. This investigation could be done by comparing coal rejects which contain about 50% ash with clean coal.
* Comparison of spouted and fluidized bed pyrolysis. The spouted bed apparatus used for the present work can be

converted to fluidized bed rather easily. However, similar results are expected.

* The use of pre-oxidation or oxidative pyrolysis to reduce the extent of agglomeration. The effect of preoxidation on tar yield is important.
* Extension of the mathematical model to predict tar yields rather than simply the total volatile yield. This could be based on the model of Chang et al.[44]

NOMENCLATURE

A	A constant of equation 2 of Table 5, s^{-1}.
A_o	The potentially available coal for tar yield.
A_p	Surface area of a single particle.
B	A constant of equation 2 of Table 5, K.
C_p	Heat capacity
D	A constant of equation 2 of Table 5.
D_p	Particle diameter.
E	Activation energy
E_o	Mean activation energy.
f	Final fraction of conversion of coal.
F_o	Coal feed rate.
F_1	Entrainment rate
G	A coefficient such that $(1+G)\ A_o$ is the potentially available coal for gas production.
G_1	Spouting gas rate.
G_2	Total gas rate out of reactor.
h_p	Heat transfer coefficient between fluid and particle.
k	Pyrolysis rate constants.
K_p	Thermal conductivity of solid particle.
m_p	Mass of a particle.
n	Order of reaction.
N_u	Nusselt number, $h_p d_p / k_f$
P	Pressure
P_r	Prandtl number, $c_{pf}\mu / k_f$

Q	Ratio of total weight loss to loss of proximate volatile matter
r_p	Radius of a particle
R	Gas constant
R_e	Particle Reynolds number based on superficial velocity for that zone, $d_p u \rho_f / \mu$
t	Time
$\bar{t}$	Average particle holding time
T	Temperature
$\bar{T}$	Average instantaneous temperature
T_b	Bulk bed solids temperature
T_p	Particle temperature
T_{p_0}	T_p at $t = 0$
T_s	Surface temperature
V	Yield of total volatiles
V^*	Ultimate yield of total volatiles
VM	Volatile content as measured by proximate analysis
VM_c	Proximate volatile matter in char
V^*_{nr}	Ultimate yield of nonreactive volatiles
V^{**}_r	Reactive volatiles
V_o	Proximate volatile matter of coal fed
V_l	Proximate volatile matter of char entrained
V_b	Proximate volatile matter of char retained in bed
W	Weight of char in bed at end of run

$\overline{W}$	Average weight of char in bed
ΔW	Weight loss = volatile yield
α	Thermal diffusivity
ϵ	Voidage (1 - volumetric fraction of solids)
σ	Standard deviation in the Gaussian distribution of activation energy

REFERENCES

1. Manurung, F. "Studies in spouted bed technique with particular reference to low temperature carbonization", Thesis (Ph.D.), University of New South Wales, 1965.

2. Barton, R.K., Rigby, G.R., and Ratcliffe, J.S. "The use of a spouted bed for the low temperature carbonization of coal", Mech. Chem. eng. Trans., 4, 105 (1968).

3. Elliott, M.A., ed. Chemistry of coal utilization, 2nd supplementary volume, New York: Wiley, 1981.

4. Howard, J.B., in Chemistry of coal utilization, 2nd supplementary volume, Chapter 12, New York: Wiley, 1981.

5. Anthony, D.B. and Howard, J.B., A.I.Ch.E.J., 22 (4), 625 (1976).

6. Wen, C.Y., and Dutta, S., Coal conversion technology, Chapter 2, Addison-Wesley, 1979.

7. Scott, D.S., in a summary of the proceedings of a workshop on the application of pyrolysis technology to the utilization of Eastern Canadian coals organized by the Research and Productivity Council in New Brunswick: Atlantic Research Laboratory technical report 30: NRCC 19903 (1982).

8. Given, P.H., "The distribution of hydrogen in coals and its relations to coal structure", Fuel, 39, 147 (1960).

9. Dryden, I.G.C., "Chemical constitution and reactions of coal", in chemistry of coal utilization, supplementary volume, H.H. Lowry, Ed., New York: Wiley, 1963, pp. 232-295.

10. Van Krevelen, D.W. Coal, Elsevier publishing company, Amsterdam, 1961.

11. Wiser, W.H., and Kertamus, N.J., "Kinetic study of the pyrolysis of a high-volatile bituminous coal", Ind. Eng. Chem., Process Des. Dev., 6, 133 (1967).

12. Franklin, R.E., "A study of the fine structure of carbonaceous solids by measurements of true and apparent densities, Part I, coals", Trans, Faraday Soc., 45, 274 (1949).

13. Franklin, R.E., "A study of the fine structure of carbonaceous solids by measurements of true and apparent densities, Part II, Carbonized coals," Trans. Faraday Soc., 45, 668 (1949).

14. Evans, D.G., and Hermann, J.A., "The porosity of Brown-coal char", Fuel, 49, 110 (1970).

15. Cannon, C.G., Griffith, M., and Hirst, W., "The carbonisation of coals", in Proc. Conf. Ultra-fine structure coals cokes, BCURA, London, 1944, p. 131.

16. Ergun, S., O'Donnell, H.J., and Parks, B.C., "Microscopic studies of rate of thermal decomposition of petrographic components of coal," Fuel, 38, 205 (1959).

17. Woods, M.F., Habberjam, G.M., Elsworth, K., and Bennet, S., "The effect of Maceral composition on the binderless briquetting of hot char," Fuel, 46, 193 (1967).

18. Lewellen, P.C., "Product decomposition effects in coal pyrolysis," M.S. Thesis, Dept. of Chemical Engineering, MIT, 1975.

19. Mills, A.F., James, R.K., and Antoniuk, D., "Analysis of coal particles undergoing rapid pyrolysis", in Future Energy Production Systems, J.C. Denton and N. Afgan, Eds., Hemisphere Publishing Company, Washington, D.C., 1976.

20. Badzioch, S., "Thermal decomposition", BCURA, Month Bull. 31(4), 193 (1967).

21. Pitt, G.J., "The kinetics of the evolution of volatile products from coal", Fuel, 41, 267 (1962).

22. Anthony, D.B., Howard, J.B., Hottel, H.C., and Meissner, H.P., "Rapid devolatilization of pulverized coal," 15th Symp. (Int.) combustion, Combustion Institute, Pittsburgh, 1975, p. 1303.

23. Badzioch, S., and Hawksley, P.G.W., "Kinetics of thermal decomposition of pulverized coal particles," Ind. Eng. Chem., Process Des. Dev., 9, 521 (1970).

24. Grace, J.R. Notes given in C.S.Ch.E. Continuing Education course on spouted beds in the Department of Chemical Engineering at the University of British Columbia, Vancouver, October, 1982.

25. Gishler, P.E., and Mathur, K.B., Method of contacting solid particles with fluids, U.S. Patent No. 2, 786, 280 to Nat. Res. Council of Can., 1957.

26. Mathur, K.B., and Epstein, N., Spouted Beds., Academic Press, 1974.

27. Barton, R.K., and Ratcliffe, J.S., "The rates of devolatilization of coal under spouted bed conditions", Mech. Chem. Eng. Trans., 5, 35 (1969).

28. Quinlan, M.J., and Ratcliffe, J.S. "A design equation for the low temperature carbonization of coal under spouted bed conditions," Mech. Chem. Eng. Trans., 5, 1 (1971).

29. Newman, A.B., "Drying of porous solids: diffusion calculations", Trans. A.I. Ch. E., Vol. 27, 1932, pp. 310-33.

30. Suuberg, E.M., "Rapid pyrolysis and hydropyrolysis of coal," Sc.D. Thesis, Dept. of Chemical Engineering, MIT, 1977.

31. Stangeby, P.C., and Sears, P.L., "Rapid pyrolysis and hydropyrolysis of Canadian coals", Fuel 60, 131-35 (1981).

32. Furimsky, E., Belanger, R., and Jorgenson, J., "The pyrolysis of Canadian coals for the production of fuels and petrochemicals", presented at Atlantic Research Lab. (NRC) "Application of pyrolyssis technology to the utilization of Eastern Canadian Coals," Fredericton, N.B., Jan 5-6, 1982.

33. Tyler, R.J., "Flash pyrolysis of coals: Devolatilization of a Victorian brown coal in a small fluidized bed reactor", Fuel, 58, 680-86 (1979).

34. Tyler, R.J., "Flash pyrolysis of coals: Devolatilization of Bituminous coals in a small fluidized bed reactor", Fuel, 59, 218-24 (1980).

35. Edwards, J.H. and Smith, I.W., "Flash pyrolysis of coals: Behaviour of three coals in 20 kg/h fluidized bed pyrolyzer", Fuel, 59, 678-81 (1980).

36. Edwards, J.H., I.W. Smith, and R.J. Tyler, "Flash pyrolysis of coals: Comparisons of results from 1 g/h and 20 kg/h reactors", Fuel, 59, 681-86 (1980).

37. Scott, D.S., Piskorz, J. and Fouda, S., "Flash pyrolysis of Canadian coals", 32nd Can. Chem. Eng. Conference, Vancouver, B.C., October 3-6, Preprint, Vol. 1, 542-555 (1982).

38. Ratcliffe, J.S. and Rigby, G.R., "Low temperature carbonization in a spouted bed", Mech. Chem. Eng. Trans. 5, 1 (1969).

39. Ray, R.B., and Sarkar, S., "Kinetics of coal pyrolysis in spouted bed", Indian Chem. Engr., April/June, Vol. 18, No. 2 (1976).

40. Dutta, S., Wen, C.Y., and Belt, R.J., Ind. Eng. Chem. Process Des. Dev., 16, 20 (1977).

41. Ramakrishnan, N.N., "Coal pyrolysis in a continuous fluidized bed", from the Proceedings of the International Conference on Coal Science, Düsseldorf, 7-9.9, 1981.

42. Wen, C.Y., Bailie, R.C., Lin, C.Y., and O'Brien, W.S., coal gasification, advances in chemistry series 131, ACS, Washington, D.C., 1974, p. 9.

43. Wen, C.Y., and chem, L.H., "A model for coal pyrolysis", Paper presented at ACS national meeting, Washington, C.C., September 9-14, 1979.

44. Chang, P.W., Durai-Swamy, K., and E.W. Knell, "Kinetics of coal pyrolysis reactions in a flash pyrolysis process", in Coal Processing Technology, 6, AIChE, New York, 1980.

45. Kayihan, F., and Reklaltis, G.V., "Modelling of staged fluidized bed coal pyrolysis reactors", Ind. Eng. chem. Process Des. Dev., 19, 15 (1980).

46. Levenspiel, O., Chemical reaction engineering, 2nd ed., New York: Wiley, 1966.

47. Shapatina, E.A., Kelyuzhnyi, V.V., and Chukanov, Z.F., "Technological utilization of fuel for Energy, 1. Thermal treatment of fuels" (1960), reviewed by S. Badzioch, BCURA Month. Bull., 25, 285 (1961).

48. Howard, J.B., and Essenhigh, R.H., "Pyrolysis of coal particles in pulverized fuel flames", Ind. Eng. Chem., Process des. Dev., 6, 74 (1967).

49. Stone, H.N., Batchelor, J.D., and Johnstone, H.F., "Low temperature carbonization rates in a fluidized bed", Ind. Eng. chem., 46, 274 (1954).

50. Van Krevelen, Van Heerden, C., and Huntjens, F.J., "Physiochemical aspects of the pyrolysis of coal and related organic compounds", Fuel, 30, 253 (1951).

51. Boyer, M.S.F., C.R. Assoc. Tech. 1'Ind. Gaz, France, Congr., 653 (1952).

52. Kobayashi, H., Howard, J.B., and Sarofim, A.F., "Coal devolatilization at high temperatures", 16th Symp. (Int.) Combustion, Combustion Institute, Pittsburgh, 1977, p. 411.

53. Holmes, J.M., Cochran, H.D., Edwards, M.S., Joy, D.S., and Lantz, P.M., "Evaluation of coal carbonization processes", in Coal Proc. Tech., 3, AIChE, New York, 1977.

54. Nowacki, D., "Coal liquefaction processes", Noyes Data Corporation, 1979.

55. Gutierrez, L., Gasification of some Western Canadian coals in fluidized bed", M.Sc., Thesis, Dept. of Chemical Engineering, The University of British Columbia, 1979.

56. Durai-Swamy, K., Che, S., Knell, E., Green, N.W., and Zahradnik, R., "Tar yields in ORC flash pyrolysis process". Preprint for ACS meeting 1979, Fuel Chemistry Symposium.

57. McCarthy, D.J., "Flash pyrolysis of Australian coals: effects of pre-oxidation and of oxygen in the inlet gases on formation of agglomerated material", Fuel, 60, 205 (1981).

58. Sitnai, O., and McCarthy, D.J., "Oxidative rapid pyrolysis of coal in a dilute phase transport reaction", in Ind. Eng. Chem. Process des. Dev., 19, 641 (1980).

59. Young, W.C., and Kearing, D.L., "Recirculating fluidized bed reactor data utilizing a tri-dimensional cold model", presented at 75th National meeting of the AIChE, Detroit, Mich., June 1973.

60. "Char oil energy development", U.S. Dept. of the Interior, Office of Coal Research, Report No. 73, Interim Report No. 1, July 1971 - June 1972, prepared by FMC Corp. Dec. 1972.

61. Miller, C.T., "Hydrocarbonization of coal in a fluidized bed", Ind. Eng. Chem. Process Des. Dev., 19, 29 (1980).

62. McCafferty, T., M.Sc., Project in progress on coal pyrolysis in the Department of Chemical Engineering, at the University of British Columbia.

63. Anthony, D.B., "Rapid devolatilization and hydrogasification of pulverized coal", Sc.D., Thesis, Dept. of chemical Engineering, MIT, 1974.

64. Torrest, R.S., and Van Meurs, P., "Laboratory studies of the rapid pyrolysis and desulphurization of a Texas lignite", Fuel, 59, 458-64 (1980.

APPENDIX A

A.1 Calculations For Isokinetic Gas Sampling:

Isokinetic sampling means that the velocities of the gases in the main pipe and in the sampling tube should be equal. In order to insure this, the velocity of the gas in the main pipe at the temperature in that area is estimated, then from the cross sectional area of the sampling tube and that velocity, the volumetric flow rate of the sample gas is calculated and then adjusted to the temperature of the sampling gas rotameter. Below is a sample calculation (Run 35).

Run 35: Forestburg coal, Temperature in reactor = 500°C mass flow rate of spouting nitrogen = 4.95 g/s, to this, an estimate of the gases, water vapour and other vapours which result from coal pyrolysis can be added:

Coal feed rate (as received) = 0.378 g/s

Coal feed rate (MAF) = 0.265 g/s

Water vapour expected to evolve = (0.378) (0.23)

= 0.09 g/s

Assume gases and vapours generated from pyrolysis represented 20% of MAF coal fed.

$\therefore$ gas and vapors evolved = (0.265) (0.2)

= 0.05 g/s

$\therefore$ total mass flow rate of gases = 4.95 + 0.09 + 0.05

= 5.09 g/s

From the above calculations, it is seen that spouting nitrogen accounts for over 97% of the gases. Hence, the mass flow rate of spouting nitrogen alone can be used for the purpose of this estimation. Also, the density of nitrogen can be assumed to represent the density of the gases. The temperature in the area of sampling tube for this run is about 400°c. The density of nitrogen at this temperature is 5.07×10^{-4} g/cm^3. The pressure is atmospheric.

$\therefore$ volumetric flow rate $= \frac{5.09}{5.07 \times 10^{-4}} = 10039$ cm^3/s

The main pipe flow area (nominal diameter 2") = 23.58 cm^2

$\therefore$ velocity of the gases $= \frac{10039}{23.58} = 425.7$ cm/s.

The sampling tube cross sectional area ($\frac{3"}{8}$ nominal diameter) = 0.7 cm^2.

$\therefore$ volumetric flow rate of sample gas at 400°C = 298 cm^3/s and at 21°C = 130 cm^3/s and hence the sample gas rotameter setting is selected accordingly by adjusting a valve upstream of the rotameter.

A.2 Product Yield Calculations

The procedure used to calculate tar, gas, and char yields is outlined below. This is followed by a detailed sample calculations. let

SN = mass flow rate of spouting nitrogen, g/s (This is the only gas input to the system)

CF = coal feed rate, g/s

CFMA = coal feed rate (MAF), g/s

SG = mass flow rate of sample gas, g/s

$$T = \frac{\text{total weight of tar collected from sample gas}}{\text{duration of tar collection}}, \text{ g/s}$$

NF = weight fraction of nitrogen in the output gas

TG = total gas output, g/s.

A material balance on the nitrogen gives the total gas output. Since the nitrogen gases evolved during pyrolysis were not measured, it is assumed that these gases are very small and negligible (calculations* showed that they are indeed negligible). Hence it is not necessary to include the nitrogen fraction in the coal and that remained in the char.

$$SN = NF \times TG$$

$$TG = \frac{SN}{NF}$$

The total gas produced due to pyrolysis = TG - SN and the gas

$$\text{yield} = \frac{TG - SN}{CFMA}.$$

The yield of any individual gas

$$= \frac{TG \times \text{weight fraction of this gas}}{CFMA}$$

$$\text{Tar Yield} = \frac{T}{SG} \times \frac{TG}{CFMA}$$

The above is multiplied by 100 to get wt.%.

Sample Calculations

For Run 32 on Forestburg coal at 580°C:

SN = 5.32 g/s, CF = 0.337 g/s, CFMA = 0.265 g/s

$T = 7.5 \times 10^{-4}$ g/s (2.7 g of tar was collected over 1 hour)

SG = 0.29 g/s.

From the gas chromotograph, the composition of the output gas (in vol.%) was obtained:

H_2 0.296

CO_2 0.412

O_2 2.294

N_2 96.676

CH_4 0.121

CO 0.201

The oxygen here is assumed to be due to air leak into the system during pumping the gas sample to the gas chromotograph. Therefore the above reading must be corrected to get oxygen free gas composition. For each part of oxygen leaked there is 0.79/0.21 part nitrogen which also must be calculated and used to correct the above reading.

Nitrogen leaked = $2.294 \times (\frac{0.79}{0.21}) = 8.63$

$\therefore$ air leaked = 2.294 + 8.63 = 10.92. This must be substracted from the gas composition and the corrected vol.% for H_2

$H_2 = 0.296 \ (\frac{100}{100-10.92})$

$= 0.332$

and so on for the others to get composition of oxygen free gas in vol.% as:

H_2:0.332, CO_2: 0.463, N_2:98.8, CH_4:0.136 and CO:0.226

This can be converted to wt.% by using the densities of the above gases to get:

H_2:0.0238, CO_2: 0.726, N_2:98.9, CH_4:0.0777, CO:0.226

Now, NF = 0.989

$SN = NF \times TG.$

$\therefore TG = \frac{5.32}{0.989} = 5.38$ g/s.

$\therefore$ gas produced due to pyrolysis = 5.38 - 5.32

= 0.06 g/s

and gas yield $= \frac{0.06}{CFMA} \times 100$

$= \frac{0.06}{0.265} \times 100$

= 22.6 wt.% of MAF coal fed.

The individual gas yield is obtained by:

$$\text{individual gas yield} = \frac{(\text{Wt.\% of this gas}) \times TG}{CFMA}$$

For H_2: hydrogen yield $= \frac{(0.0238)\ (5.38)}{0.265} = 0.48$ wt.% MAF

this is repeated to get the yield of other gases. Yields of all gases, char and tar for all the runs are given in Appendix B.

$$\text{Tar yield} = \left(\frac{T}{SG}\right) \times \frac{TG}{CFMA} \times 100$$

$$= \left(\frac{7.5 \times 10^{-4}}{0.29}\right) \left(\frac{5.38}{0.265}\right) \times 100$$

= 5.2% (MAF)

$$\text{Char yield} = \frac{\text{total weight of char collected (MAF)}}{\text{total weight of coal fed (MAF)}} \times 100$$

For this run the total weight of coal fed (as received)

= 1721 g over 76 minutes.

$\therefore$ coal fed (MAF) = 1207 g.

The weight of char collected (dry) = 835 g.

The ash content of this char is 13.8%

$\therefore$ weight of char collected (MAF) = 719.8 g.

$\therefore$ char yield = $\frac{719.8}{1207}$ x 100 = 59.6%

A simple computer program was written to perform the above calculations. *The calculations shown below indicate that the nitrogen gases (nitrogen or nitrogen oxides) evolved from the coal due to pyrolysis are indeed negligible.

For Run 32 on Forestburg coal:

From Table 12 the nitrogen content of this coal is 1.71% MAF and from the char analysis for this run, the nitrogen content of the char is 1.98 (MAF).

The rate of nitrogen gases produced = Nitrogen in coal - Nitrogen in char.

CFMA = 0.265 g/s

The MAF char for this run was produced at a rate = 0.158 g/s

$\therefore$ the rate of nitrogen gases produced =

$$(0.265)\frac{(1.71)}{100} - (0.158)\frac{(1.98)}{100} = 1.4 \times 10^{-3} \text{ g/s.}$$

while SN = 5.32 g/s.

Therefore the rate of nitrogen gases produced represents $\frac{1.4 \times 10^{-3}}{5.32}$ x 100 (0.03%) of the nitrogen input which is indeed negligible. In addition, should it become necessary to include the nitrogen produced due to pyrolysis, provision should be made to measure them by the gas chromotograph.

Sample Calculations of the Pyrolysis Rate Constant (k)

All the values given below are on MAF basis.

k is calculated from equation 6.7

For run 35 on Forestburg coal, we have the following values for the parameters:

$F_0 = 0.26$ g/s, $F_1 = 0.01$ g/s, $\overline{W} = 398$ g, $Q = 1.3$, $V_0 = 0.47$

The char yield = 0.704

$\therefore \Delta W = 1 - 0.704 = 0.296$

$\therefore$ By using equation 6.13, V_b is calculated to be 0.344

$\therefore \overline{t} = 2224$ s.

Now we have all the parameters to calculate k from equation 6.7

$\therefore k = 9.21 \times 10^{-4}\ s^{-1}$

Sample Calculations for Pyrolytic Water

For run 32 on Forestburg coal (moisture content $\sim$ 23%):

Coal feed rate (as received) = 0.337 g/s.

$\therefore$ Water expected to be released = 0.337 x 0.23 = 0.078 g/s.

N_2 flowing through the system = 5.32 g/s.

Assuming that the gas (mainly N_2) leaving the system at 20°C is saturated with water vapour. The vapour pressure of water at this temperature is 17.5 mm Hg.

$\therefore$ Water that is not condensed = $5.32\ (\frac{17.5}{760})(\frac{18}{28}) = 0.079$ g/s.

$\therefore$ No pyrolytic water is expected to condense under these conditions.

APPENDIX B
Experimental Data and Results

Table 24 - Forestburg coal; experimental conditions and product yield

Run No.	Coal Feed Rate Kg/h	Temperature °C	Weight of Char Kg	Yields, Wt% of MAF Coal Fed		
				Tar	Gas	Char
11	3.59	480	3.292	-	12.4	69.9
12	3.036	500	3.575	-	15.2	80.4
13	3.036	600	-	-	27.2	-
22	2.203	500	1.476	7.1	-	74.7
23	2.647	530	2.327	-	-	64.9
24	3.891	450	2.525	3.3	10.2	78.6
25	3.628	520	2.781	3.3	20.1	68.5
26	1.468	500	1.050	7.4	-	66.9
27	7.643	500	3.263	4.0	14.6	68.1
28	1.48	500	1.163	-	9.6	70.5
29	6.134	500	3.558	1.2	15.9	69.2
30	4.55	500	2.941	2.4	15.5	69.4
31	3.658	480	2.585	2.2	8.3	69.6
32	1.358	580	0.835	5.2	22.9	59.6
33	1.123	530	0.752	21	15.7	66.9
34	1.049	540	0.690	19.9	16.9	65.4
35	1.36	500	0.953	13.2	13.8	70.4
36	0.386	500	0.276	35.1	1.8	66.9
37	0.6	515	0.332	12.5	2.6	64.4
38	1.286	580	0.812	5.9	-	63.5
39	0.94	520	0.365	-	-	64.2
40	1.096	560	0.687	6.8	18.0	65.9
41	1.278	520	0.822	-	-	66.9
42	1.487	500	-	5.1	8.3	-
43	1.114	520	-	10.4	12.1	-
44	1.114	560	0.782	6.2	19.2	66

Table 25 - Sukunka coal; experimental data and results

Run No.	Coal Feed Rate Kg/h	Temperature °C	Weight of Char Kg	Yields, Wt% of MAF Coal Fed		
				Tar	Gas	Char
16	2.043	500	-	-	6.32	-
17	2.033	530	-	-	5.29	-
18	5.361	480	3.178	-	2.7	74.1
19	1.113	620	-	-	5.14	-
20	9.307	550	-	-	-	-
21	1.782	500	1.476	11.2	3.4	72.0
45	1.739	600	-	30.6	3.57	-
46	0.622	580	-	36.1	2.2	-
47	0.622	520	0.499	11.9	1.9	68.4
48	1.372	520	1.074	11.9	4.1	69.7
49	1.456	560	1.456	15.9	7.3	72
52	0.767	550	0.466	-	1.9	66.9
54	0.933	615	0.757	26.1	3.7	64.7
55	0.794	590	-	-	-	-
56	1.562	560	0.816	16.5	5.8	65.5
58	1.279	580	0.781	20.4	5.7	63.3
59	1.529	540	-	16.5	4.9	-
60	1.311	580	0.536	17.5	7.5	64.8
61	1.142	640	-	25.3	10.1	-
63	1.704	580	-	15.3	4.9	-
64	1.307	560	-	15.5	7.4	-
65	1.307	560	-	16.7	7	-
66*	1.040	580	-	17.6	7.6	-
67*	1.050	580	-	22.4	5.9	-
73	1.215	520	0.591	11.0	6	74.5
75	1.215	500	0.601	10.7	4.8	77.4
76	1.215	580	0.451	17.6	5.4	68.3
77*	1.15	580	0.315	26.7	6.2	59.7

*For runs 66,67 and 77 the particle size of coal feed was (in U.S. standard) -6+8, -16+25, -25+30 respectively while for all other runs it was -6+16.

Table 26 - Balmer A coal; experimental data and results

Run No.	Coal Feed Rate Kg/h	Temperature °C	Weight of Char Kg	Yields, Wt% of MAF Coal Fed		
				Tar	Gas	Char
72	1.027	535	0.886	8.4	3.75	79.7
68	1.217	565	0.896	8.6	4.0	80.3
69	1.54	600	1.451	7.1	3.0	82.9
70	1.715	620	1.316	12.1	3.5	76.0
78	1.246	650	1.066	8.9	4.7	81.1

Table 27 - Balmer B coal; experimental data and results

Run No.	Coal Feed Rate Kg/h	Temperature °C	Weight of Char Kg	Yields, Wt% of MAF Coal Fed		
				Tar	Gas	Char
84	0.956	545	0.937	13.6	5.4	77.2
80	1.056	580	0.895	19.4	5.8	69.9
82	0.956	600	0.805	18.1	6.3	74.4
79	1.47	620	1.172	12.9	7.7	73.6
83	0.956	640	0.771	14.7	8.98	71.9

Table 28 - Percentage of Ash in Char from Various Coals

Coal	Temperature °C	Wt.% Ash
Forestburg	500	11.9
	530	12.5
	560	12.6
	580	13.8
Sukunka	520	15.9
	580	16.2
	600	18
	640	18.7
Balmer B	545	14.3
	580	14.6
	640	15.9

Reproducibility

From runs 32, 38, 40 and 44, reproducibility of the results was calculated. For example, reproducibility of tar yield from Forestburg coal at 560°C was calculated from runs 40 and 44 as follows:

$$\text{Average tar yield} = \frac{6.2 + 6.8}{2} = 6.5$$

$$\therefore \text{Error} = \pm 0.3$$

$$\therefore \text{Reproducibility} = \frac{\pm 0.3}{6.5} \times 100 = \pm 4.6\%$$

Reproducibility of the tar yield was also calculated from runs 32 and 38 to be ± 6%. Thus the average reproducibility of ± 5% was reported. The same method was used to obtain a reproducibility of ± 3% for the gas and ± 2% for the char yields. Further indications of reproducibility may be seen in tables 15 - 17.

Table 29 - Typical ash analysis for the coals studied*

Compound	Coal Type		
	Forestburg	Balmer	Sukunka
SiO_2	37.8	61.2	66.4
Al_2O_3	20.11	29.6	19.2
Fe_2O_3	6.60	2.6	2.9
Mn_3O_4	-	-	-
TiO_2	0.40	1.7	0.7
P_2O_5	0.40	0.8	trace
CaO	15.12	2.4	2.5
MgO	1.00	0.7	1.7
SO_3	13.67	1.7	1.8
Na_2O	4.60	0.0	0.7
K_2O	0.50	0.4	1.4

*These are typical analyses given by the coal suppliers.

APPENDIX C

Kinetic Model for the Case W≠ Constant

From Equation (6.2) we have:

$$F_o V_o - k V_b W - F_1 V_b = W \frac{d V_b}{dt} + V_b \frac{dW}{dt} \qquad (C.1)$$

If we take W = at, i.e. a linear increase of char accumulation with time, then

$$\frac{dW}{dt} = a$$

Therefore equation (C.1) becomes:

$$F_o V_o - k V_b W - F_1 V_b = at \frac{d V_b}{dt} + aV_b \qquad (C.2)$$

$$\frac{dV_b}{dt} + V_b\left(k + \frac{F_1}{at} + \frac{1}{t}\right) = \frac{F_o V_o}{at} \qquad (C.3)$$

This is a first order linear equation which can be solved by the integrating factor (R) method.

$$R = \exp\left(kt + \frac{F_1 + a}{a} \ln t\right).$$

multiplying equation (C.3) by this integrating factor gives:

$$\frac{dV_b}{dt}\left[\exp\left(kt + \frac{F_1 + a}{a} \ln t\right) + V_b\left(k + \frac{F_1}{at} + \frac{1}{t}\right) \exp\left(kt + \frac{F_1 + a}{a} \ln t\right)\right.$$

$$= \frac{F_o V_o}{at} \exp\left(kt + \frac{F_1 + a}{a} \ln t\right). \qquad (C.4)$$

Integrating equation (C.4) gives:

$$V_b \exp(kt + \frac{F_1 + a}{a} \ln t) = \frac{F_o V_o}{a} \int_o^t \frac{\exp(kt + \frac{F_1 + a}{a} \ln t)}{t} dt$$

$$V_b e^{kt} e^{\ln(t)^{\frac{F_1 + a}{a}}} = \frac{F_o V_o}{a} \int_o^t \frac{e^{kt} e^{\ln(t)^{\frac{F_1 + a}{a}}}}{t} dt$$

$$V_b e^{kt} t^{\frac{(F_1 + a)}{a}} = \frac{F_o V_o}{a} \int_o^t e^{kt} t^{\frac{F_1}{a}} dt.$$

Let $A = \frac{F_1 + a}{a}$, $B = \frac{F_1}{a}$

$$V_b e^{kt} t^A = \frac{F_o V_o}{a} \int_o^t e^{kt} t^B dt.$$

The solution for this equation is:

$$V_b \quad t^A = \frac{F_o V_o}{a} \left[\quad \sum_{r=0}^{B} (-1)^r \frac{B!\, t^{B-r}}{(B-r)!\, k^{r+1}} \right] \qquad (C.5)$$

Another Method

Another solution to equation (6.2) could be developed as follows: From equation (6.2) we have:

$$F_o V_o - k V_b W - F_1 V_b = \frac{d(W V_b)}{dt} \qquad (C.6)$$

By assuming the rate of entrainment to be very small and negligible, $F_1 \to 0$ we get

$$F_o V_o - k V_b W = \frac{d(W V_b)}{dt} \qquad (C.7)$$

Integrate with $t = 0$ $V_b W = 0$ to get

$$V_b W = \frac{F_o V_o}{k} (1 - e^{-kt}) \qquad (C.8$$

Overall mass balance gives (note that $F_1 \to 0$).

$$F_o - k V_b W = \frac{dW}{dt} \qquad (C.9)$$

Insert (C.8) to get

$$F_o - F_o V_o(1 - e^{-kt}) = \frac{dW}{dt} \qquad (C.10)$$

Integrate

$$W = (F_o - F_o V_o)t + \frac{F_o V_o}{k} (1 - e^{-kt}) \qquad (C.11)$$

k can be calculated from equation (C.11).

From (C.8) and (C.11) we get

$$V_b = \frac{\frac{F_o V_o}{k} (1 - e^{-kt})}{(F_o - F_o V_o)t + \frac{F_o V_o}{k} (1 - e^{-kt})}$$